NASA TECHNICAL NOTE

NASA TN D-5963

NASA TN D-5963
C. 1

AN APPROACH GUIDANCE METHOD USING A SINGLE ONBOARD OPTICAL MEASUREMENT

by Harold A. Hamer and Katherine G. Johnson

Langley Research Center
Hampton, Va. 23365

NATIONAL AERONAUTICS AND SPACE ADMINISTRATION • WASHINGTON, D. C. • OCTOBER 1970

1. Report No.	2. Government Accession No.
NASA TN D-5963	

4. Title and Subtitle

AN APPROACH-GUIDANCE METHOD USING A SINGLE ONBOARD OPTICAL MEASUREMENT

5. Report Date: October 1970

6. Performing Organization Code:

7. Author(s)

Harold A. Hamer and Katherine G. Johnson

8. Performing Organization Report No.: L-7053

9. Performing Organization Name and Address

NASA Langley Research Center
Hampton, Va. 23365

10. Work Unit No.: 125-17-06-05

11. Contract or Grant No.:

12. Sponsoring Agency Name and Address

National Aeronautics and Space Administration
Washington, D.C. 20546

13. Type of Report and Period Covered: Technical Note

14. Sponsoring Agency Code:

15. Supplementary Notes

16. Abstract

An empirical method has been developed for onboard guidance within the sphere of influence of a celestial body. For guidance maneuvers made at a relatively large distance from the body, only one preselected measurement from a star to the body is required. Although the method is designed to control the magnitude of the periapsis radius (or entry angle), the periapsis position and velocity automatically remain close to the nominal values. For lunar approach, error analysis with an assumed one-sigma error of 10 seconds of arc in the optical angular measurements and a one-sigma velocity-cutoff error of 0.2 m/sec has shown that perilune radius can be controlled to a one-sigma accuracy of from 7 to 13 km, depending on the time the approach guidance is performed.

17. Key Words (Suggested by Author(s))	18. Distribution Statement
Approach guidance Onboard navigation guidance Translunar trajectories	Unclassified – Unlimited

19. Security Classif. (of this report)	20. Security Classif. (of this page)	21. No. of Pages	22. Price*
Unclassified	Unclassified	80	$3.00

*For sale by the Clearinghouse for Federal Scientific and Technical Information
Springfield, Virginia 22151

AN APPROACH-GUIDANCE METHOD USING A SINGLE ONBOARD OPTICAL MEASUREMENT

By Harold A. Hamer and Katherine G. Johnson
Langley Research Center

SUMMARY

An empirical method is developed for onboard guidance within the sphere of influence of a celestial body. The procedure requires only limited onboard calculations and leads to approach-guidance predictions sufficiently accurate for emergency or backup operations. The method is applied to lunar-approach trajectories and is studied in detail for certain lunar missions.

The procedure relies heavily on use of precalculated data and is unique in that only a single angular measurement from the star to the moon is required, provided that it is made at or near the lunar sphere of influence. If the approach guidance is delayed to a time closer to the moon, an additional measurement of the subtended angle of the moon is required. The method is designed specifically to control the magnitude of the perilune radius, but the perilune position and velocity values automatically remain close to the nominal values. An error analysis with an assumed one-sigma error of 10 seconds of arc in the optical angular measurements and a one-sigma velocity-cutoff error of 0.2 m/sec has shown that the perilune radius can be controlled to a one-sigma accuracy of from 7 to 13 km, depending on the time the approach guidance is performed. The effects of maneuvering errors, star location, and empirical approximation errors on the approach guidance are discussed.

For manned flight, the required angular measurements can be readily made from onboard the spacecraft by a sextant-type instrument. For unmanned flight, the measurements can be made automatically by pointing the spacecraft (or tracker instrument) in a predetermined direction to a star and then sighting to the planet with a scanner-type instrument.

INTRODUCTION

In space missions the navigation and guidance is normally accomplished by automatic procedures which employ earth-based radar measurements. The inclusion of

procedures which utilize onboard measurements is a desirable feature, both for manned and unmanned flights. For example, in interplanetary flight, the planet ephemeris error can lead to unacceptable errors in the trajectory position relative to the planet when only earth-based measurements are used. This position error is most significant during the approach phase, that is, when the spacecraft is within the sphere of influence of the planet. Some type of onboard measurements relative to the planet may be required to correct this position error.

Over the years a number of studies have been made to develop onboard guidance procedures for controlling the approach to a celestial body. (For example, see refs. 1 to 6.) In general, these methods require several types of measurements and the measurements must be repeated a number of times. The guidance correction is ordinarily based on a statistical filtering technique which requires extensive calculations and computing equipment, and the methods may also require more than one guidance maneuver.

The method presented in this paper is unique in that only a single onboard position fix is required to determine the guidance correction. This fix is made at a chosen time and, when used in conjunction with some simple empirical approximations derived from two-body theory, is sufficient to control the periapsis magnitude with a reasonable degree of accuracy by using only one guidance maneuver. In this paper, the method is studied in regard to the approach phase of earth-moon trajectories, but it can also be applied to reentry control for moon-earth trajectories. (See ref. 7.) The method warrants investigation for application to interplanetary-trajectory control.

For guidance at or near the lunar sphere of influence, the only measurement required is the included angle between a star and the target body. If the approach guidance is made closer to the moon, a subtended-angle measurement is also required for determining the range. An analysis is included which shows that for acceptable accuracy, the star must be in a specified direction with respect to the nominal trajectory. The direction of this star and that of the guidance-velocity vector can be predetermined as can most of the calculations for deriving the magnitude of the guidance correction. These characteristics make the method particularly useful for manual operation.

The accuracy characteristics of the method are examined by means of a Monte Carlo error analysis. The analysis includes the effects of measurement error, thrust-cutoff error, and approximation error which is caused by assumptions in the empirical procedure. The results were obtained by use of the Jet Propulsion Laboratory n-body trajectory program. (See ref. 8.)

SYMBOLS

D	position deviation in direction of specified star
l,m,n	direction cosine of line of sight to star with respect to X-, Y-, and Z-axis, respectively
R	lunar radius
r	range to moon center
r_e	range to earth center
r_p	perilune radius
Δr_{mc}	incremental range to earth center at time of midcourse-position fix, $r_{e,a} - r_{e,n}$
Δr_p	incremental perilune radius, $r_{p,a} - r_{p,n}$
T	time from earth injection
T_p	time to nominal perilune time
T_{pf}	time of midcourse-position fix
Δt	time increment (appendix A)
V	vehicle velocity
V_p	perilune velocity
ΔV	guidance-velocity correction
x,y,z	position coordinates in Cartesian axis system in which X-axis is in direction of Aries, XY-plane is parallel to earth equatorial plane, and Z-axis is in direction of north celestial pole
$\dot{x},\dot{y},\dot{z}$	velocity coordinates in Cartesian axis system

x_r, y_r, z_r	position coordinates in rotating Cartesian axis system in which X_r-axis lies along earth-moon line, X_rY_r-plane is in earth-moon plane, and Z_r-axis is in northerly direction
α	semisubtended angle of moon
β	angle between nominal range vector and major axis of position-error ellipsoid
γ	flight-path angle
δ	angle formed at vehicle between line to star and its projection in the instantaneous earth-moon-vehicle plane
ϵ	eccentricity of orbit (appendix C)
ζ	angle between nominal velocity vector and major axis of velocity-error ellipsoid
θ	included angle between star and celestial-body center
θ_1, θ_2	angular measurements used for determining α and θ
Θ	angle formed at vehicle between line to moon center and projection of line to star in the instantaneous earth-moon-vehicle plane
λ	angle between approach-guidance-velocity vector and vehicle-velocity vector
μ	product of universal gravitational constant and mass of moon
σ	standard deviation or root-moon-square value
φ	true anomaly
ψ	in-plane angle between second midcourse $\overline{\Delta V}_S$ and $\overline{V}_n$
$\|\|$	absolute value

Subscripts:

A	value immediately following approach-guidance correction
a	actual
add	additional approach-guidance velocity to account for second midcourse manuever
D	position deviation
F	first midcourse correction
m	measured value
n	nominal value
R	moon radius
r	range to moon center
r,mc	range to earth center at time of midcourse-position fix
r,p	perilune radius
S	second midcourse correction
s	position deviation from nominal trajectory, $\left[(x_a - x_n)^2 + (y_a - y_n)^2 + (z_a - z_n)^2\right]^{1/2}$
u	velocity deviation from nominal trajectory, $\left[(\dot{x}_a - \dot{x}_n)^2 + (\dot{y}_a - \dot{y}_n)^2 + (\dot{z}_a - \dot{z}_n)^2\right]^{1/2}$
V,p	perilune velocity

α semisubtended angle of moon

θ star-to-body angle

A bar over a symbol indicates a vector.

BASIC METHOD

Synopsis

The approach-guidance procedure presented herein is designed to correct perilune-magnitude error. The direction of the approach-guidance velocity correction is preset; the manuever can be applied at any preselected time within the lunar sphere of influence. The direction in which the correction is usually applied is perpendicular to the nominal velocity vector and in the orbital plane. This direction is essentially optimum for most distances from the moon.

Midcourse guidance.- The approach-guidance procedure is an outgrowth of the onboard midcourse-guidance procedure developed in reference 9 and is designed to correct errors resulting from the use of this type of midcourse guidance. In practice, the midcourse guidance would be required to correct the actual trajectory in order to remove perturbations due to errors attributed to injection and other sources. To reduce the amount of analysis required for this paper only one such perturbed trajectory was employed for most of the approach-guidance analysis. Some data, however, are given to show that the approach-guidance method is capable of handling a family of trajectories originating from a wide range of injection errors. The injection errors considered were essentially spherically distributed and had one-sigma values of roughly 3 km in position and 3 m/sec in velocity. These perturbations are relatively large with respect to present-day values. (For the smaller injection errors associated with normal operation, the onboard approach guidance could be used in lieu of any other type of midcourse guidance.)

A fixed-time-of-arrival law was used for the onboard midcourse guidance. (See ref. 9.) The aim point was selected at the lunar sphere of influence. The first midcourse maneuver was performed at 10 hours from injection for 70-hour translunar trajectories and at 15 hours for 90-hour translunar trajectories, the position fix being taken 1/2 hour before the maneuver. These trajectories span the range of reasonable trip times. Because the first midcourse maneuver corrects only for the position error at the aim point, a second midcourse maneuver is normally required at the aim point to correct the spacecraft-velocity vector back to the nominal vector.

Approach guidance.- The approach-guidance method is empirical in nature and most of the calculations are preflight calculations. In these calculations the guidance-velocity requirements are developed from two-body relationships, wherein a closed-form expression relating perilune and upstream conditions can be written. These conditions can be related to deviations from the nominal trajectory. The deviations can be determined by simple onboard optical angular measurements.

Results obtained from Monte Carlo samples of trajectories perturbed at first midcourse are used to show that within the sphere of influence, the position deviation in a certain direction predicts the perilune radius and perilune velocity with relatively high accuracy. The guidance velocity required to correct the perilune radius is then determined empirically as a function of this deviation. It is this precalculated variation which the navigator employs for the onboard approach guidance. The only onboard calculation required is the simple computation of the deviation by use of the measured and nominal values of the onboard measurements.

Errors considered in guidance procedures.- The random perturbations after first midcourse were assumed to be caused by onboard measurement error alone; the effect of maneuvering errors would be negligible. At second midcourse the effect of measurement error was considered, inasmuch as this maneuver is derived from the first midcourse measurements. Although small, the effect of velocity-cutoff error was included in the second midcourse correction. Because of the relatively small second midcourse correction required, the effect of error in the pointing direction was neglected. In the approach-guidance procedure, types of errors considered were: measurement errors, velocity-cutoff errors, and approximation errors caused by use of the empirical procedure. The effect of approximation error in the midcourse guidance is essentially eliminated by the approach guidance. It should be noted that n-body trajectories are used throughout this paper in developing the method and in performing the error analyses.

General Considerations

The onboard midcourse-guidance procedure of reference 9 reduces the error at the aim point significantly; however, the remaining errors must be reduced further by means of some type of approach guidance. The approach-guidance procedure presented herein proposes to correct such errors resulting from the use of this type of midcourse guidance. Some typical errors resulting from the midcourse procedure are shown in figure 1. The data are shown for two magnitudes of range-measurement error inasmuch as this error has a predominant effect on the aim-point accuracy. The range of aim points covered includes all points from the sphere of influence to perilune.

The accuracy characteristics of the approach-guidance procedure are dependent upon the errors associated with the midcourse procedure. As previously stated, the

maneuvering errors at midcourse are negligible compared with the measurement errors made in estimating the required midcourse correction. The measurements include a range determination and three star-to-body angles. Details of the midcourse procedure can be found in reference 9. The facts pertinent to the present study are that the predominant measurement errors and the position-determination errors are generally in the direction of the vehicle-velocity vector. Hence, the midcourse-guidance error is essentially an error in the magnitude of ΔV rather than in its direction and can be accurately controlled in the approach-guidance procedure. As an example of the midcourse-guidance errors, one-sigma values along the three axes of the error ellipsoid relating to the covariance matrix of midcourse-velocity errors are 1.38, 0.505, and 0.226 m/sec. These magnitudes pertain to the data shown in figure 1 for range-measurement error $\sigma_{r,mc}$ = 22 km. The values signify that the error at first midcourse is predominantly along the major axis of the ellipsoid; the angle between the major axis and the spacecraft-velocity vector is about 2^{o} in this case.

Thrust Assumptions

In the approach-guidance procedure, the thrust is considered to be impulsive in effect; that is, the burning time is negligible relative to the trajectory time scale. The impulsive correction is assumed to be applied in a constant direction in the nominal plane of motion at initialization of the thrust maneuver. Unless otherwise noted, the velocity-correction vector is perpendicular to the nominal velocity vector. Except for the effect of engine-cutoff error, the guidance correction is assumed to be perfectly executed. These assumptions are all appropriate inasmuch as their effect on the overall results is negligible. Finally, a high-thrust device for implementing the approach-guidance maneuver is assumed.

Approach-Guidance Procedure

The approach guidance can be applied at a predetermined time anywhere within the lunar sphere of influence. Most of the required calculations are performed before the flight by using information on the nominal trajectory. In regard to the midcourse procedure, the approach guidance must be applied at or beyond the aim point where the second midcourse maneuver is made. These two maneuvers can be conveniently combined even though in practice some time is required to make the simple approach-guidance measurements and calculations. A delay of several minutes in the guidance does not appreciably affect the overall accuracy of the system. Longer delays, if necessary, can easily be taken into account in the procedure.

Measurement equations.- The approach-guidance procedure is based on the determination at a given time of the deviation of the trajectory in position from the nominal trajectory. (See fig. 2.) As will be shown, for a strong correlation with the perilune conditions r_p and V_p, the deviation must be measured in a predetermined direction to a specified star. From the figure, the deviation D is given by

$$D = r_m \cos \theta_m - r_n \cos \theta_n \tag{1}$$

where r_n and θ_n are nominal values. Normally, two measurements are required: the range to the moon r_m and the angle θ_m included between the star and the center of the moon. In this paper, the range is assumed to be measured by the semisubtended angle α (that is, $r = R/\sin \alpha$ where R is the known radius of the moon). The two measurements must be referenced to a common time. Since it may not be possible to make simultaneous measurements, a method for updating the measurements is given in appendix A. As will be pointed out, θ_n at the sphere of influence should be approximately 90^o, in which case the effect of error in range is negligible and

$$D \approx r_n\left(\cos \theta_m - \cos \theta_n\right) \tag{2}$$

Thus no range measurement is required.

Guidance-velocity determination.- As previously stated, there is a strong correlation between the deviation D, taken in a certain direction, and the perilune conditions r_p and V_p. This correlation is shown in figure 3. In this figure, D is determined at a time near the sphere of influence and the measurement star is in the nominal orbital plane and perpendicular to the nominal range vector to the moon. The trajectories A and B are perturbed differently at injection; trajectory A resulted in a Δr_{mc} of -419 km at the time of the first midcourse-position fix, whereas trajectory B resulted in a Δr_{mc} of -1287 km. In both cases, the velocity-error vector was about 17.5^o from the vehicle-velocity vector; for trajectory B the position-error vector was about 79.5^o from the vehicle-position vector. Each data point in figure 3 represents the result caused by random measurement errors in correcting the trajectories at midcourse. Trajectory results are shown for two magnitudes of range-measurement error. The smoothness of the data for the two trajectories indicates that the approach-guidance accuracy would be insensitive to the magnitude of injection error.

The strong correlation between D and the perilune conditions is a clue that D can be used empirically to determine the guidance-velocity correction required to attain the desired perilune radius. The equation which relates the approach-guidance-velocity magnitude to the conditions at perilune, and hence to the deviation D is as follows:

$$\Delta V = \frac{V\left[r^2 \cos\gamma \cos(\gamma + \lambda) - r_{p,n}^2 \cos\lambda\right]}{r_{p,n}^2 - r^2 \cos^2(\gamma + \lambda)} \pm \frac{r_{p,n}\left\{\left(r^2 - r_{p,n}^2\right) V^2 \sin^2\lambda + \left[r^2 \cos^2(\gamma + \lambda) - r_{p,n}^2\right]\left(\frac{2\mu}{r_{p,n}} - \frac{2\mu}{r}\right)\right\}^{1/2}}{r_{p,n}^2 - r^2 \cos^2(\gamma + \lambda)} \tag{3}$$

where

$$\cos\gamma = \frac{r_p V_p}{rV} \tag{4}$$

The equation was derived from the principle of conservation of angular momentum, as shown in appendix B. This equation is not used by the navigator onboard the spacecraft, but it is used in a preflight analysis to determine the variation of ΔV with D.

In the equation, λ is the angle between the ΔV vector and the vehicle-velocity vector, which is a predetermined value; γ is the flight-path angle. The quantities r and V are the values of range and velocity for the perturbed trajectory at the time of the approach correction. The quantity $r_{p,n}$ is the nominal or desired perilune radius, whereas r_p and V_p are the values of perilune radius and perilune velocity of the perturbed trajectory. The values of $r_{p,n}$ and λ are constant. For a given time, changes in r and V do not significantly affect ΔV; the variables r_p and V_p are the main contributors of ΔV. These variables, in turn, are dependent upon γ as is seen in equation (4).

Star direction.- For the approach-guidance method the star must be in a given direction with respect to the nominal trajectory, and it is not necessary that the variations such as those shown in figure 3 be linear. The approach-guidance accuracy is closely related to the amount of scatter in the perilune-radius predictions; hence, it is imperative that the scatter be kept to a minimum. Examples of scatter for various directions of the deviation D at $T_p = 14.617$ hours are shown in figure 4. It is obvious that minimum scatter is obtained for a deviation (star measurement) in or near the nominal orbital plane and approximately perpendicular to the nominal range vector. The instantaneous nominal earth-moon-vehicle plane is used as the reference plane since it is within 0.667° of the selenocentric orbital plane of the spacecraft.

Figure 5 presents data for various times within the sphere of influence. (Note the staggered vertical scale. The scale should be read so that in all cases the curve at $D = 0$ would pass through the nominal value of r_p, which is roughly 3404 km.) In

figure 5(a) examples are shown where the nominal θ is held constant; that is, the direction of the star is always perpendicular to the nominal range vector at the corresponding time T_p. The direction of the star changes from case to case, and the scatter becomes unacceptable as the approach-guidance measurement is delayed to times near the moon. The characteristics of the scatter in figure 5(b) show that the optimum direction of the star does not change with time. The indicated change in the true anomaly depicts the angle through which the range vector rotates and hence the change in the nominal value of θ with time. For example, at $T_p = 14.617$ hours, θ_n would be 90^o; whereas at $T_p = 4.617$ hours, θ_n would be about 80^o (or 100^o). It is apparent from figure 5(b) that regardless of the time that the measurement is made, the star must be in a direction perpendicular to the nominal range vector at the sphere of influence. This direction is illustrated in figure 2.

The optimum direction of the star is apparently in the orbital plane and perpendicular to the nominal range vector at the sphere of influence. The characteristics of the scatter in figure 6 show that the star can be as much as 2^o away from the optimum direction and still give adequate accuracy. Although it is not shown, an in-plane displacement from the perpendicular direction much greater than 2^o would not be acceptable. Note the amount of scatter in figure 4(c) for which the displacement is about 9.5^o. Out-of-plane displacement up to at least 30^o does not appreciably affect the accuracy insofar as scatter is concerned; however, it does affect the measurement sensitivity as shown in figure 7.

From the sketch in the upper part of figure 7, it can be determined from the right spherical trigonometric relationship

$$\cos \theta = \cos \Theta \cos \delta$$

that

$$\frac{d\theta}{d\Theta} = \left(\frac{\cos^2 \delta - \cos^2 \theta}{1 - \cos^2 \theta} \right)^{1/2}$$

where $\frac{d\theta}{d\Theta}$ could be called the measurement-sensitivity factor. For a star direction perpendicular to the orbital plane, this factor is zero; this statement means that a measurement in this direction gives no indication of the in-plane trajectory deviation, which is essential for controlling the magnitude of r_p. (The out-of-plane deviation would be important for methods which control the location of r_p.) Inasmuch as figure 5 shows that the nominal value of θ changes with time T_p, the data in figure 7 are shown for a change of $\pm 10^o$. This amount of change shows little or no effect on the sensitivity factor. It is seen in figure 7 that an out-of-plane displacement of 30^o has only about 10-percent effect on the sensitivity.

Optimum direction and time of ΔV.- For guidance made within the lunar sphere of influence, the optimum direction of the ΔV vector is in the orbital plane and essentially perpendicular to the nominal velocity vector. This condition is illustrated in figure 8 which is an example of the correction of one perturbed trajectory which had a position error of 271 km at the sphere of influence (T_p = 14.617 hr). Note that close to the moon (T_p = 2.617 hr), the optimum direction for ΔV is about 80^o; however, the change in ΔV from that at $\lambda = 90^o$ is negligible. Also, as expected, the figure shows that for minimum fuel requirements, the optimum time for the guidance maneuver is at the sphere of influence. The increase in fuel requirements as the maneuver is delayed to times closer to the moon is also illustrated in figure 9. The variation shown applies to the energy level of the translunar trajectory shown in figure 10 and is only approximate because it was determined for one particular perturbed trajectory. However, for any other perturbed trajectory, the values would not differ appreciably from those shown in figure 9.

Except where otherwise stated, the nominal translunar trajectory illustrated in figure 10 was employed throughout the analysis. The trajectory required 70 hours and 37 minutes to reach perilune; it is plotted in a rotating-axis system to show the relative positions of the earth, moon, and vehicle at any given time.

Preflight analysis.- Again, it should be stated that the perturbations of r_p and V_p from their nominal values are the principal contributors to the approach-guidance ΔV magnitude. Inasmuch as r_p and V_p are functions of the deviation D (see fig. 3), these quantities can be used to determine the approach-guidance correction ΔV as a function of D. Determination of this relationship can be made before flight which means that the navigator need measure only the angles necessary to calculate D in order to determine the velocity correction required.

The preflight procedure employed for determining ΔV as a function of D can be stated as follows:

(1) By use of an n-body trajectory program, a number of perturbed trajectories (for example, 50) are generated from the point of the first midcourse correction to perilune, the perturbations being chosen randomly, based on the covariance matrix of errors after the first midcourse correction. During this process the second midcourse correction is applied at the aim point, no errors in execution being assumed. Actually, at midcourse the trajectories can be randomly perturbed about the nominal rather than around any or all trajectories perturbed by injection error; the effects would be the same in either case, as indicated in figure 3. Perturbing trajectories about the nominal eliminates the tedious task of generating a random sample of perturbed injection trajectories. This procedure also eliminates one step in the error analysis, that of having to account for the second midcourse maneuver. The small errors at second midcourse due to the perturbations at first midcourse would remain; however, their effect is negligible.

(2) For each such trajectory, the deviation D at the time of the approach-guidance maneuver is computed and r_p and V_p are recorded. By using these data, r_p and V_p are plotted as functions of D as in figure 3, and a curve is faired through the points. For onboard determination, D is calculated by equation (1) or (2); however, for preflight analysis, D can be calculated from the equivalent equation

$$D = l(x_a - x_n) + m(y_a - y_n) + n(z_a - z_n)$$

(3) For each value of D, corresponding values of r_p and V_p are read from the faired curves. From these values of r_p and V_p along with the corresponding values of r and V at the time of the approach guidance, a value of ΔV is computed by using equation (3) to yield a point ΔV,D. The resulting plot of ΔV as a function of D is used by the navigator to determine the required approach-guidance correction.

Results of the foregoing preflight procedure are shown in figures 11 to 14 for several trajectories and times of approach-guidance measurement. Figure 11 presents the variation of perilune radius with the deviation D. For all cases hereinafter, the deviation is in the nominal orbital plane and in a direction perpendicular to the nominal range vector at the lunar sphere of influence. The deviations are determined for the times T_p in the figures. The first three parts of figure 11 pertain to the 70-hour translunar trajectory illustrated in figure 10, the two different nominal values of r_p being obtained by slightly changing the earth-injection conditions. Figure 11(d) applies to a 90-hour translunar trajectory. The slope of the curve in this figure is reversed because this trajectory is designed for counterclockwise motion about the moon.

In the prediction of perilune radius by D, the scatter gives a good indication of the approach-guidance accuracy. Inspection of the plots for the various conditions shows that the scatter is not materially affected by the type of trajectory or the time of guidance measurement T_p. It can be noted in figure 11(c), however, that the scatter increases for perturbed trajectories falling below the lunar surface. Also, the variation in this figure is more nonlinear than in the other parts of figure 11; however, this nonlinearity has no effect on the guidance accuracy. The scatter in figure 11(d) is somewhat conservative in that it indicates more error than would ordinarily be obtained in practice. The extra scatter is due to the manner in which the midcourse-velocity errors were applied as discussed in the section "Approach-Guidance Accuracy Characteristics."

Figure 12 presents corresponding data on the variation of perilune velocity with the deviation D. It should be stated that the scatter for this quantity is not as important to the guidance accuracy as that for perilune radius. (Here again, in fig. 12(d), the slope is reversed because of the change in direction of the trajectory about the moon.)

Since flight-path angle appears in the preflight calculation of ΔV (eq. (3)), comparison was made between the two-body value of γ as calculated from r_p and V_p (eq. (4)) and the actual value determined directly in the n-body trajectory program. The results are shown in figure 13, where γ and D are given for the time near the lunar sphere of influence (T_p = 14.617 hr). The two-body data are relatively smooth because they were determined from the faired r_p and V_p curves in figures 11(a) and 12(a). The difference of about 0.7^o between the two curves is due to two-body approximation. This difference makes it imperative to use equation (4) to calculate γ for determining the ΔV, inasmuch as ΔV was derived from two-body theory.

Figure 14 presents corresponding data on the variation with the deviation D of approach-guidance velocity as determined from the r_p and V_p values in figures 11 and 12. As previously stated, this variation is calculated by a preflight analysis of a number of perturbed trajectories; thus, the onboard computation of ΔV is eliminated. The signs for ΔV merely indicate whether the guidance-velocity pointing angle λ is 90^o or -90^o. Except for the angular measurements needed to calculate D, the variation of ΔV with D is the only information required by the navigator. For the trajectory of figure 14(d), the plot shows an error in ΔV of 0.3 m/sec at $D = 0$. The effect of this error, which may be due to the two-body approximation, can be corrected by merely offsetting the curve by 0.3 m/sec.

The data in figure 14 are relatively smooth because faired values of r_p and V_p were used. The data of figure 15, however, were derived by using actual or unfaired values of r_p (fig. 11(a)) and V_p (fig. 12(a)) to determine ΔV; the scatter shown in this figure represents the velocity-correction error that would occur in practice because of the approximation. The deviation applies to a measurement time at the lunar sphere of influence (T_p = 14.617 hr); the dashed line, determined from data of figure 9, represents the ΔV requirement 5 hours after the time of measurement.

Theoretical Considerations

Error characteristics.- Position- and velocity-error ellipsoids representing characteristics of trajectory errors within the lunar sphere of influence due to onboard midcourse-guidance error are shown in figures 16 to 19. The guidance error is primarily due to a measurement error. Figure 16 gives the length of the axes of the position-error ellipsoid. The major axis is much greater than the other axes; hence, its direction may be considered to be representative of the direction of the position errors. The orientation of the major axis is shown in figure 17. In the upper plot, it is noted that the major axis lies always within 5^o of the orbital plane. This feature provides the capability for determining the approach-guidance requirement by using only one star measurement.

The characteristics of the velocity-error ellipsoid are shown in figures 18 and 19. For figure 19, the major axis of the velocity-error ellipsoid is generally within 1° of the orbital plane. It can be seen in figure 19 that the error in the direction perpendicular to the velocity vector would be generally as large as the error along the velocity vector. It is the error in the perpendicular direction that has an effect on the perilune radius. As shown in figure 1, this velocity error can be several meters per second. Hence, it must be concluded that this error is correlated with D in order for the approach-guidance procedure to perform so well.

Derivation of guidance relationships.- Attempts were made in the study to derive the relationship r_p/D; however, no theoretical derivation was found. The only procedure shown thus far for determining the relationship between r_p and D is by generating a sample of trajectories randomly perturbed at first midcourse. This method requires calculations for a large number (for example, 50) of trajectories. In order to circumvent this problem, the following semiempirical procedure was developed for determining the variation of r_p with D; typical results are shown in figure 20.

First, several magnitudes of D were arbitrarily selected, as shown by the symbols in figure 20. These values were then converted to magnitudes in the direction of the major axis of the position-error ellipsoid by dividing D by $\sin\beta$. (See fig. 17.) The direction cosines of the major axis were then used to obtain the change in the x, y, and z selenocentric position coordinates for the various points. The change in the vehicle velocity (error) for the various points was determined from the ratio of σ_u/σ_s in figure 1. For example, for T_p of 14.617 hours, this ratio is 0.0074 $\frac{m/sec}{km}$. The change in the nominal velocity vector was obtained by putting this error in the direction of the major axis of the velocity-error ellipsoid. (See fig. 19.) For the nominal trajectory used (fig. 10), which corresponds to clockwise motion about the moon, the selenocentric velocity magnitude should be reduced for positive values of D and increased for negative values of D. This procedure would be reversed if the star direction were opposite to that in figure 2.

For the semiempirical method, one needs the covariance matrix of midcourse errors and a knowledge of the pertinent error ellipsoids. This knowledge is obtained from trajectory-error-propagation programs by propagating the covariance matrix of the midcourse-guidance errors along the nominal trajectory. The orientation and shape of the error ellipsoids can be determined by simple matrix manipulation. (For example, see ref. 9.) The semiempirical method is only approximate because of the use of the major axes of the error ellipsoids to represent position- and velocity-error characteristics and because of the nonlinearity effects in propagating covariance matrices. The method, however, compares closely with the actual results, as shown in figure 20.

Appendix C contains several equations for calculating the ratio $\Delta(\Delta V)/\Delta r_p$. Figure 21 presents actual data for this variation. Comparisons of actual and theoretical values given in figures 21(a), 21(b), and 21(d) show the equations to be very accurate. The theoretical expressions may be useful for various approach-guidance procedures in which r_p is determined by some quantity other than D. (For example, in ref. 4, perilune radius is determined from measurements of the orbital angular velocity and body subtended angle.) It is of interest to note that the variation is extremely linear for maneuvers made near the moon, (fig. 21(b)) and for trajectories designed to pass near the moon (fig. 21(c)).

Combination of maneuvers.- The foregoing figures correspond to the case where the approach-guidance maneuver is made after the second midcourse maneuver. Analysis of trajectories for which the aim point (time of second midcourse maneuver) was selected to be at nominal perilune time has shown that the approach-guidance procedure cannot be used without a second midcourse maneuver. Hence, the midcourse aim point must be chosen to be at or prior to the time of the approach-guidance measurements. The second midcourse maneuver can be conveniently combined with the approach-guidance maneuver, inasmuch as ΔV_S is approximately linear with Δr_{mc} and its direction is roughly the same for any injection error, as shown in figures 22 and 23, respectively. Each symbol represents a different perturbed trajectory due to injection error. Figure 22 represents position- and velocity-injection errors up to 10 km and 10 m/sec, respectively, and pertains to an aim point at $T = 56$ hours ($T_p = 14.617$ hr). For these values, the figure shows that ΔV_S can be predicted by Δr_{mc}, the range measurement at first midcourse. For position errors much higher than 10 km the scatter would become excessive. Figure 23 shows the precise in-plane angles of the second midcourse-guidance-velocity vector for the different perturbed trajectories. The angles are given with respect to the nominal velocity vector of the spacecraft and are shown to be roughly the same, especially at the larger values of Δr_{mc} where the magnitude of ΔV_S is relatively large. The degree of scatter shown in the figure is not significant; therefore, an average value can be used. The dispersions in the out-of-plane direction are even less than those shown in figure 23.

The linear results of figure 24 were determined from each of the perturbed trajectories by applying the faired ΔV_S values of figure 22 at an average angle of 15^o from the nominal velocity vector. Figure 24, in effect, shows the change in perilune radius due to the second midcourse velocity ΔV_S. Even though $\overline{\Delta V_S}$ would ordinarily be applied at angles ranging from about 10^o to 35^o (fig. 23), the small amount of scatter shown in figure 24 indicates that the perilune radius can be effectively corrected when ΔV is applied at a constant angle. Hence, the direction of $\overline{\Delta V_S}$ can be converted to a direction perpendicular to $\overline{V}_n$ with little loss in accuracy.

To include the effect of $\overline{\Delta V_S}$ in the approach ΔV magnitude, which is in a perpendicular direction, the following equation is used:

$$\frac{\Delta V_{add}}{\Delta r_{mc}} = \left(\frac{\Delta r_p}{\Delta r_{mc}}\right)\left(\frac{\Delta(\Delta V)}{\Delta r_p}\right)$$

where $\Delta r_p/\Delta r_{mc}$ is obtained from figure 24 and $\Delta(\Delta V)/\Delta r_p$ from figure 21(a). In this case

$$\frac{\Delta V_{add}}{\Delta r_{mc}} = -0.065 \times 0.0200 = -0.0013 \ \frac{m/sec}{km}$$

The quantity ΔV_{add} is an additional increment in the approach-guidance velocity and is added to $\overline{V}$ in the manner indicated in appendix B. In order for the navigator to include the effect of $\overline{\Delta V_S}$ in the approach-guidance maneuver, only a knowledge of the range measurement at first midcourse is required. It should be emphasized that if $\overline{\Delta V_S}$ is not applied in this manner, it must be applied prior to the approach guidance, inasmuch as no correlation exists between the deviation D and $\overline{\Delta V_S}$.

APPROACH-GUIDANCE ACCURACY CHARACTERISTICS

In this section, the errors associated with the approach-guidance procedure are defined and analyzed. The analysis covers the range from the lunar sphere of influence to a point near the moon. It is assumed that there are no errors in the onboard calculations due to human limitations.

Effect of Approximation Error

Table I summarizes the amount of perilune-magnitude error due to scatter for the various conditions illustrated in figures 11(a) to 11(d). This scatter error is an approximation error due to assumptions in the empirical approach-guidance procedure and is essentially the standard deviation of the difference between the data points and the faired line in each plot. The standard deviations given in the table, however, were obtained from a Monte Carlo analysis; that is, for each perturbed trajectory the faired value of ΔV was added to the corresponding $\overline{V}$ and the trajectory propagated to perilune.

Conditions 1 and 2 differ only in the value of V used in calculating the guidance velocity (eq. (3)); as indicated, this difference has little effect on the guidance accuracy. Comparison of conditions 1 and 3 shows that the second midcourse correction can be combined with the approach-guidance maneuver with no loss in accuracy. Comparison of conditions 2 and 4 shows that the error due to scatter decreases as the approach-guidance

measurement is delayed to times closer to the moon. As the nominal perilune is lowered (condition 5), the scatter error increases.

As previously stated, the results for condition 6 are conservative because of the manner in which the midcourse errors were simulated for this translunar trajectory. The errors were more nearly spherically distributed than would occur in practice from onboard midcourse measurements and lead to a higher inaccuracy in the approach-guidance procedure. In this case, the one-sigma values along the three axes of the error ellipsoid were 1.45, 1.11, and 0.168 m/sec. These values signify that the errors in the direction of the major and mean axes are roughly the same, and, in addition, the angle between the major axis and the spacecraft-velocity vector is about 83°. Figure 25 is an example of the approach-guidance scatter error for the 70-hour translunar trajectory with an approximate spherical distribution of velocity errors in the midcourse guidance application, which might occur in certain types of midcourse procedures. The error distribution was obtained by incorporating errors at midcourse in each of the three components of the spacecraft nominal velocity. The errors were applied by including permutations of 0, ±1, and ±2 m/sec. For figure 25, $\sigma_{r,p} = 25.6$ km, which, for all practical purposes, represents the absolute maximum scatter error for controlling approach trajectories by the present method.

As a matter of interest, the scatter errors for some of the parameters at perilune are shown in table II. The off-nominal position and velocity deviations are σ_s and σ_u, respectively. The value $\sigma_{V,p}$ represents a change in the perilune-velocity magnitude; σ_u corresponds to changes in the three components of velocity (that is, to a change in the direction of the velocity vector). The reason for the large difference between these two values is evident in figure 19 which shows that the velocity errors at perilune are generally in a direction 90° from the velocity vector.

It is interesting to note that if perfect midcourse guidance is applied to the highly perturbed trajectory referred to in figure 3, the perilune-magnitude error is approximately 25 km. This error is caused by the linear approximation made in using transition matrix theory. As indicated by one-sigma perilune errors listed in table I, the approach-guidance method corrects a large part of this error.

Effect of Measurement Error

One important effect on the approach-guidance accuracy is caused by the error in the required onboard measurements. The measurement-error equations are developed in appendix D. The nominal values of the measurement angles are given in figure 26 as a function of time to perilune. Also shown is the nominal variation of range to the moon. The change in the angle from the star to the moon results from the fact that the optimum star-measurement direction does not change as T_p decreases.

Figure 27 presents results on the effect of measurement error and the combined effect with approximation (scatter) error. The analysis pertains to a nominal 70-hour translunar trajectory with a perilune radius of 3403.6 km; however, the results would be about the same for other trip times and perilune radii. In the upper plot of figure 27, the solid curve shows the variation of σ_r, the one-sigma error in determining range by measuring the subtended angle of the moon. (See eq. (D3).) The one-sigma error in measuring the semisubtended angle was assumed to be 10 seconds of arc. The dashed curve shows the range-determination accuracy when the nominal value for range at the corresponding time is used; that is, the range is not measured. The error caused by using the nominal value is given by

$$\sigma_r = \sigma_s \cos \beta$$

where the position error σ_s is obtained from figure 1 and the angle β is given in figure 17. As noted in the upper plot of figure 27, the dashed curve applies to trajectories with a fairly small midcourse-measurement error $\sigma_{r,mc} = 10$ km. For $\sigma_{r,mc} = 20$ km, the values for the dashed curve would approximately double, and so on. The effect of the larger midcourse-measurement errors is shown by the other dashed curves in figure 27.

The quantity σ_D is the one-sigma error in the deviation D due to the measurement errors σ_r and σ_θ. The curves for σ_D were obtained from equation (D2) by using values of σ_r from the upper plot by assuming $\sigma_\theta = 10$ seconds of arc. As indicated in the lower plot of figure 27, the different dashed lines correspond to cases where $r_a \doteq r_n$ for three families of trajectories caused by different magnitudes of midcourse-measurement error.

The data points shown for $\Delta r_p/\Delta D$ were obtained from figure 5(b). This ratio is used to determine the effect of measurement error on the perilune-radius accuracy:

$$\sigma_{r,p} = \frac{\Delta r_p}{\Delta D} \sigma_D$$

The data points for the effect of scatter error were obtained from table I.

The lower plot in figure 27 shows the perilune-radius error due to the combined effects of measurement and scatter error as determined by

$$\sigma_{r,p} = \left[\left(\frac{\Delta r_p}{\Delta D} \sigma_D \right)^2 + \left(\sigma_{r,p} \right)^2_{\text{scatter}} \right]^{1/2}$$

It can be seen from the various plots that the effect of approach-guidance measurement error is small in comparison with that of scatter error. In fact, doubling the measurement error would not increase $\sigma_{r,p}$ significantly. For the solid line in the lower plot of figure 27, the approach-range measurement is included, and, consequently, the magnitude of the midcourse-range-measurement error $\sigma_{r,mc}$ is insignificant. If the guidance measurements are made at distances relatively far from the moon, the range measurement does not substantially improve the approach-guidance accuracy, especially for low values of $\sigma_{r,mc}$. Actually, at the sphere of influence where the nominal value of θ is 90^{o}, the range-determination error has no effect on the approach-guidance accuracy. (See appendix D.) Also, if approach-guidance measurements are made closer to the moon, the nominal value of θ at the sphere of influence may vary by several degrees with no increase in scatter error. (See fig. 6.) For example, from figure 26, it can be seen, that if θ_n at $T_p = 14.617$ hours were 88^{o} or 92^{o}, the time at which no range measurement would be required ($\theta_n = 90^{o}$) would be shifted by about 4 hours.

Effect of Maneuvering Error

The effect of approach-guidance maneuvering errors on the perilune-radius accuracy was examined. (See figs. 28 and 29.) Since maneuver timing error represents error in the direction of range, it is considered to be negligible, especially at or near the sphere of influence where the range error has no effect. In fact, timing error need not be considered in any type of onboard guidance procedure inasmuch as errors of 1 or 2 minutes applied to the midcourse procedure of reference 9 lead to aim-point errors of only several kilometers.

Pointing error.- The effect of pointing-direction error is shown in figure 28. No statistical analysis was performed; rather, the individual effects of the in-plane and out-of-plane components of this error were determined. The plane referred to is the instantaneous nominal earth-moon-vehicle plane which is essentially the selenocentric orbital plane of the vehicle. The data were calculated for only one perturbed trajectory, but are representative of any perturbed trajectory. The results indicate that the effect of pointing error can be considered to be negligible; that is, errors of several degrees would have no great effect on the approach-guidance accuracy when the nominal λ is selected as 90^{o}.

Velocity-cutoff error.- Inasmuch as the approach-guidance ΔV magnitude is relatively low, especially near the lunar sphere of influence (fig. 15), the effect of guidance-velocity-cutoff error was investigated statistically and is shown in figure 29. The guidance-velocity-requirement curve in the upper plot used in determining this effect is taken from figure 9.

The curve showing the effect of cutoff error on the perilune-radius error was determined from the inverse of the velocity requirement by the following equation:

$$\sigma_{r,p} = \frac{\Delta r_p}{\Delta(\Delta V)}\left(0.2 \times 10^{-3}\right) \tag{5}$$

where the value 0.2 is the one-sigma error, in meters per second, assumed in cutoff velocity.

The lower plot in figure 29 shows the variation in the overall error in perilune radius with time of terminal-guidance measurement, as determined by the equation

$$\sigma_{r,p} = \left[\left(\sigma_{r,p}\right)^2_{\text{cutoff}} + \left(\sigma_{r,p}\right)^2_{\text{scatter}} + \left(\frac{\Delta r_p}{\Delta D}\sigma_D\right)^2\right]^{1/2}$$

In general, 40 percent of the error is attributed to each of the first two sources and the remaining 20 percent to the measurement error. The cutoff error in figure 29 applies when $\lambda = 90^o$. Application of the ΔV vector at other values of λ (fig. 8) reduces the effect of cutoff error as is shown by equation (5). Another error in the guidance-velocity magnitude, called the proportional error, is a small constant percentage of ΔV and was found to be negligible.

The effect of a cutoff error of 0.2 m/sec was also determined for some of the other quantities at perilune for condition 2 given in table II. The effect was to increase $\sigma_{V,p}$ from 1.99 to 2.90 m/sec and to increase σ_s and σ_u to only 27.20 km and 11.40 m/sec, respectively.

With respect to times near the sphere of influence, the perilune-radius error can be reduced by about one-half if approach guidance is delayed to 5 hours from the moon. The fuel requirements, however, will be tripled, as shown by the upper plot in figure 29.

Effect of Ephemeris Error

Even though the lunar ephemeris error is very small (1 or 2 km), its effect on the approach-guidance accuracy was examined. Larger ephemeris errors were included to give some indication of the effect on the approach-guidance procedure when controlling interplanetary trajectories. Ephemeris error affects the accuracy of the guidance procedure because the guidance measurements are referenced to a nominal trajectory which, in turn, is based on a certain location of the moon. This type of error was introduced into the procedure by changing the ephemeris of the moon in the n-body trajectory program. In figure 30, it is seen that the approach-guidance procedure compensates, to a large extent, for the effect of ephemeris error. For example, for ephemeris error in the direction of the moon's motion, the error in controlling perilune radius to the nominal value is only about 20 percent of the ephemeris error. The angle between the nominal range vector and the earth-moon line is about 51^o; therefore, the perilune error would be

different if the ephemeris error were in the direction perpendicular to the nominal range vector. In fact, this direction generally has the greatest effect on interplanetary approach-guidance error, even though it is the direction for minimum ephemeris error (ref. 10). Although trajectory characteristics near a planet are not identical to those within the lunar sphere of influence, the results in figure 30 would roughly apply to interplanetary flight.

Prediction of Perilune Time

The variation of time of perilune passage with approach-guidance velocity is shown in figure 31 for a number of perturbed trajectories. As stated in the figure, the perturbed trajectories are due to one-sigma midcourse-range-measurement errors of 22 km. The magnitude of this error, however, affects the magnitude of approach ΔV and not the degree of scatter in the data. A prediction of this time, based on the magnitude of approach ΔV, may be important for deboost into lunar orbit. The scatter of the data about the faired line indicates a one-sigma prediction capability of about 82 seconds. The maximum error shown is only about 180 seconds.

CONCLUSIONS

A method for determination of approach-velocity corrections for a space vehicle has been presented. The method has been applied to the approach phase of earth-moon trajectories; however, it will also apply to reentry control for moon-earth trajectories. The method is unique in that only a single onboard position measurement is required to determine the guidance correction for controlling the perilune-radius magnitude. This position measurement is in the form of a deviation from a nominal trajectory and normally requires a subtended-angle measurement and a star-to-body angular measurement. Use is made of preflight calculations of the nominal trajectory and of various parameters for trajectories perturbed about this trajectory. These calculations not only provide the ΔV-magnitude variation with deviation, but preselect the measurement star and direction of the velocity-correction vector. These preflight determinations are the only requirements for the approach method, other than performing the measurements. The characteristics of the method are such that perilune accuracy of around 10 km can be obtained even though large differences may exist between the actual and nominal trajectories. From the error analysis performed on the method, the important results concerning the onboard approach-guidance method are:

1. The method is especially applicable to controlling errors resulting from onboard midcourse-measurement procedures.

2. The method can be applied anywhere within the lunar sphere of influence.

3. The measurement star must be in a specified direction for adequate guidance accuracy. This direction is perpendicular ($\pm 2^{\circ}$) to the direction of the nominal range vector at the lunar sphere of influence and does not change with time within the sphere. For highest sensitivity, the star should be near the orbital plane; however, angles up to 30° or more could be tolerated.

4. A range determination (for example, by measuring the subtended angle of moon) is not necessary if the guidance maneuver is made far from the moon, that is, near the lunar sphere of influence.

5. For one-sigma errors of 10 seconds of arc in the onboard angular measurements, the one-sigma error in controlling perilune radius is approximately 13 km. This error includes a one-sigma error of 0.2 m/sec in the cutoff velocity and corresponds to times near the lunar sphere of influence. If approach guidance is delayed to 5 hours from the moon, the perilune error is reduced by about one-half. The fuel requirements, however, are tripled.

6. Only a small part of the perilune-radius error is attributed to measurement error, if it is assumed that the one-sigma measurement error is 10 seconds of arc. In general, the cutoff-velocity error contributes 40 percent of the error, as does the effect of approximation error associated with the empirical procedure.

7. The approach-guidance procedure is insensitive to other types of maneuvering errors such as timing and pointing direction.

8. Whereas the method is designed principally to control the magnitude of the perilune radius, it has been shown also to control perilune position and velocity within reasonable limits.

9. It has been shown that the present guidance method compensates, to a large degree, for the effect of ephemeris error.

Langley Research Center,
National Aeronautics and Space Administration,
Hampton, Va., July 24, 1970.

APPENDIX A

EQUATIONS FOR UPDATING GUIDANCE MEASUREMENTS

The two angular measurements, θ and α, normally used in determining the approach-guidance velocity must be referenced to a common time. With the type of measurement scheme shown in the sketch, both measurements could be made essentially at

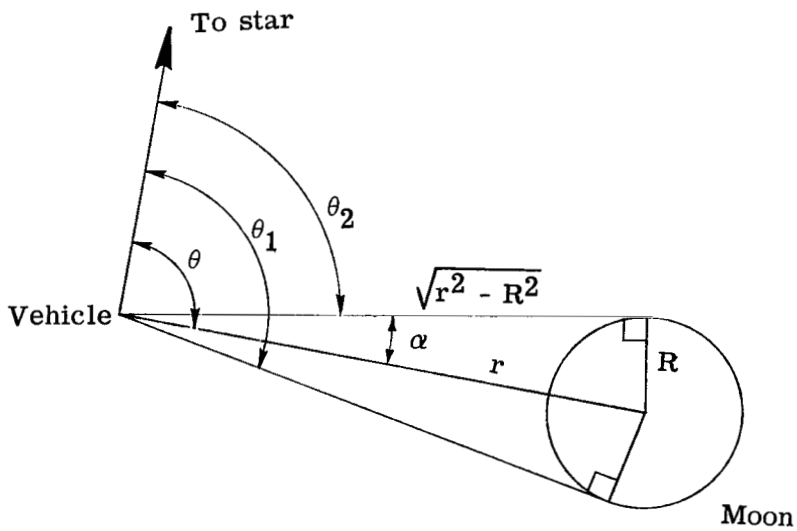

$$\theta = \frac{\theta_1 + \theta_2}{2}$$

$$\alpha = \frac{\theta_1 - \theta_2}{2}$$

the same time so that updating would not be necessary. However, if some other measurement scheme were employed or if more than one set of measurements were needed to reduce the measurement error, updating the measurements could be required.

Either measurement can be updated to a common time (small increments of time only) by means of data such as that presented in figure 32 and by the following equations:

$$\theta = \theta_m + \frac{d\theta}{dt} \Delta t$$

$$\alpha = \alpha_m + \frac{d\alpha}{dt} \Delta t$$

where Δt is the increment between the measurement time and the common time. In converting a measurement to a common time, the corresponding value of the rate of change of angle with time along the nominal trajectory, $d\theta/dt$ or $d\alpha/dt$, must be selected for the given time T_p. The value of T_p would need to be known only approximately; hence, the nominal value would suffice. The values of $d\theta/dt$ and $d\alpha/dt$, shown in figure 32, are precalculated from the equations which follow.

The rate of change of the measurement θ (angle between star and moon center) with time along a nominal trajectory is given by

$$\frac{d\theta}{dt} = \frac{\partial\theta}{\partial x}\frac{dx}{dt} + \frac{\partial\theta}{\partial y}\frac{dy}{dt} + \frac{\partial\theta}{\partial z}\frac{dz}{dt}$$

where dx/dt, dy/dt, and dz/dt are known values for the nominal trajectory in the selenocentric coordinate system and, as can be determined from equations given in reference 11, the partials for the angular measurements θ are

$$\frac{\partial\theta}{\partial x} = \frac{x(my + nz) - l(y^2 + z^2)}{r^2\left[r^2 - (lx + my + nz)^2\right]^{1/2}}$$

$$\frac{\partial\theta}{\partial y} = \frac{y(lx + nz) - m(x^2 + z^2)}{r^2\left[r^2 - (lx + my + nz)^2\right]^{1/2}}$$

$$\frac{\partial\theta}{\partial z} = \frac{z(lx + my) - n(x^2 + y^2)}{r^2\left[r^2 - (lx + my + nz)^2\right]^{1/2}}$$

If the star is in the orbital plane, the equation for $d\theta/dt$ is equivalent to the rate of change of true anomaly with respect to time.

The rate of change of the measurement α (semisubtended angle of moon) with time along a nominal trajectory is given by

$$\frac{d\alpha}{dt} = \frac{\partial\alpha}{\partial x}\frac{dx}{dt} + \frac{\partial\alpha}{\partial y}\frac{dy}{dt} + \frac{\partial\alpha}{\partial z}\frac{dz}{dt}$$

where, again, the derivatives with respect to time are commonly known values for the nominal trajectory and the partials for the angular measurement α, which can be determined from the relation

$$\alpha = \tan^{-1}\frac{R}{\sqrt{r^2 - R^2}}$$

are

$$\frac{\partial\alpha}{\partial x} = -x\frac{R}{r^2\sqrt{r2 - R^2}}$$

$$\frac{\partial \alpha}{\partial y} = -y \frac{R}{r^2 \sqrt{r^2 - R^2}}$$

$$\frac{\partial \alpha}{\partial z} = -z \frac{R}{r^2 \sqrt{r^2 - R^2}}$$

APPENDIX B

DERIVATION OF VELOCITY CORRECTION REQUIRED TO ATTAIN DESIRED PERILUNE

From the law of conservation of angular momentum

$$r_{p,n}^2 V_{p,n}^2 = r^2 V_A^2 \cos^2\gamma_A = r^2 V_A^2 \cos^2(\gamma + \Delta\gamma) \tag{B1}$$

where γ is the flight-path angle prior to the approach-guidance correction, and γ_A and V_A represent values immediately following the correction.

Expanding equation (B1) gives

$$r_{p,n}^2 V_{p,n}^2 = r^2 V_A^2 (\cos\gamma \cos\Delta\gamma - \sin\gamma \sin\Delta\gamma)^2$$

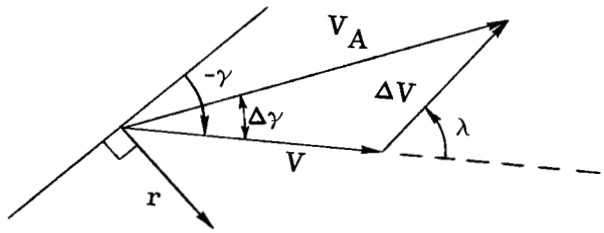

Solving for $\Delta\gamma$ from the sketch gives

$$r_{p,n}^2 V_{p,n}^2 = r^2 V_A^2 \left[\frac{\cos\gamma(V + \Delta V \cos\lambda)}{V_A} - \frac{\sin\gamma\, \Delta V \sin\lambda}{V_A}\right]^2$$

or

$$r_{p,n}^2 V_{p,n}^2 = r^2 \left[\cos\gamma(V + \Delta V \cos\lambda) - \sin\gamma\, \Delta V \sin\lambda\right]^2$$

Expansion yields

$$r_{p,n}^2 V_{p,n}^2 = r^2 \left[\cos^2\gamma(V + \Delta V \cos\lambda)^2 + \Delta V^2 \sin^2\gamma \sin^2\lambda - 2\,\Delta V(V + \Delta V \cos\lambda) \sin\gamma \cos\gamma \sin\lambda\right] \tag{B2}$$

or

$$r_{p,n}^2 V_{p,n}^2 = r^2 \left[\Delta V^2 \cos^2(\gamma + \lambda) + 2V\,\Delta V \cos\gamma \cos(\gamma + \lambda) + V^2 \cos^2\gamma\right] \tag{B3}$$

But

$$V_{p,n}^2 - \frac{2\mu}{r_{p,n}} = V_A^2 - \frac{2\mu}{r} \tag{B4}$$

and from the sketch, it is seen that

$$V_A^2 = V^2 + \Delta V^2 + 2V\,\Delta V \cos\lambda \tag{B5}$$

Substituting equations (B4) and (B5) into equation (B3) yields

$$r_{p,n}^2\left(V^2 + \Delta V^2 + 2V\,\Delta V\cos\lambda - \frac{2\mu}{r} + \frac{2\mu}{r_{p,n}}\right)$$

$$= \Delta V^2 r^2 \cos^2(\gamma+\lambda) + 2V\,\Delta V r^2 \cos\gamma\cos(\gamma+\lambda) + V^2 r^2\cos^2\gamma$$

whence

$$\Delta V^2\left[r_{p,n}^2 - r^2\cos^2(\gamma+\lambda)\right] + 2V\,\Delta V\left[r_{p,n}^2\cos\lambda - r^2\cos\gamma\cos(\gamma+\lambda)\right]$$
$$+ V^2\left(r_{p,n}^2 - r^2\cos^2\gamma\right) + r_{p,n}^2\left(\frac{2\mu}{r_{p,n}} - \frac{2\mu}{r}\right) = 0$$

Solving for the velocity correction yields

$$\Delta V = \frac{V\left[r^2\cos\gamma\cos(\gamma+\lambda) - r_{p,n}^2\cos\lambda\right]}{r_{p,n}^2 - r^2\cos^2(\gamma+\lambda)}$$
$$\pm \frac{r_{p,n}\left\{\left(r^2 - r_{p,n}^2\right)V^2\sin^2\lambda + \left[r^2\cos^2(\gamma+\lambda) - r_{p,n}^2\right]\left(\frac{2\mu}{r_{p,n}} - \frac{2\mu}{r}\right)\right\}^{1/2}}{r_{p,n}^2 - r^2\cos^2(\gamma+\lambda)} \tag{B6}$$

The value of γ is derived from

$$\cos\gamma = \frac{r_p V_p}{rV} \tag{B7}$$

where r_p and V_p are the predicted perilune values. (See figs. 11 and 12.) The alternate signs of the second term in equation (B6) correspond to correcting to either side of

the moon. The sign which results in the lesser value of ΔV would ordinarily be chosen. It should be noted that ΔV is added to (subtracted from) $\overline{V}$ if the nominal trajectory is designed to rotate clockwise (counterclockwise) about the moon (viewed from northerly direction) as shown in figure 2.

APPENDIX C

VELOCITY REQUIREMENT FOR APPROACH GUIDANCE

Several analytical expressions for the variation of approach-guidance velocity ΔV with perilune radius r_p are presented in this appendix. The velocity requirement $\Delta(\Delta V)/\Delta r_p$ is useful for error analysis (see fig. 29) and as mentioned in the main text, for obtaining ΔV if r_p can be determined directly from some type of approach-guidance measurement. Values resulting from each of the following expressions were essentially the same and are compared with actual values in figure 21.

The first equation presented is the exact expression for velocity requirement (at small values of ΔV) and was determined by differentiating equation (B6) with respect to r_p. The resulting equation is

$$\frac{\partial(\Delta V)}{\partial r_p} = \frac{2r^2 V r_p \cos(\gamma+\lambda)\left[\cos\gamma + \cos\lambda\cos(\gamma+\lambda)\right]}{\left[r^2\cos^2(\gamma+\lambda) - r_p^2\right]^2}$$

$$\pm \frac{\left\{(rV\sin\lambda)^2 - (r_pV\sin\lambda)^2 + \left[r^2\cos^2(\gamma+\lambda) - r_p^2\right]\left(\frac{2\mu}{r_p} - \frac{2\mu}{r}\right)\right\}^{1/2}\left[r^2\cos^2(\gamma+\lambda) + r_p^2\right]}{\left[r^2\cos^2(\gamma+\lambda) - r_p^2\right]^2}$$

$$\mp \frac{r_p^3V^2r\sin^2\lambda + \mu r^3\cos^2(\gamma+\lambda) + \mu r r_p^2 - 2\mu r_p^3}{r r_p\left[r^2\cos^2(\gamma+\lambda) - r_p^2\right]\left\{(rV\sin\lambda)^2 - (r_pV\sin\lambda)^2 + \left[r^2\cos^2(\gamma+\lambda) - r_p^2\right]\left(\frac{2\mu}{r_p} - \frac{2\mu}{r}\right)\right\}^{1/2}}$$

Simplified expressions which were derived from work accomplished in reference 12 are

$$\frac{\partial V}{\partial r_p} = \pm \frac{\frac{V_p\epsilon}{1+\epsilon}}{r\left[1 - \frac{3+\epsilon}{1+\epsilon}\left(\frac{r_p}{r}\right)^2 + \frac{2}{1+\epsilon}\left(\frac{r_p}{r}\right)^3\right]^{1/2}}$$

for optimum-angle thrust direction and

$$\frac{\partial V}{\partial r_p} = \pm \frac{\frac{V_p\epsilon}{1+\epsilon}}{r - \frac{r_p^2}{r}}$$

for thrust in the direction of the local horizontal (which is near optimum).

APPENDIX D

MEASUREMENT-ERROR EQUATIONS

Derived in this appendix are the equations used in analyzing the effect of measurement error in the approach-guidance procedure. The measurement equation is

$$D = r_m \cos \theta_m - r_n \cos \theta_n = r_m \cos \theta_m - \text{Constant}$$

where D is the position deviation calculated from the measurements r_m and θ_m. It is seen that

$$dD = \cos \theta \, dr - r \sin \theta \, d\theta \tag{D1}$$

or

$$\Delta D = \cos \theta \, \Delta r - r \sin \theta \, \Delta\theta$$

Uncorrelated Measurements

If it is assumed that Δr and $\Delta\theta$ are random uncorrelated errors,

$$\sigma_D^2 = (\cos \theta \, \sigma_r)^2 + (r \sin \theta \, \sigma_\theta)^2 \tag{D2}$$

where nominal values for r and θ can be used. The quantity σ_θ is normally taken as constant, whereas σ_r is a function of range. For times near $T_p = 14.614$ hours ($\theta \approx 90^o$),

$$\sigma_D^2 \approx r^2 \sigma_\theta^2$$

where σ_θ is the standard deviation of the star-to-moon angular measurement error. Inasmuch as the range-measurement error is insignificant for $\theta \approx 90^o$, the nominal value can be used in place of the range measurement when D is calculated.

For times closer to the moon, the range measurement, and hence its error σ_r, become significant. The error in range determination is caused by error in the subtended-angle measurement α and uncertainty in the knowledge of the moon's radius R. From the equation

$$R = r \sin \alpha$$

it is seen that

$$dR = r \cos \alpha \, d\alpha + \sin \alpha \, dr$$

or

$$\sin \alpha \, \Delta r = \Delta R - r \cos \alpha \, \Delta \alpha$$

so that

$$\sigma_r^2 = \left(\frac{\sigma_R}{\sin \alpha}\right)^2 + \left(r \cot \alpha \, \sigma_\alpha\right)^2 = \left(\frac{r}{R} \sigma_R\right)^2 + \left(r \cot \alpha \, \sigma_\alpha\right)^2$$

Now, since α is small

$$\sigma_r^2 = \left(\frac{r}{R} \sigma_R\right)^2 + \left(r \frac{r}{R} \sigma_\alpha\right)^2$$

or

$$\sigma_r^2 = \frac{r^2}{R^2}\left(\sigma_R^2 + r^2 \sigma_\alpha^2\right) \tag{D3}$$

Correlated Measurements

If the angles θ and α are measured by the method suggested in appendix A, their errors would be correlated. From the equations given in the sketch in appendix A, it is seen that

$$d\theta = \frac{1}{2}\left(d\theta_1 + d\theta_2\right)$$

$$d\alpha = \frac{1}{2}\left(d\theta_1 - d\theta_2\right)$$

Also

$$r \approx \frac{R}{\alpha}$$

so that

$$dr = -\frac{r^2}{R} d\alpha = \frac{r^2}{2R}\left(d\theta_2 - d\theta_1\right)$$

If the relations for dr and $d\theta$ are substituted into equation (D1), then

$$dD = \frac{\cos\theta}{2}\left(\frac{r^2}{R}\right)\left(d\theta_2 - d\theta_1\right) - \frac{r\sin\theta}{2}\left(d\theta_1 + d\theta_2\right)$$

or

$$\Delta D = \frac{r}{2}\left[\left(\frac{r\cos\theta}{R} - \sin\theta\right)\Delta\theta_2 - \left(\frac{r\cos\theta}{R} + \sin\theta\right)\Delta\theta_1\right]$$

If it is assumed that θ_1 and θ_2 are measured separately, that is, $\Delta\theta_1$ and $\Delta\theta_2$ are random uncorrelated errors with equal variances σ_θ^2,

$$\sigma_D^2 = \frac{r^2}{4}\left[2\left(\frac{r^2}{R^2}\cos^2\theta + \sin^2\theta\right)\sigma_\theta^2\right] \tag{D4}$$

or

$$\sigma_D = \frac{\sqrt{2}}{2}\, r\left(\sin^2\theta + \frac{r^2}{R^2}\cos^2\theta\right)^{1/2}\sigma_\theta$$

For times near $T_p = 14.614$ hours ($\theta \approx 90^\circ$),

$$\sigma_D \approx 0.707 r\sigma_\theta$$

It is interesting to note that in this case, the errors are smaller than those for the previous case (eq. (D2)).

In equation (D4), the error in R has not been taken into account. Including the error in R gives

$$\sigma_D' = \left(\sigma_D^2 + \frac{r^2}{R^2}\sigma_R^2\right)^{1/2}$$

where σ_D is determined from equation (D4) and the prime denotes the inclusion of the uncertainty in lunar radius.

REFERENCES

1. Friedlander, Alan L.; and Harry, David P., III: An Exploratory Statistical Analysis of a Planet Approach-Phase Guidance Scheme Using Angluar Measurements with Significant Error. NASA TN D-471, 1960.

2. Harry, David P., III; and Friedlander, Alan L.: An Analysis of Errors and Requirements of an Optical Guidance Technique for Approaches to Atmospheric Entry With Interplanetary Vehicles. NASA TR R-102, 1961.

3. Hartwell, J. Graham; Danby, J. M. A.; and Jones, Arthur L.: Planetary Approach Navigation. Navigation, vol. 11, no. 2, 1964, pp. 125-144.

4. Taylor, Arthur J.; and Wagner, John T.: On-Board Approach Guidance for a Planet-Orbiter. J. Spacecraft Rockets, vol. 3, no. 12, Dec. 1966, pp. 1731-1737.

5. Seaman, Lewis T.; and Brown, Harold E.: Planetary Approach Guidance for a Martian Mission. Transactions of 1967 National Symposium on "Saturn V/Apollo and Beyond," vol. III, Steven S. Hu, ed., Amer. Astronaut. Soc., c.1967.

6. Murtagh, Thomas B.: Planetary Probe Guidance Accuracy Influence Factors for Conjunction-Class Missions. NASA TN D-4852, 1969.

7. Hamer, Harold A.: Approach-Guidance Requirements for Simplified Onboard Control of Moon-to-Earth Trajectories. Proceedings of the ION National Space Meeting on Space Navigation – Theory and Practice in the Post Apollo Era, Inst. Navigation, Feb. 1970, pp. 285-299.

8. Warner, M. R.; Nead, M. W.; and Hudson, R. H.: The Orbit Determination Program of the Jet Propulsion Laboratory. Tech. Mem. No. 33-168 (Contract NAS 7-100), Jet Propulsion Lab., California Inst. Technol., Mar. 18, 1964.

9. Hamer, Harold A.; Johnson, Katherine G; and Blackshear, W. Thomas: Midcourse-Guidance Procedure With Single Position Fix Obtained From Onboard Optical Measurements. NASA TN D-4246, 1967.

10. Anon.: The Deep Space Network for the Period January 1 to February 28, 1967. Space Programs Sum. No. 37-44, Vol. III (Contract No. NAS 7-100), Jet Propulsion Lab., California Inst. Technol., Mar. 31, 1967.

11. Hannah, Margery E.; and Mayo, Alton P.: A Study of Factors Affecting the Accuracy of Position Fix for Lunar Trajectories. NASA TN D-2178, 1964.

12. Boltz, Frederick W.: Minimum Thrust for Correcting Keplerian Orbits With Application to Interplanetary Guidance. NASA TN D-4945, 1968.

TABLE I.- EFFECT OF SCATTER ERROR ON ACCURACY OF CONTROLLING PERILUNE DISTANCE

Condition	Nominal trip time, hr	$r_{p,n}$, km	$T_{p,n}$, hr	Value of V used in equation (3)	Second midcourse-approach-guidance maneuvers	$\sigma_{p,n}$, km
1	70.617	3403.6	14.617	V_n	Separate	8.78
2	70.617	3403.6	14.617	V_a	Separate	8.60
3	70.617	3403.6	14.617	V_n	Combined	8.27
4	70.617	3403.6	4.617	V_a	Separate	5.5
5	71.07	1892.8	15.07	V_n	Separate	10.52
6	90	2237.3	15.0	V_n	Separate	14.79

TABLE II.- EFFECT OF SCATTER ERROR ON ACCURACY OF CONTROLLING PARAMETERS AT PERILUNE

[Condition 2 of table I]

Parameter	σ
Inclination, deg	0.36
Longitude, deg	0.37
Latitude, deg	0.17
V_p, m/sec	1.99
s, km	25.32
u, m/sec	11.14

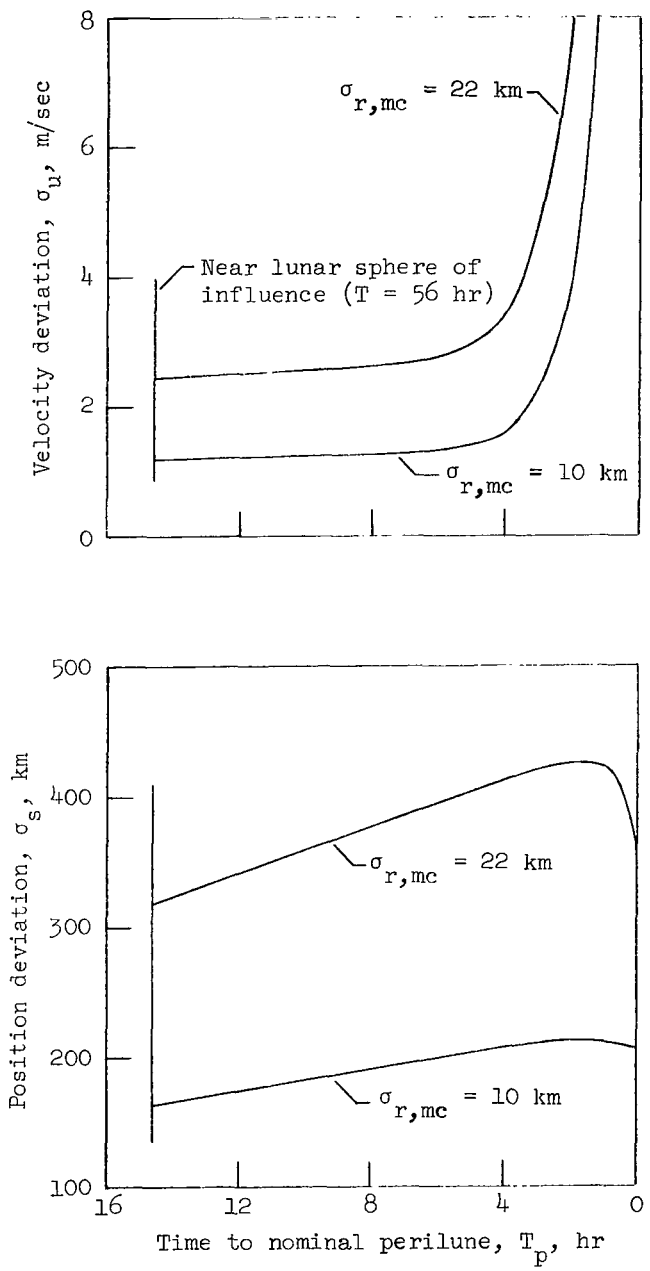

Figure 1.- Aim-point errors resulting from midcourse-guidance-measurement error. Data include angular-measurement errors; σ_θ = 10 seconds of arc.

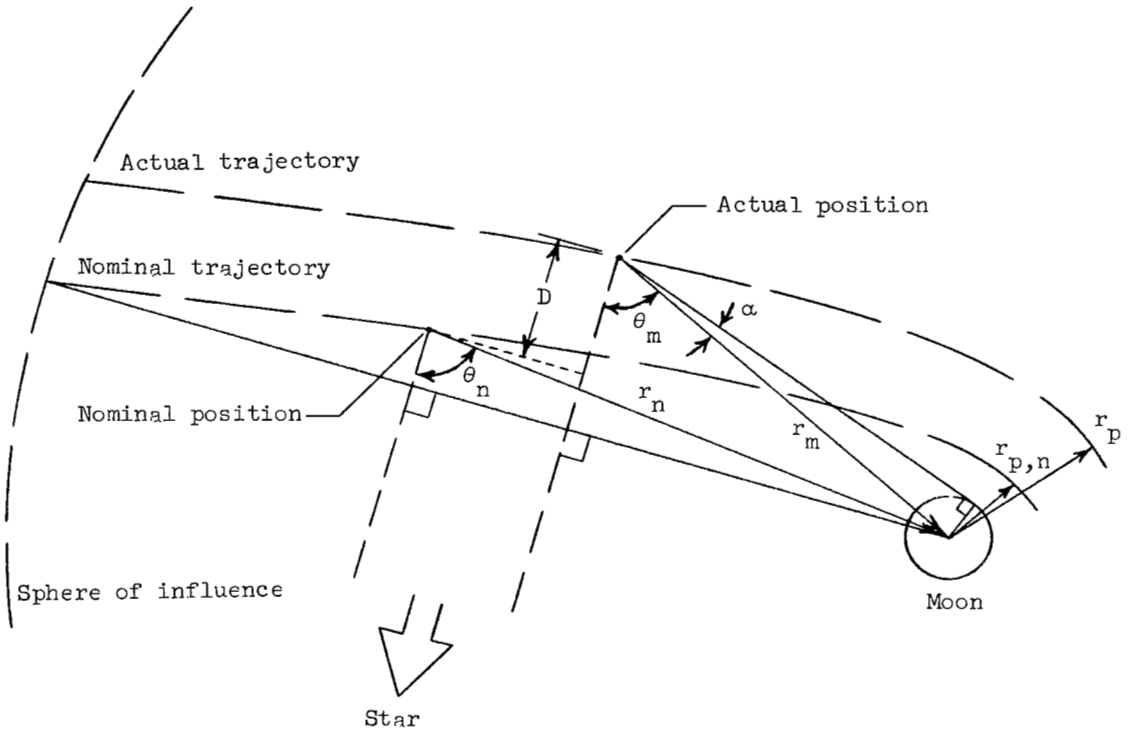

$$D = r_m \cos \theta_m - r_n \cos \theta_n$$

Figure 2.- Schematic sketch showing measurements required for approach-guidance procedure. (Trajectories are not necessarily coplanar.)

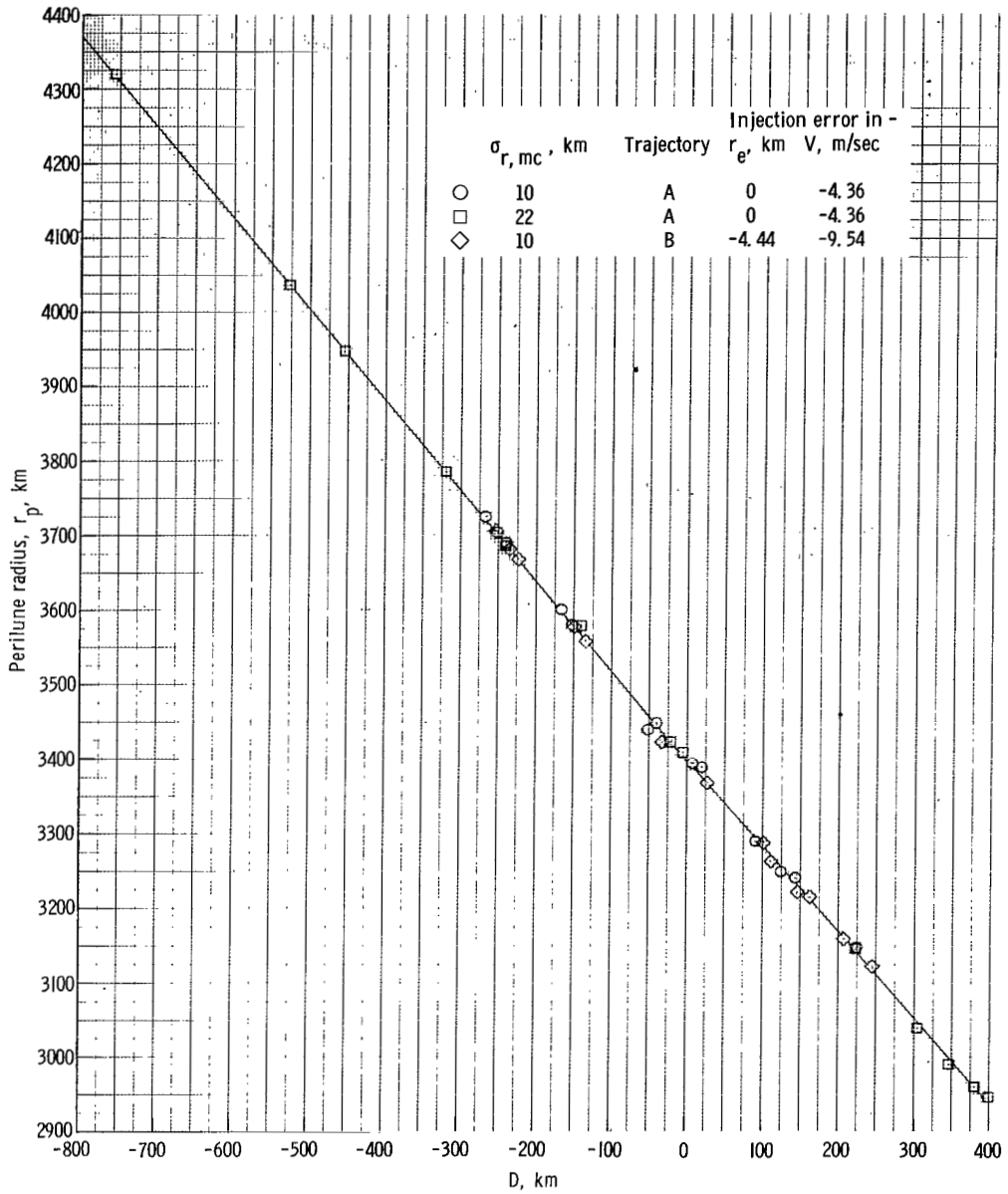

(a) Perilune radius.

Figure 3.- Variation of perilune conditions with deviation D at T_p = 14.617 hr for various perturbed trajectories. The direction of D is in the nominal orbital plane and perpendicular to the nominal range vector to the moon.

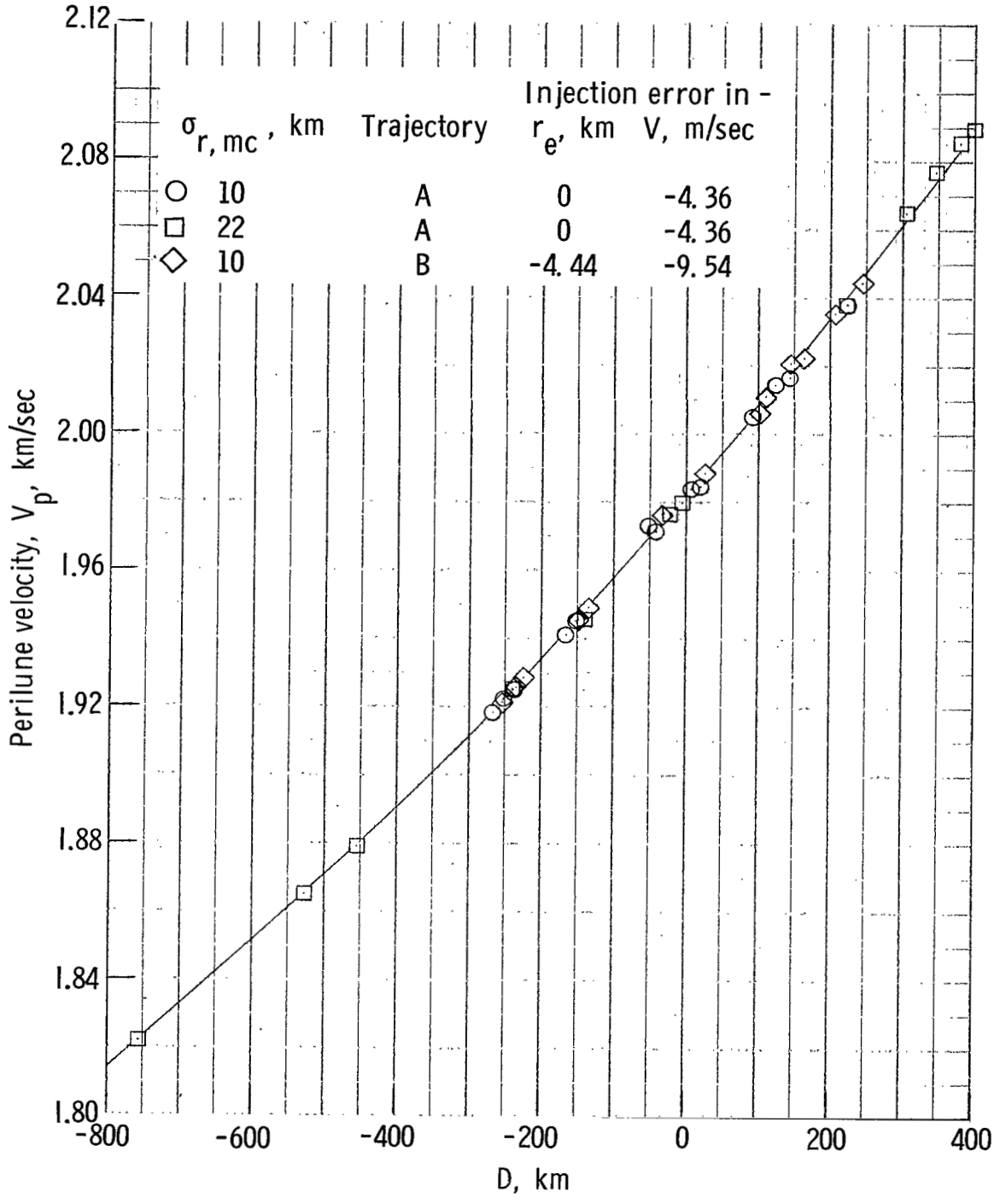

(b) Perilune velocity.

Figure 3.- Concluded.

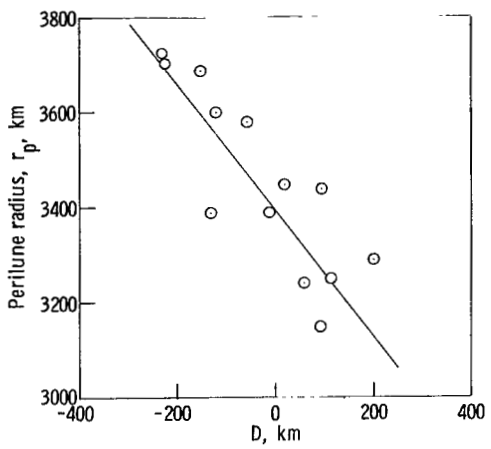

(a) Star in direction of selenocentric velocity vector (close to earth-moon-vehicle plane).

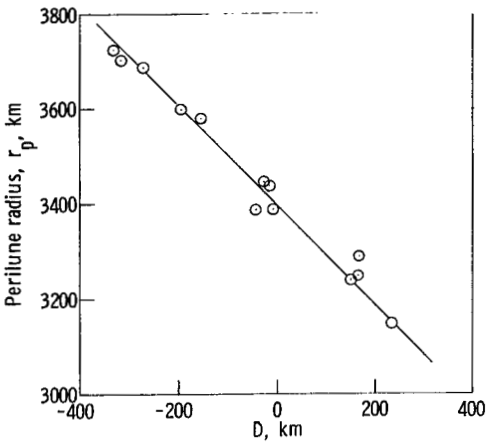

(b) Star in direction of major axis of position-error ellipsoid (about 4.7° out of earth-moon-vehicle plane.

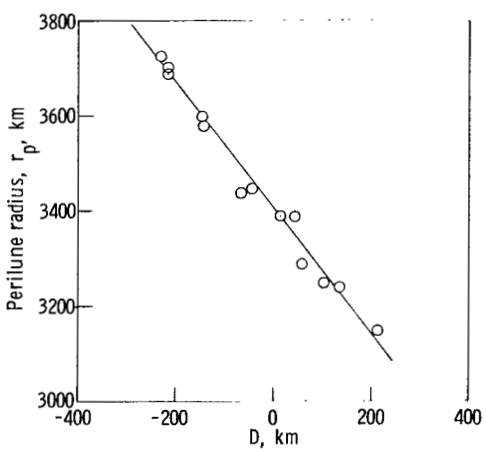

(c) Star in earth-moon-vehicle plane and in direction perpendicular to hyperbolic asymptote (about 3.5° and 9.5° from perpendicular to selenocentric velocity and radius vector, respectively).

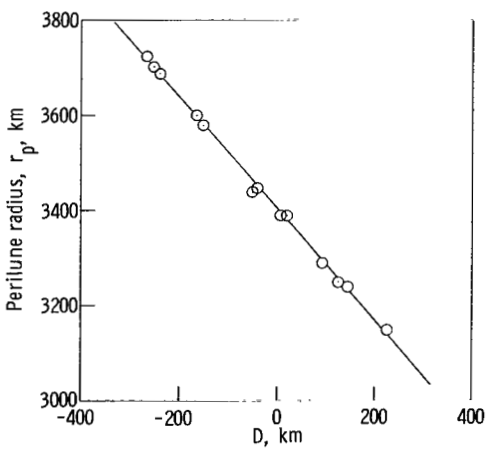

(d) Star in earth-moon-vehicle plane and in direction perpendicular to selenocentric radius vector.

Figure 4.- Comparison of scatter at T_p = 14.617 hr for deviations in different directions. $\sigma_{r,mc}$ = 10 km. (Lines are faired through data points.)

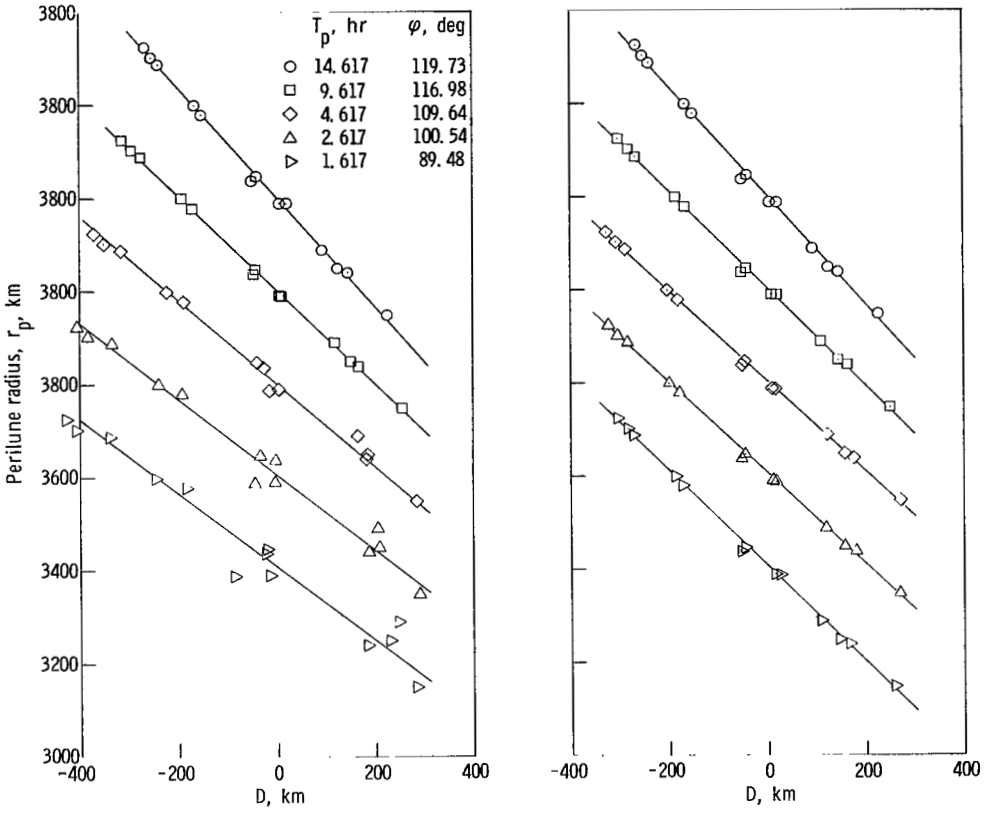

(a) Star in earth-moon-vehicle plane and in direction perpendicular to selenocentric radius vector.

(b) Star in earth-moon-vehicle plane and in same direction for all times, that is, in direction perpendicular to selenocentric radius vector at T_p = 14.617 hr.

Figure 5.- Comparison of scatter for deviations taken at different times. $\sigma_{r,mc}$ = 10 km. Note staggered vertical scale.

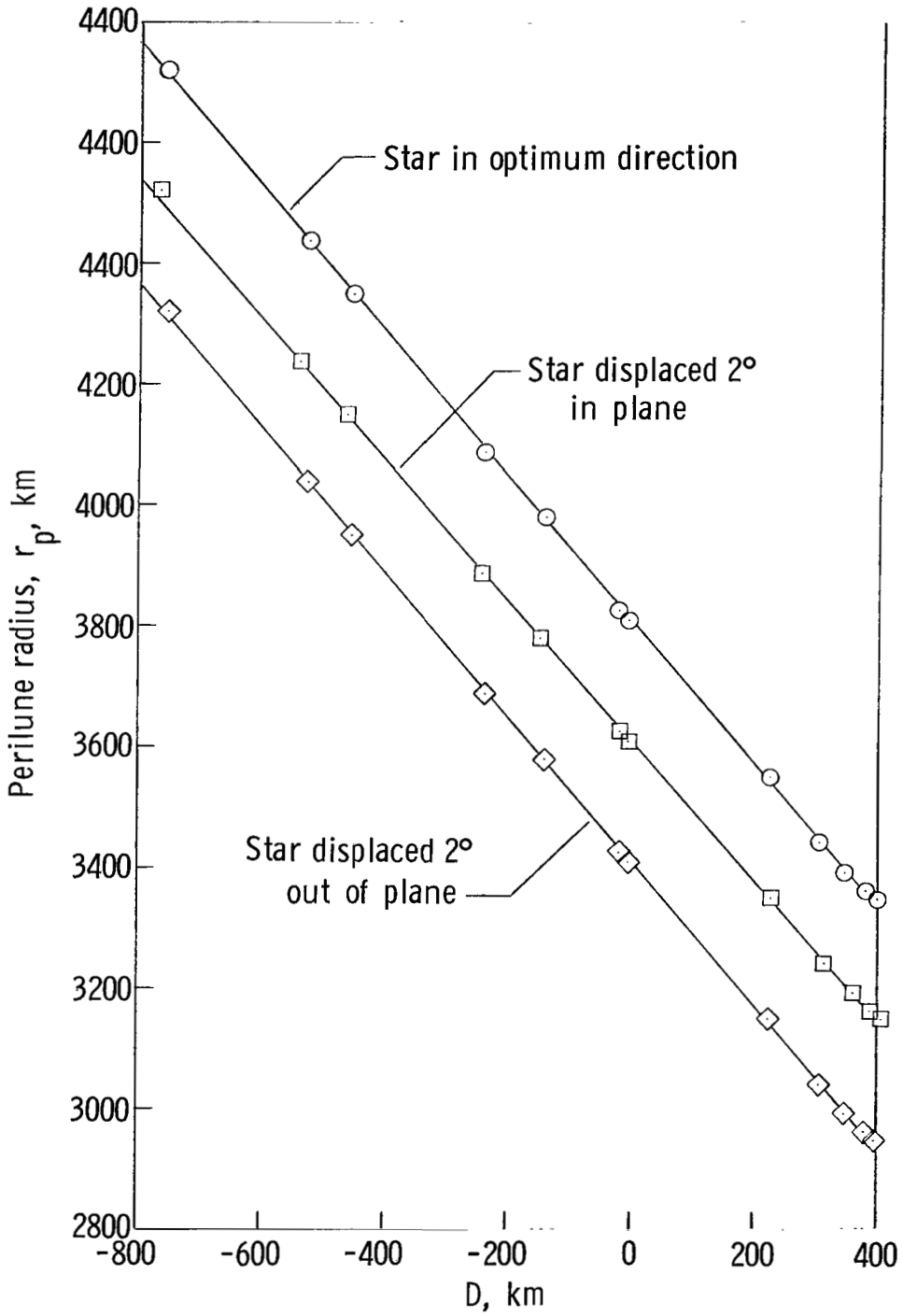

Figure 6.- Effect on scatter of displacing star from optimum direction. T_p = 14.617 hr; $\sigma_{r,mc}$ = 22 km. Note staggered vertical scale.

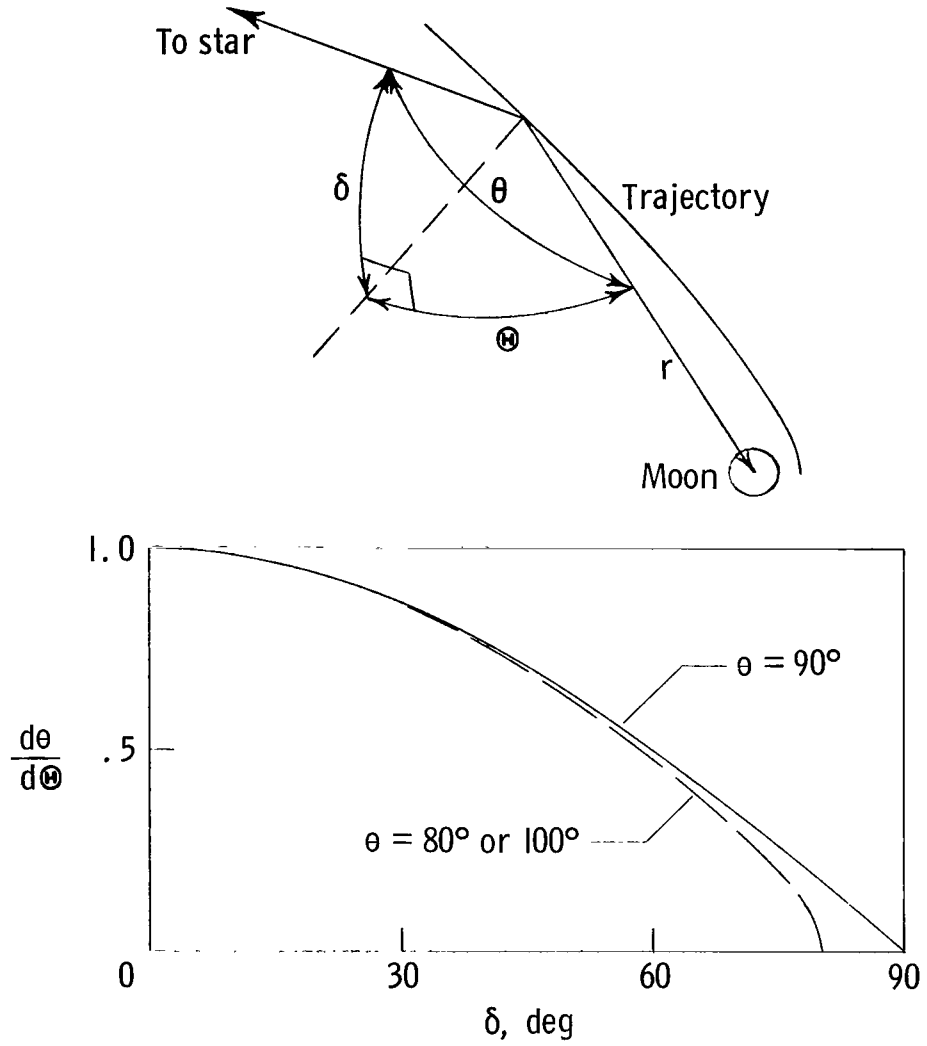

Figure 7.- Measurement sensitivity as a function of out-of-plane displacement of measurement star.

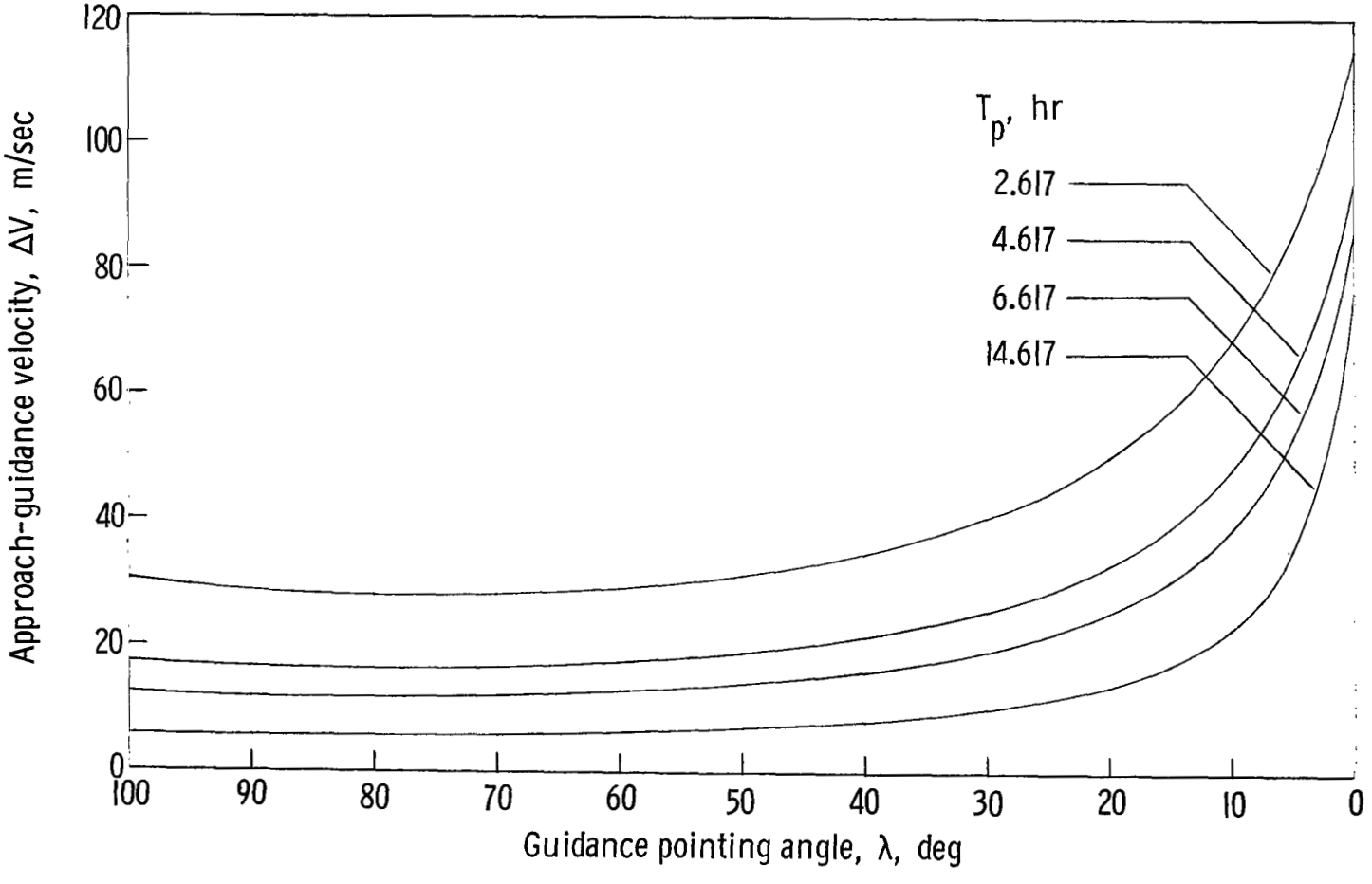

Figure 8.- Example of velocity-correction requirements for a typical perturbed trajectory.

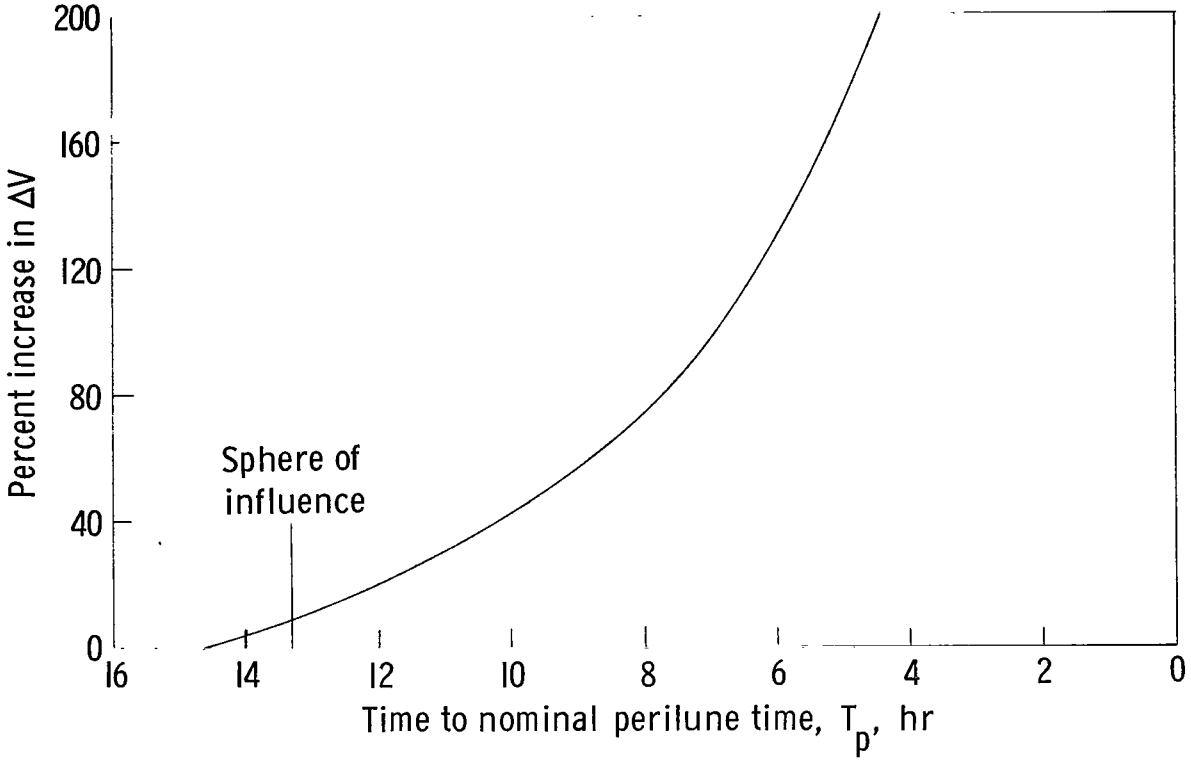

Figure 9.- Approximate increase in approach-guidance correction over that required near the sphere of influence. $\lambda = 90^{\circ}$.

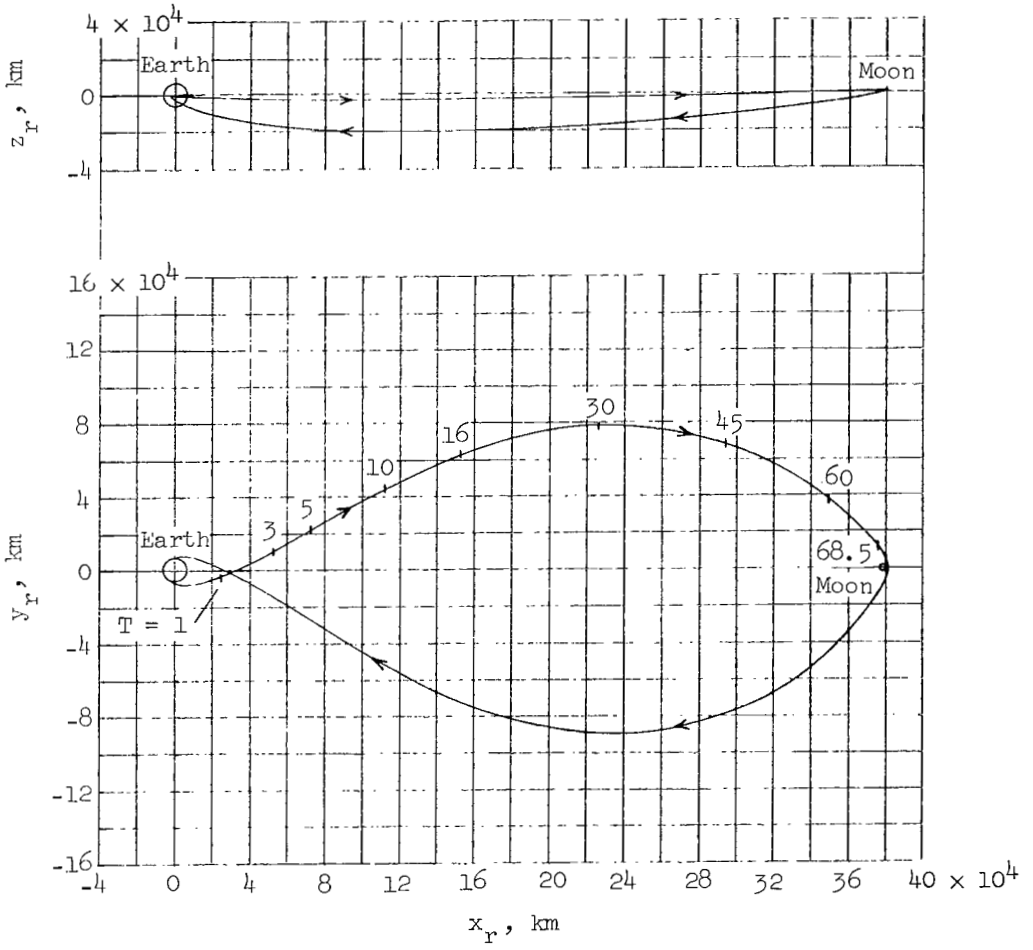

Figure 10.- Nominal trajectory used for most of the analysis in this paper.

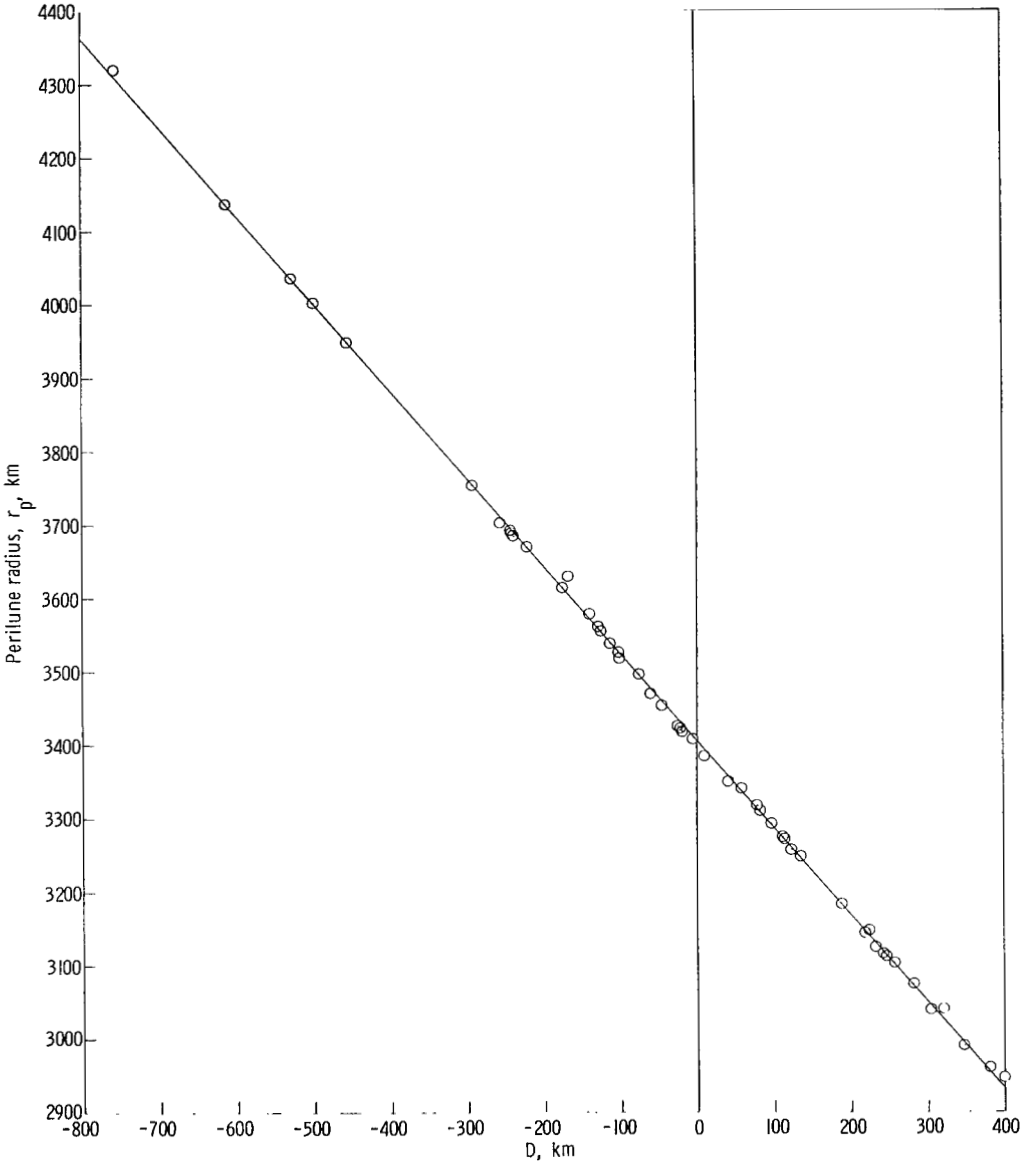

(a) 70-hr translunar trajectory; $r_{p,n}$ = 3403.6 km; T_p = 14.617 hr.

Figure 11.- Variation of perilune radius with D for 50 perturbed trajectories. $\sigma_{r,mc}$ = 22 km.

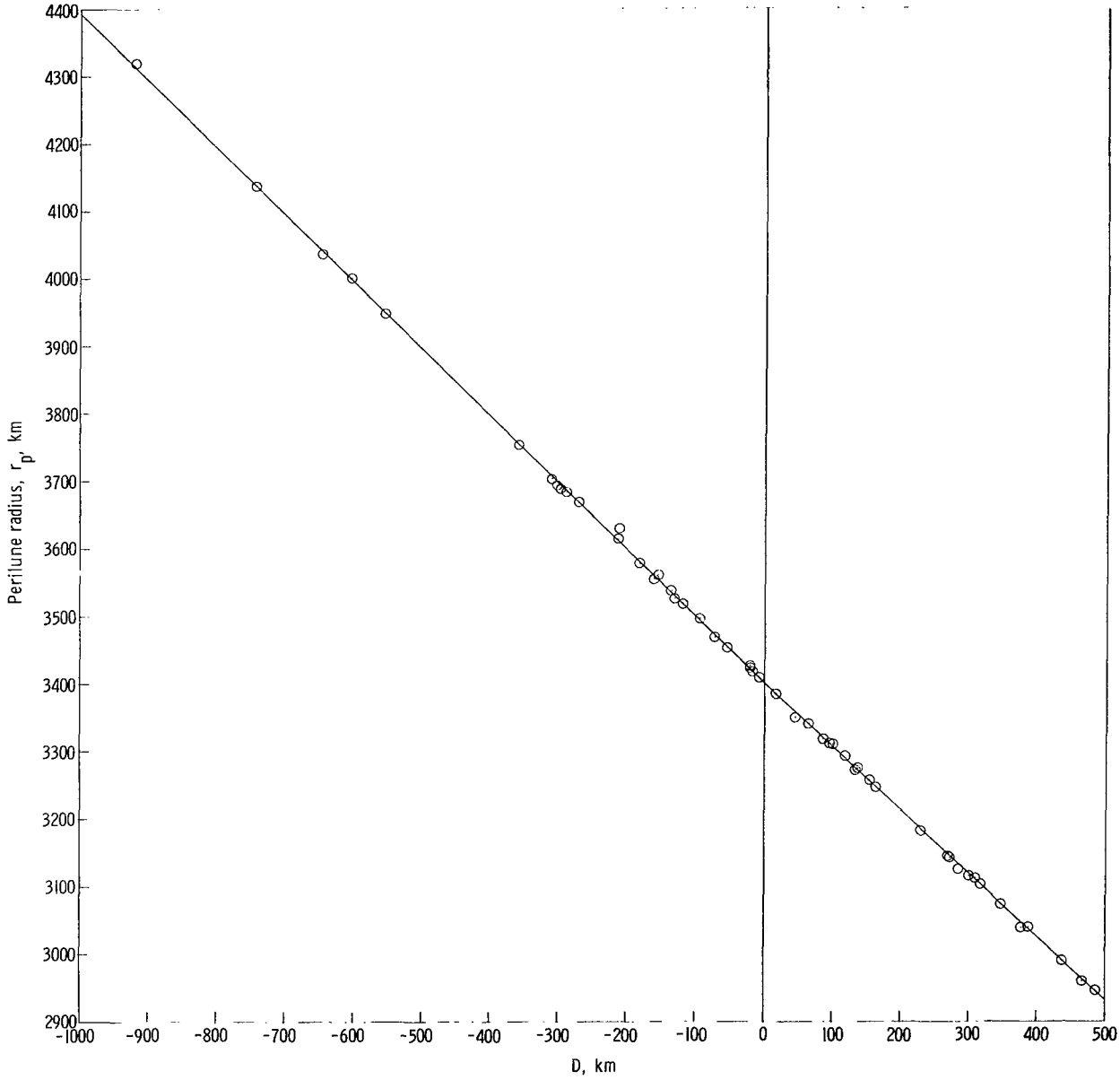

(b) 70-hr translunar trajectory; $r_{p,n}$ = 3403.6 km; T_p = 4.617 hr.

Figure 11.- Continued.

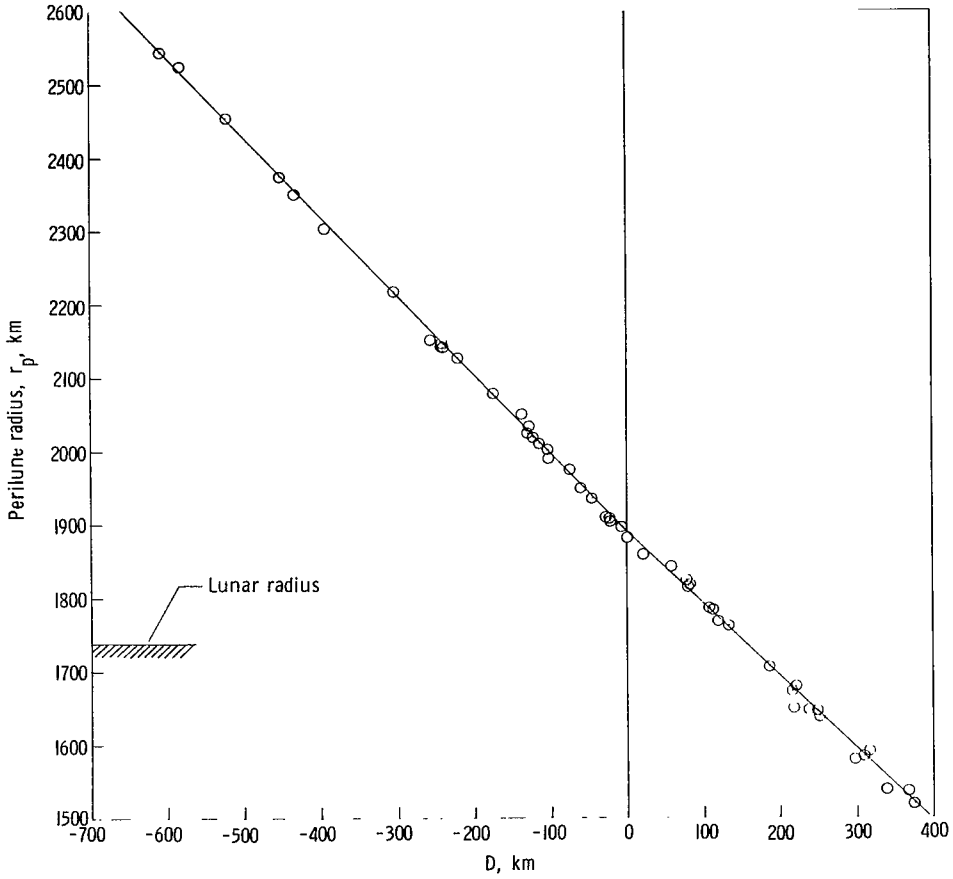

(c) 70-hr translunar trajectory; $r_{p,n}$ = 1892.8 km; T_p = 15.07 hr.

Figure 11.- Continued.

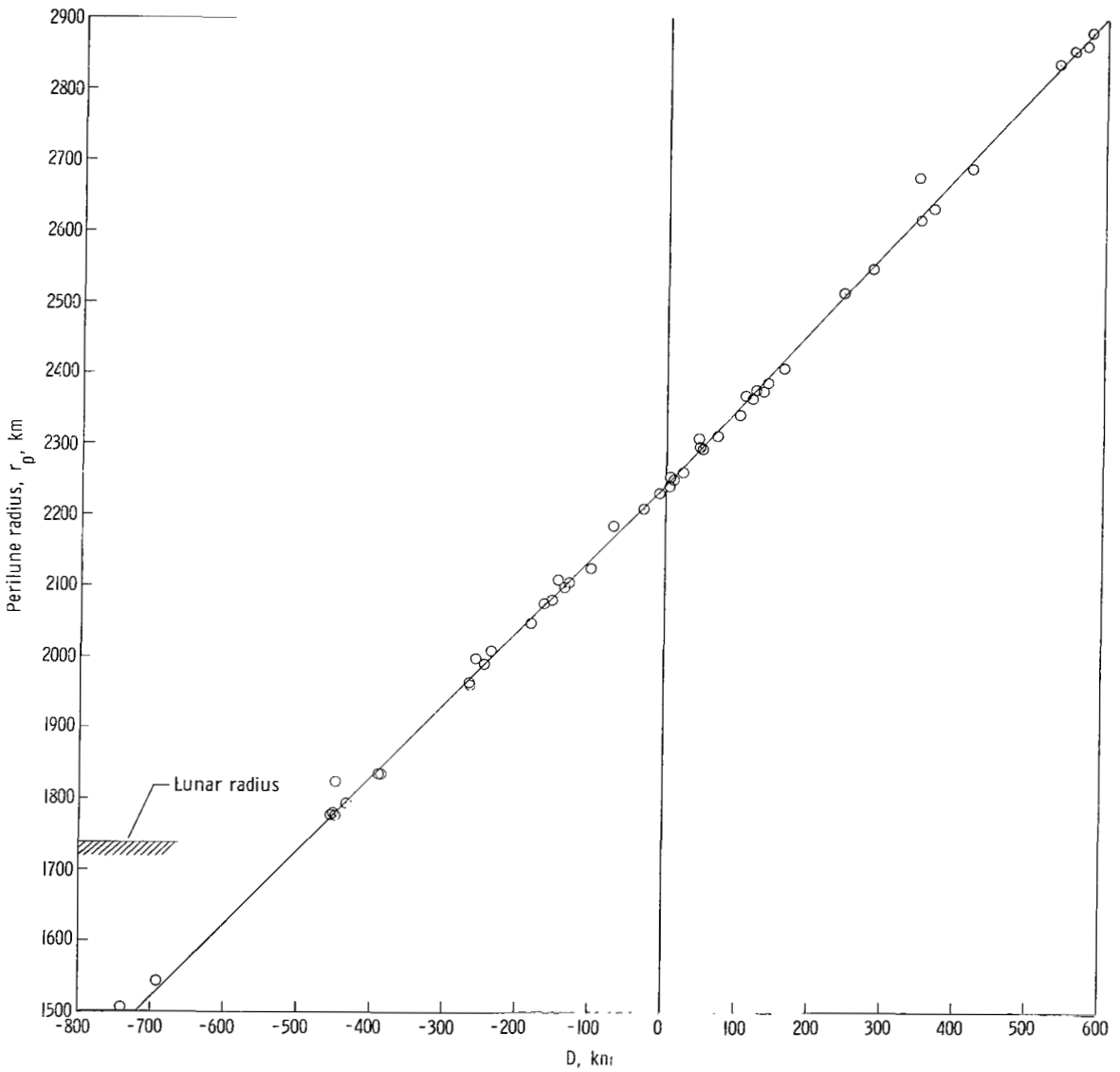

(d) 90-hr translunar trajectory; $r_{p,n}$ = 2236.6 km; T_p = 15.0 hr.

Figure 11.- Concluded.

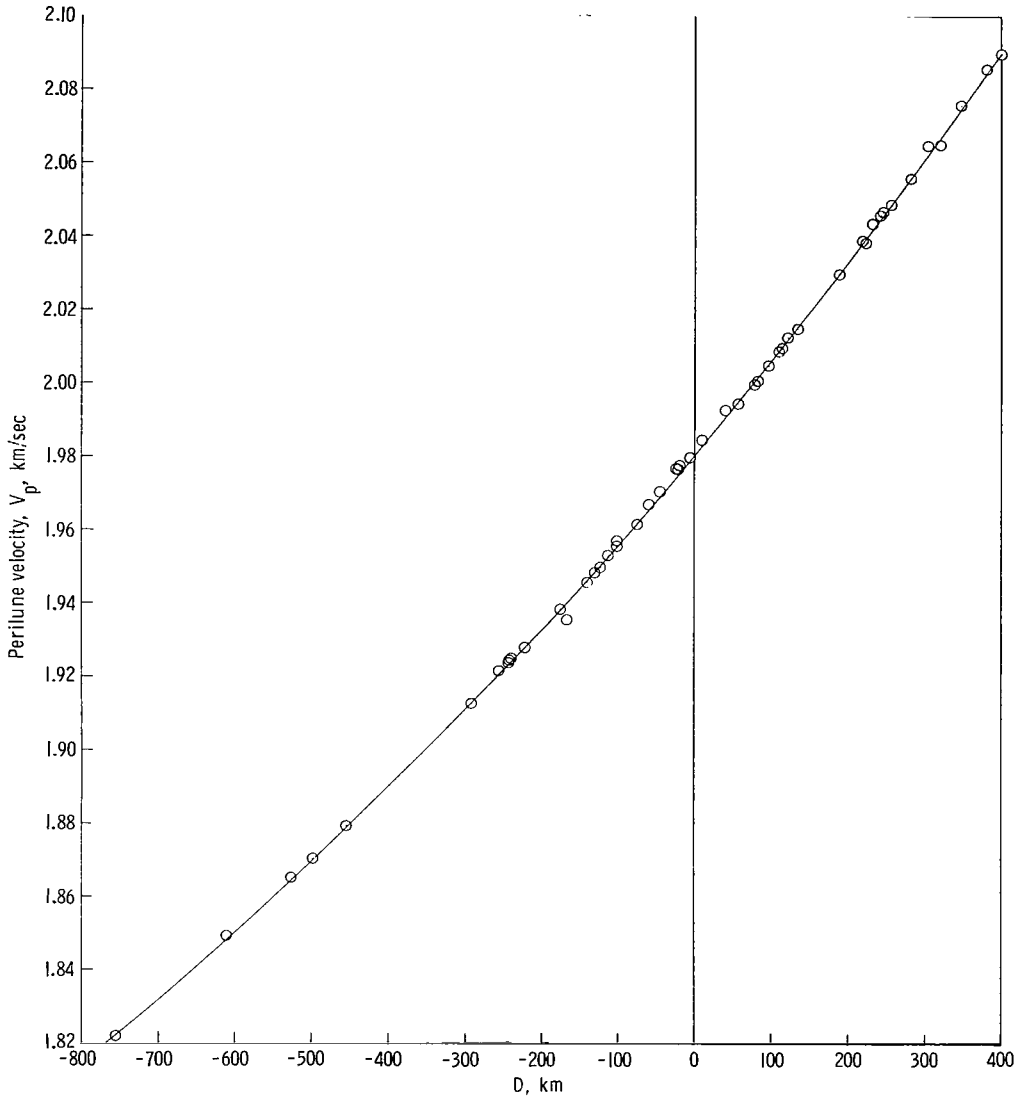

(a) 70-hr translunar trajectory; $r_{p,n}$ = 3403.6 km; $V_{p,n}$ = 1.9805 km/sec; T_p = 14.617 hr.

Figure 12.- Variation of perilune velocity with D for 50 perturbed trajectories. $\sigma_{r,mc}$ = 22 km.

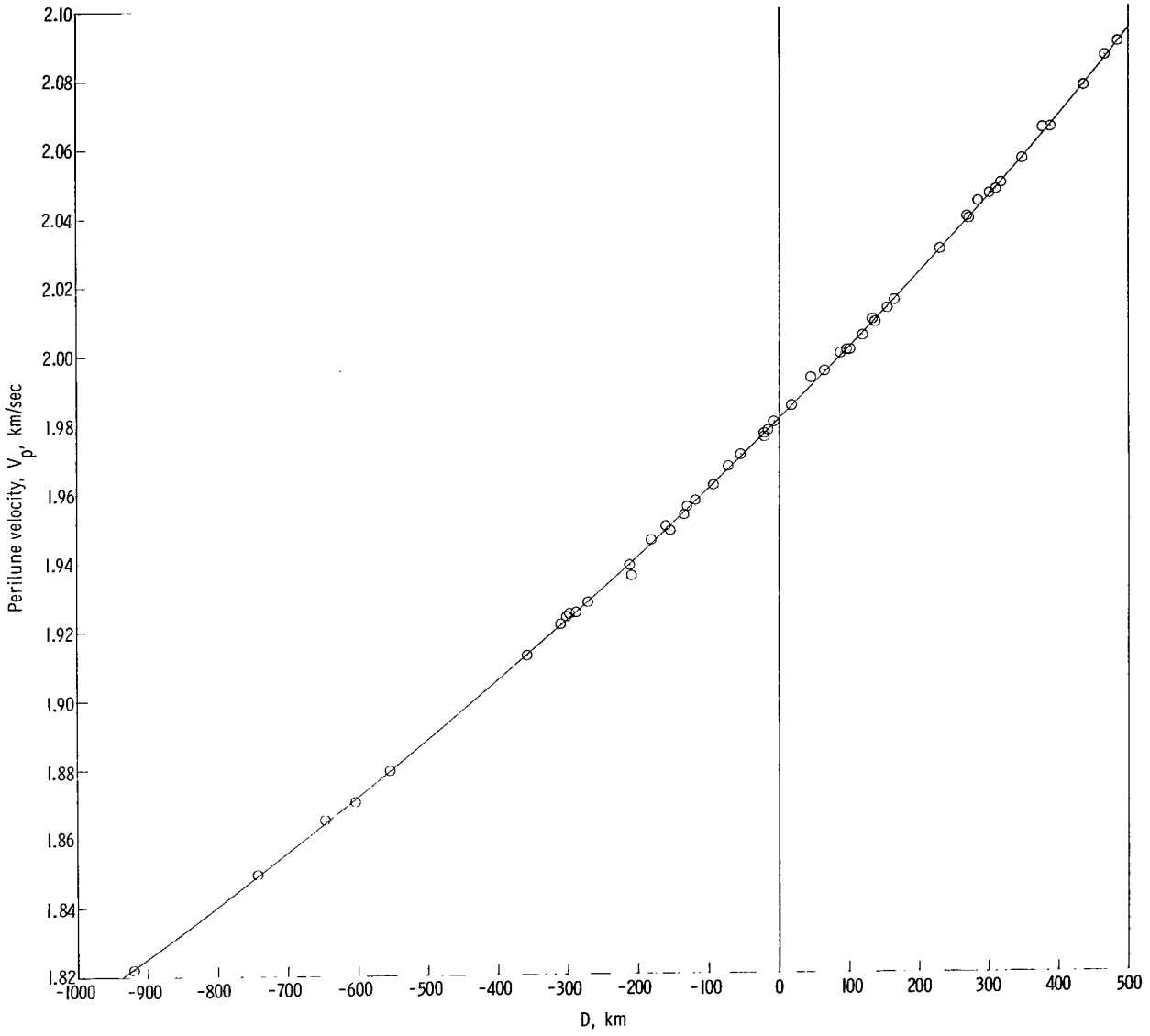

(b) 70-hr translunar trajectory; $r_{p,n}$ = 3403.6 km; $V_{p,n}$ = 1.9805 km/sec; T_p = 4.617 hr.

Figure 12.- Continued.

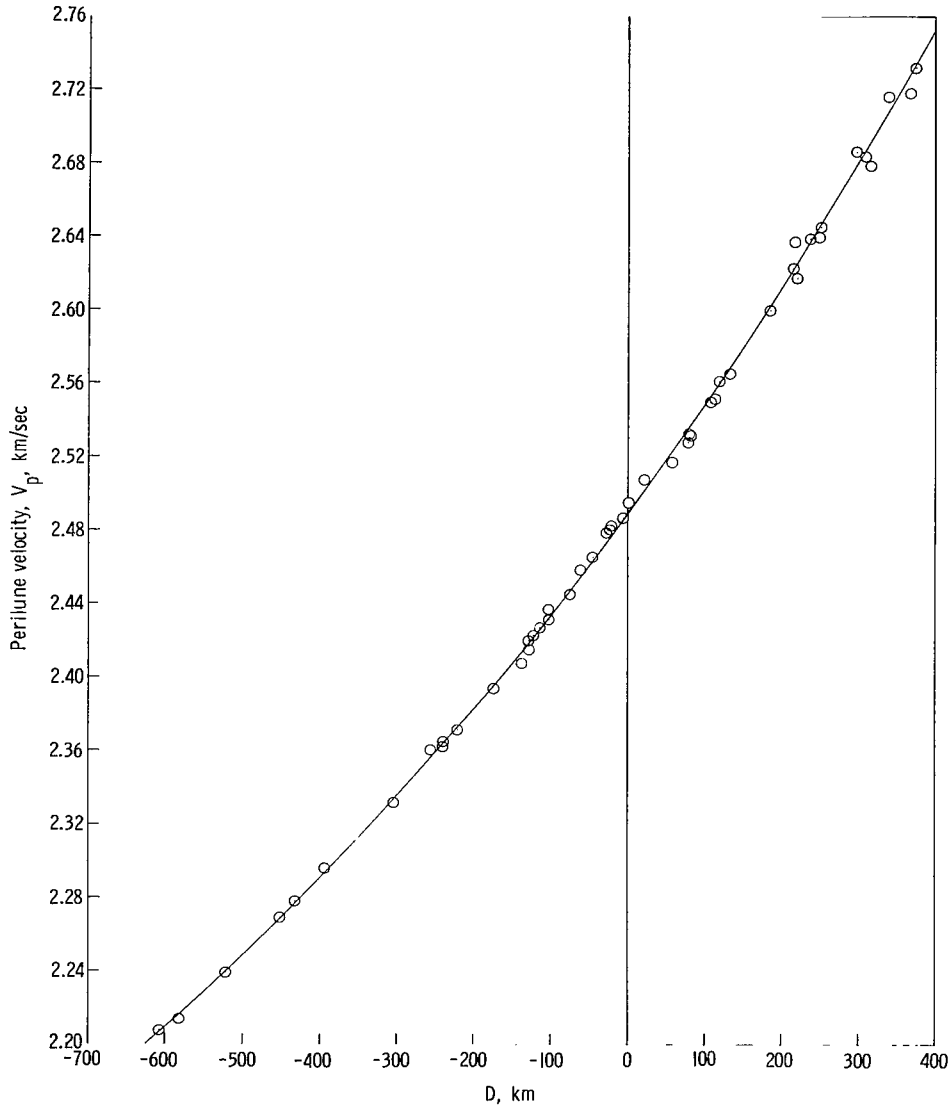

(c) 70-hr translunar trajectory; $r_{p,n}$ = 1892.8 km; $V_{p,n}$ = 2.4883 km/sec; T_p = 15.07 hr.

Figure 12.- Continued.

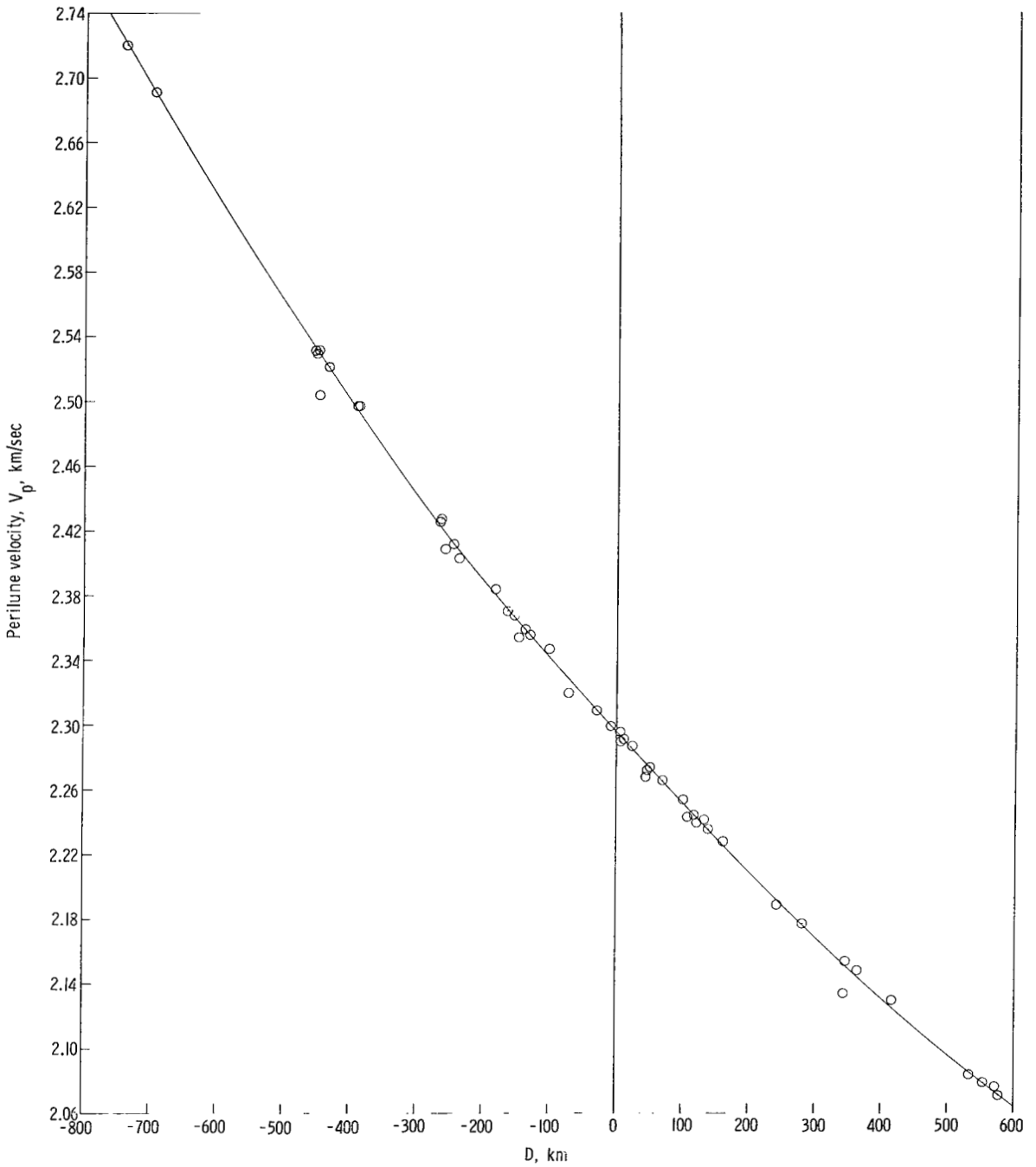

(d) 90-hr translunar trajectory; $V_{p,n}$ = 2.2957 km/sec; T_p = 15.0 hr.

Figure 12.- Concluded.

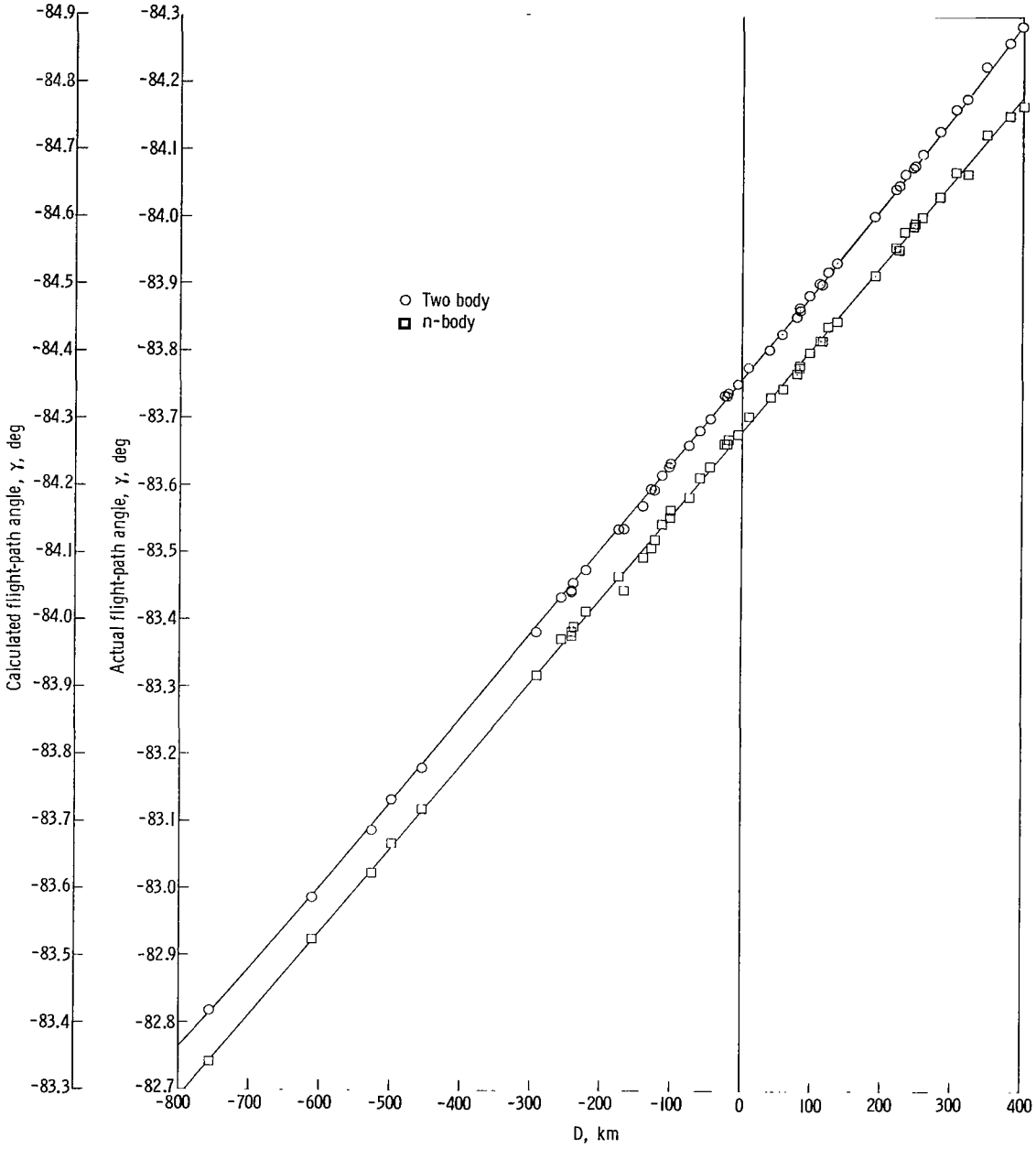

Figure 13.- Variation of flight-path angle with D for 50 perturbed trajectories. T_p = 14.617 hr; $\sigma_{r,mc}$ = 22 km. Calculated (two body) value of flight-path angle obtained from equation (4).

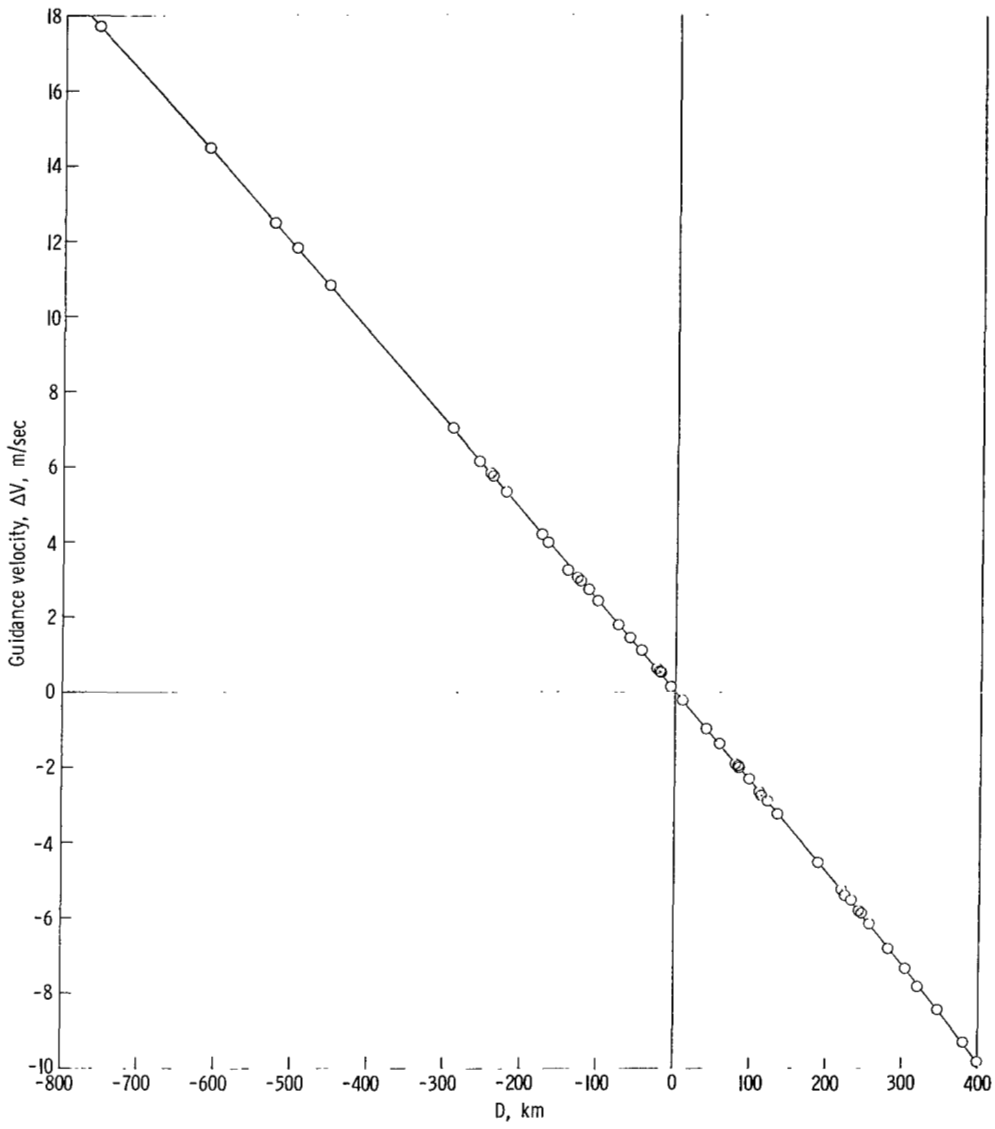

(a) 70-hr translunar trajectory; $r_{p,n}$ = 3403.6 km; T_p = 14.617 hr.

Figure 14.- Variation of approach-guidance velocity with D for 50 perturbed trajectories. $\sigma_{r,mc}$ = 22 km.

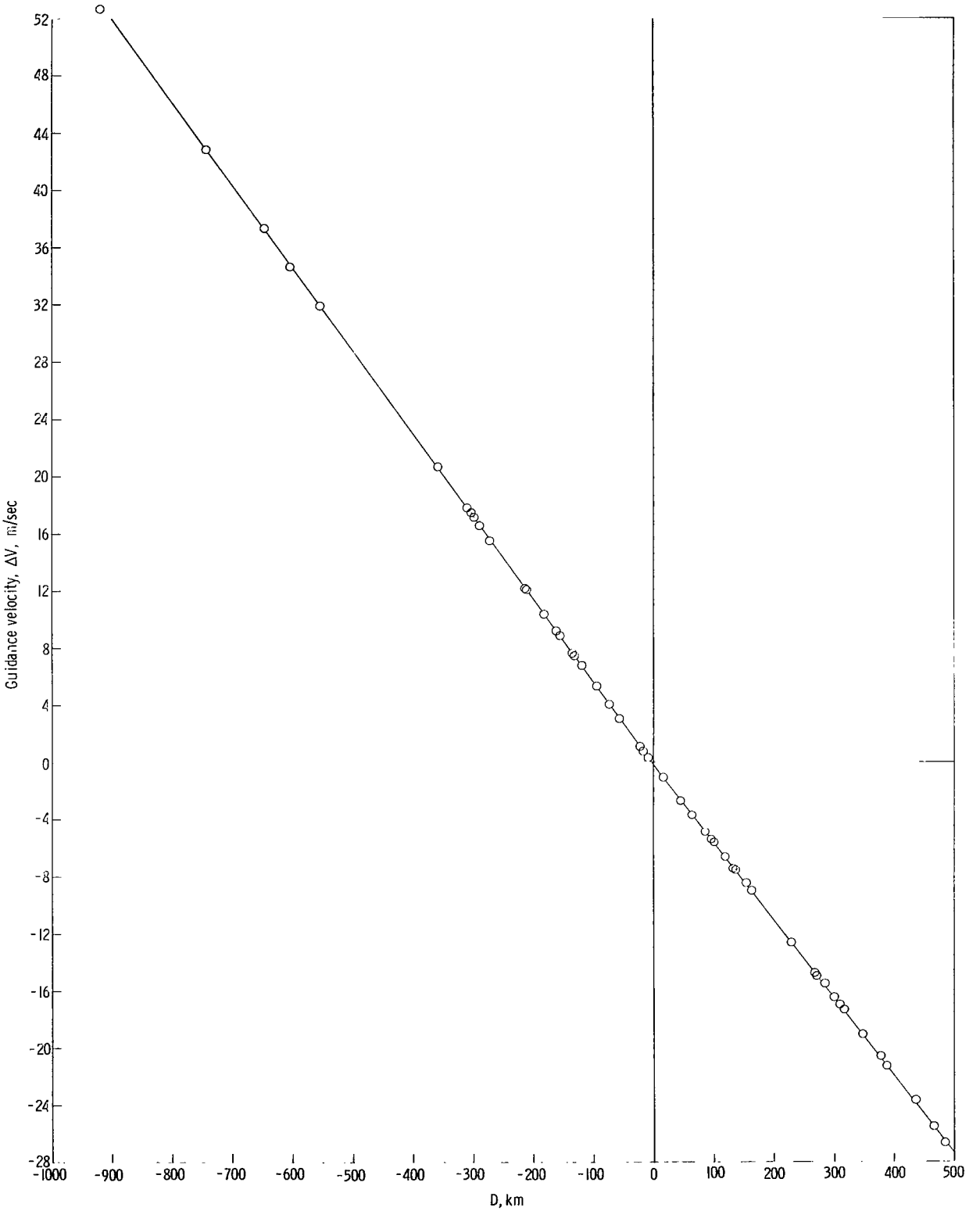

(b) 70-hr translunar trajectory; $r_{p,n}$ = 3403.6 km; T_p = 4.617 hr.

Figure 14.- Continued.

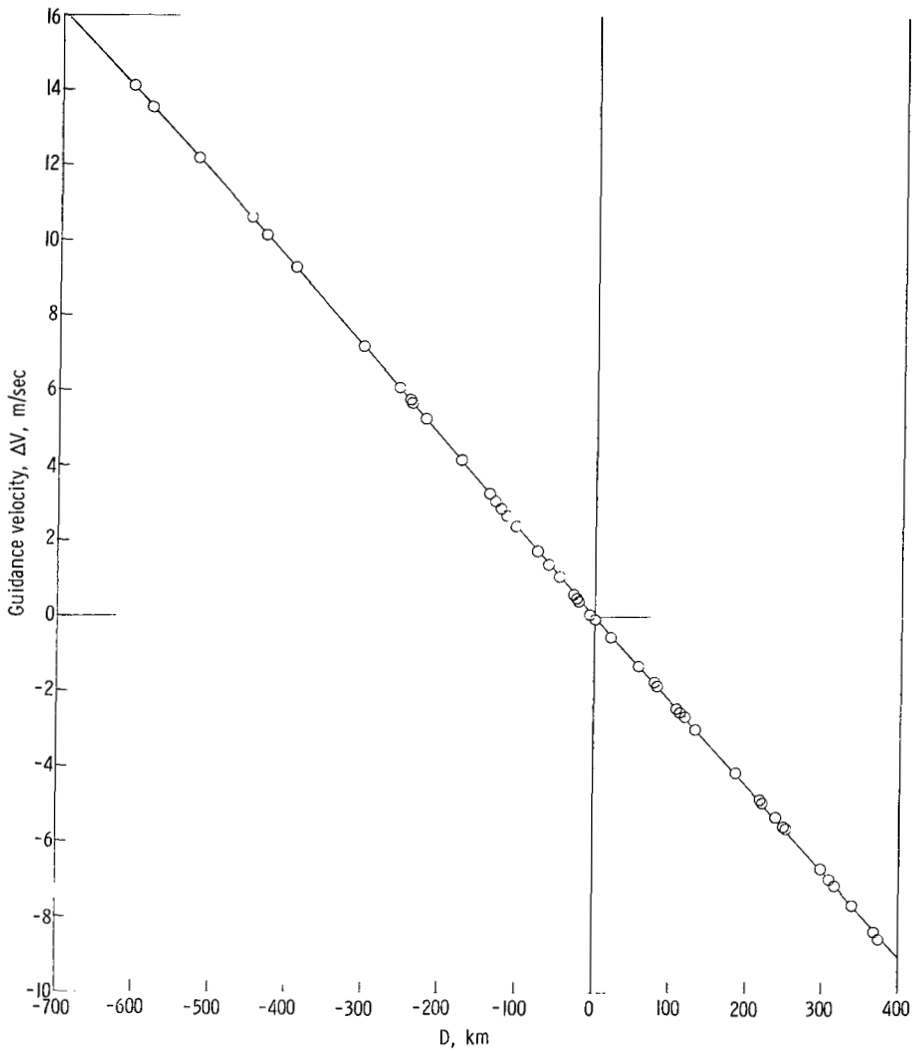

(c) 70-hr translunar trajectory; $r_{p,n}$ = 1892.8 km; T_p = 15.07 hr.

Figure 14.- Continued.

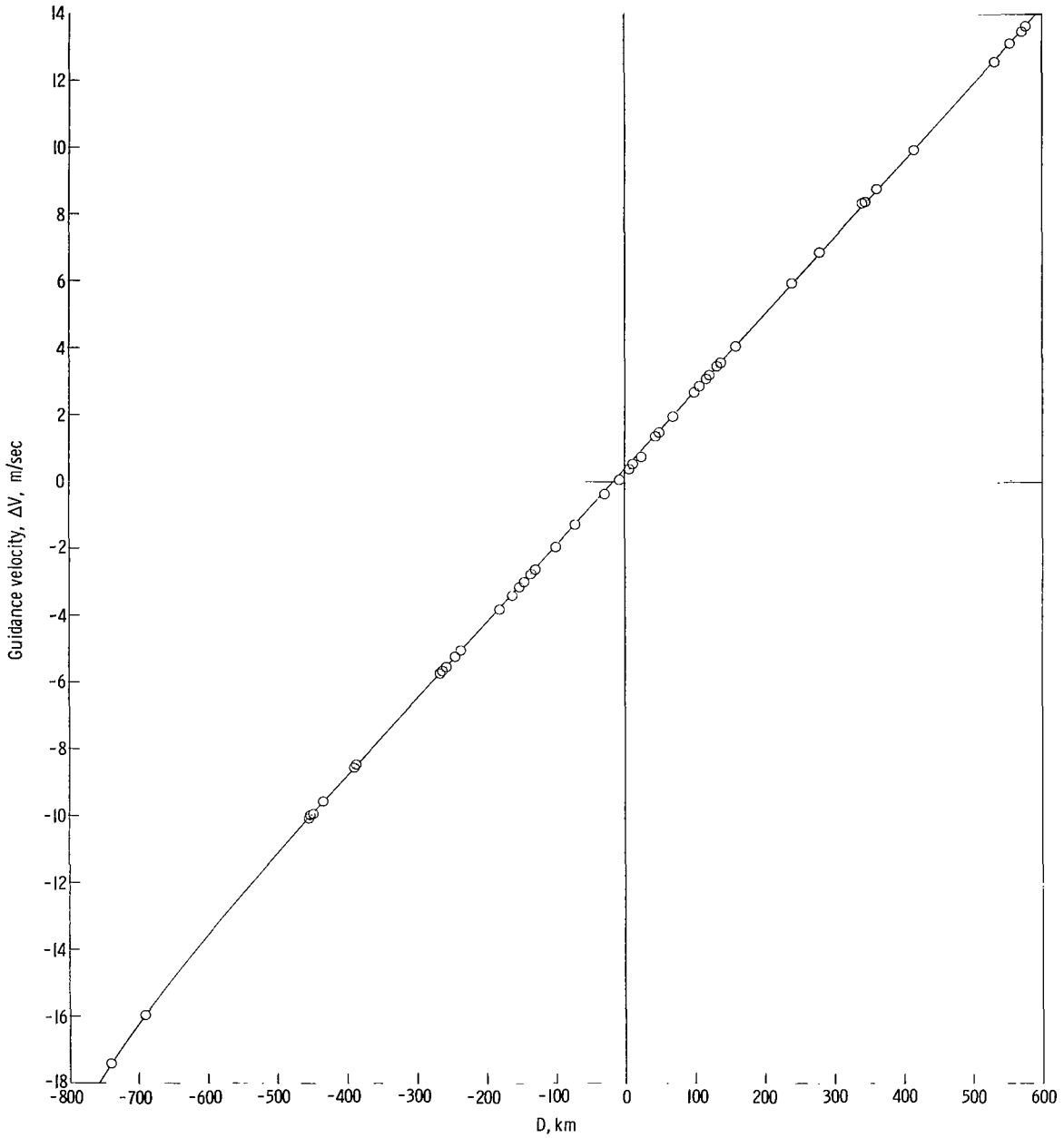

(d) 90-hr translunar trajectory; $r_{p,n}$ = 2236.6 km; T_p = 15.0 hr.

Figure 14.- Concluded.

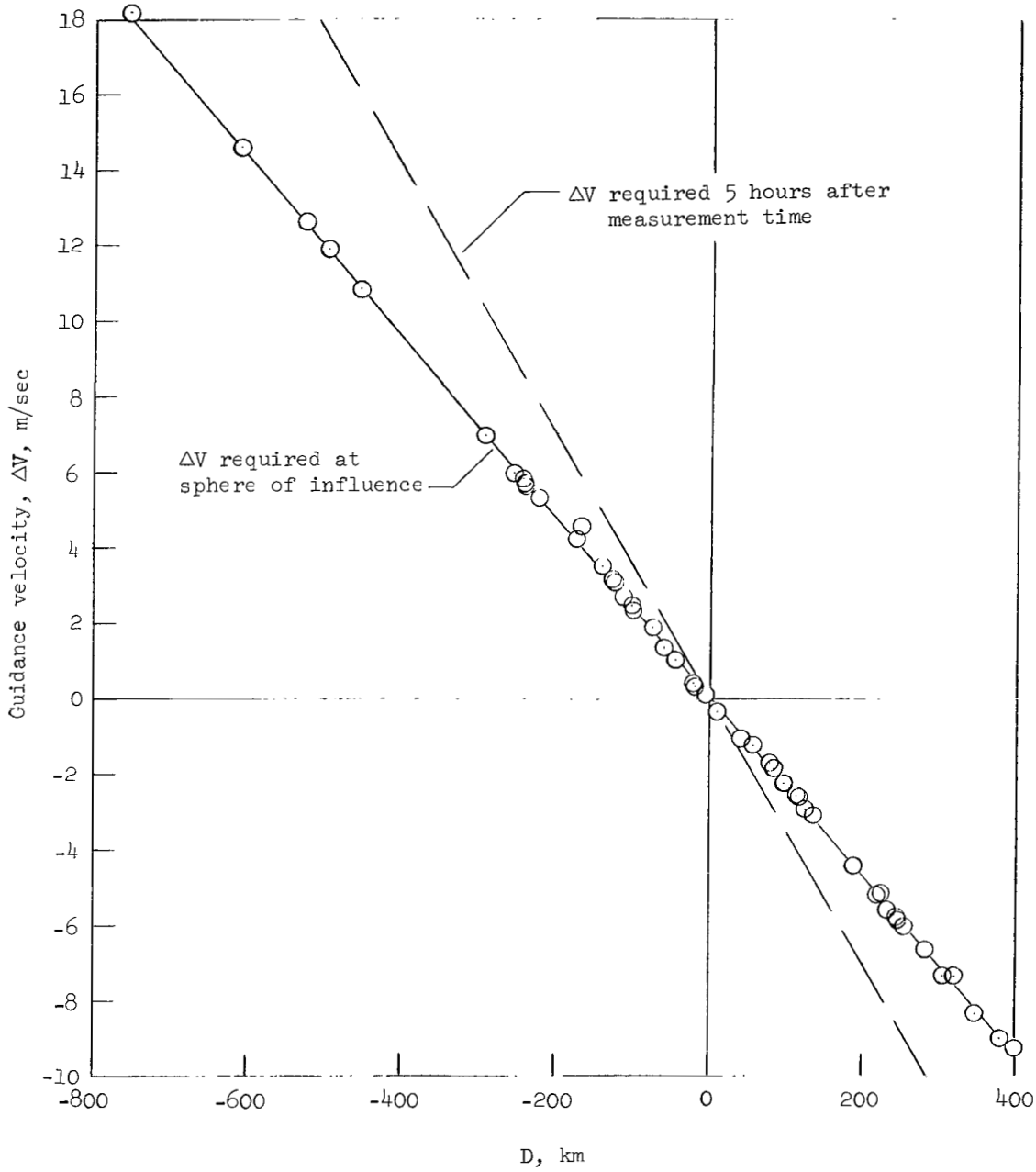

Figure 15.- Variation of approach-guidance-velocity requirements with D for two times. Measurements made at sphere of influence.

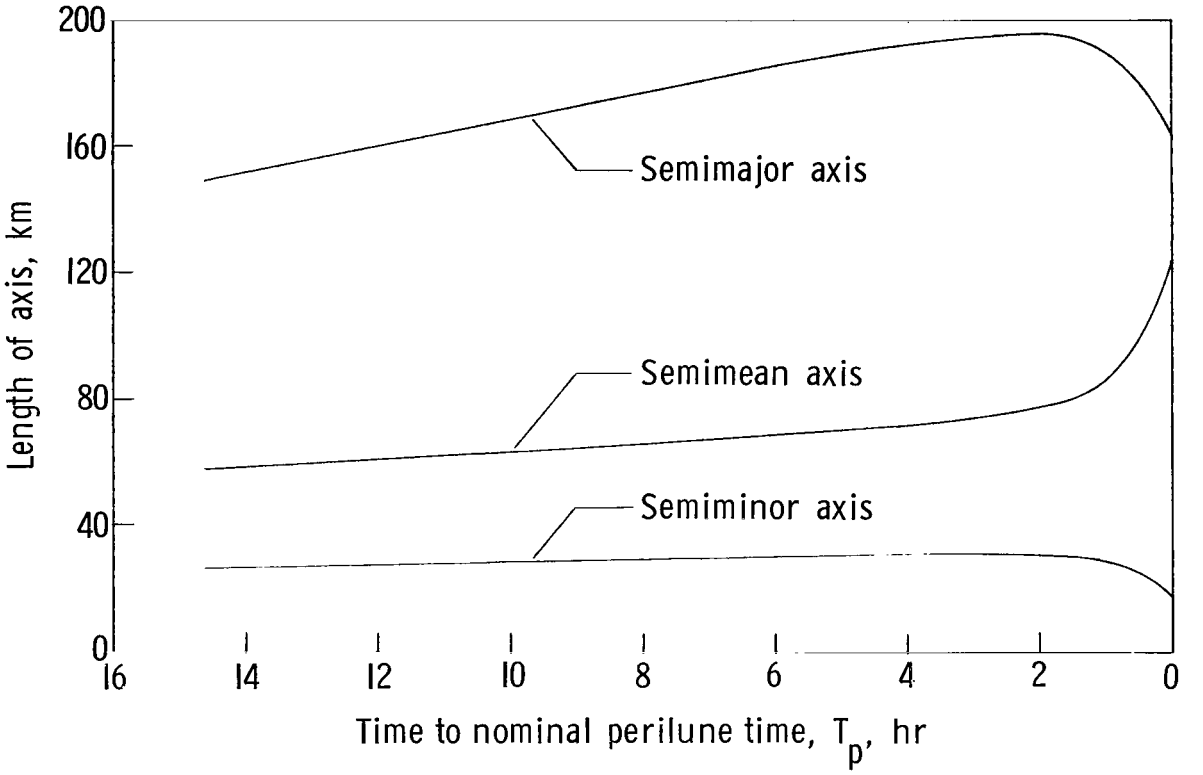

Figure 16.- Magnitude of axes of one-sigma position-error ellipsoid resulting from measurement error in onboard midcourse-guidance procedure. $\sigma_{r,mc}$ = 10 km; σ_θ = 10 seconds of arc.

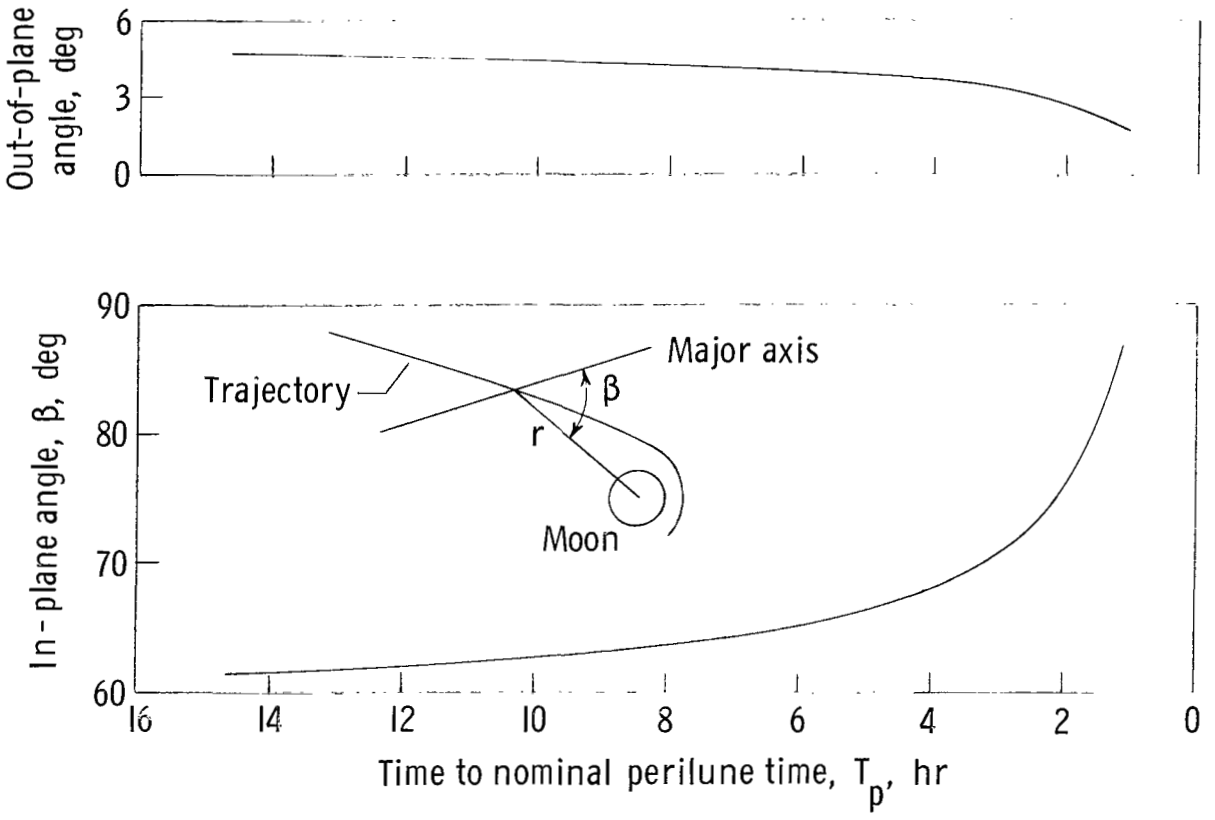

Figure 17.- Orientation of major axis of position-error ellipsoid caused by measurement error in onboard midcourse-guidance procedure.

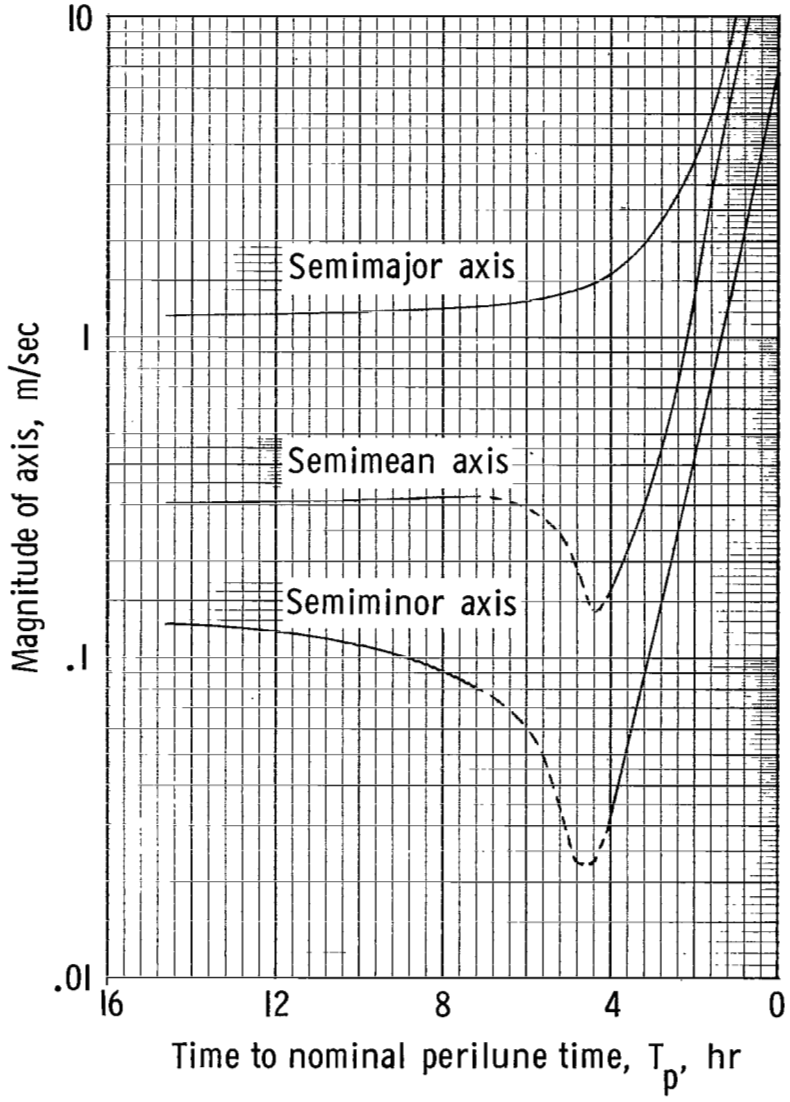

Figure 18.- Dimensions showing shape of one-sigma velocity-error ellipsoid resulting from measurement error in onboard midcourse-guidance procedure. $\sigma_{r,mc}$ = 10 km; σ_θ = 10 seconds of arc.

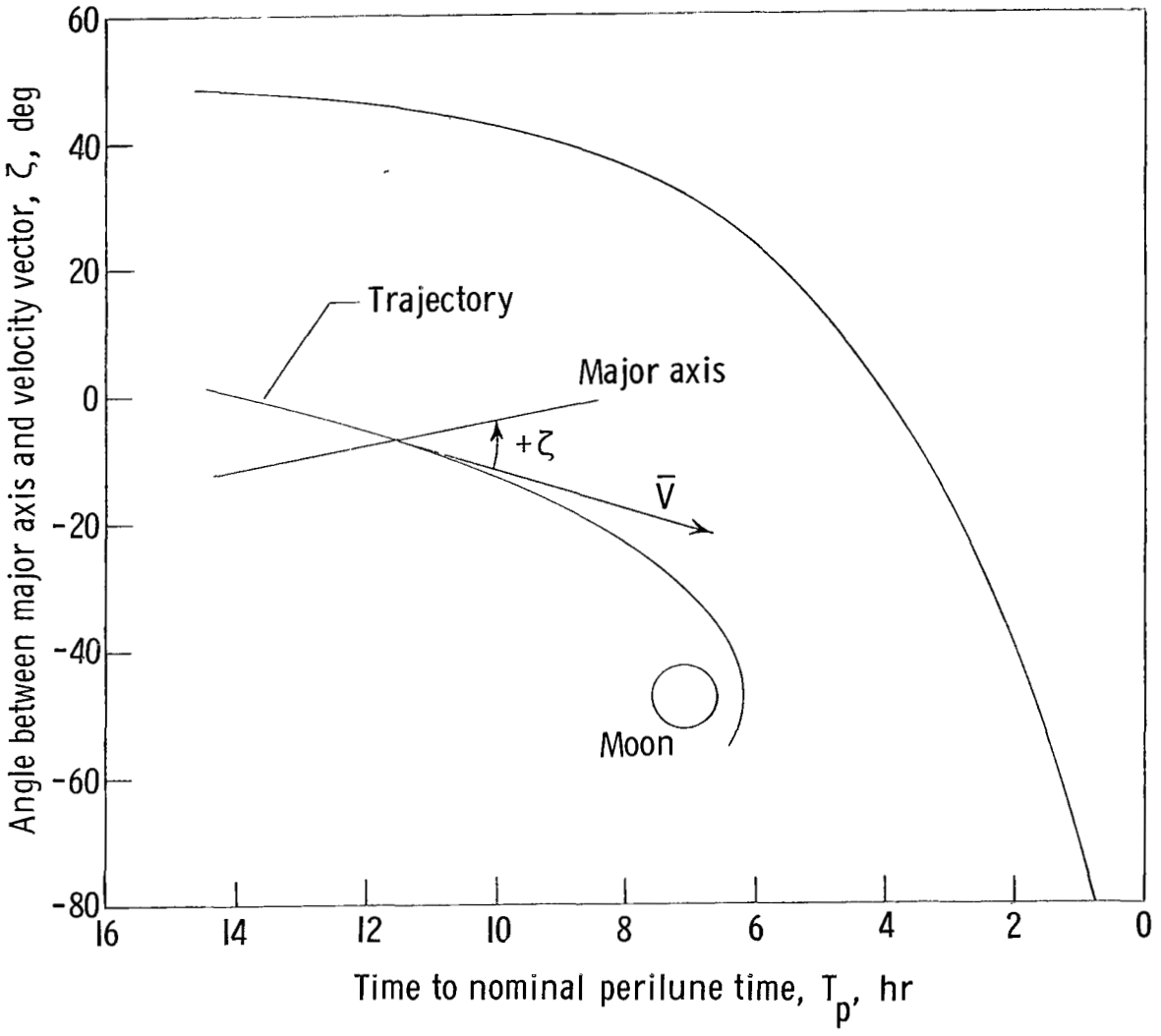

Figure 19.- Orientation of major axis of velocity-error ellipsoid (approximately in orbital plane) caused by measurement error in onboard midcourse-guidance procedure.

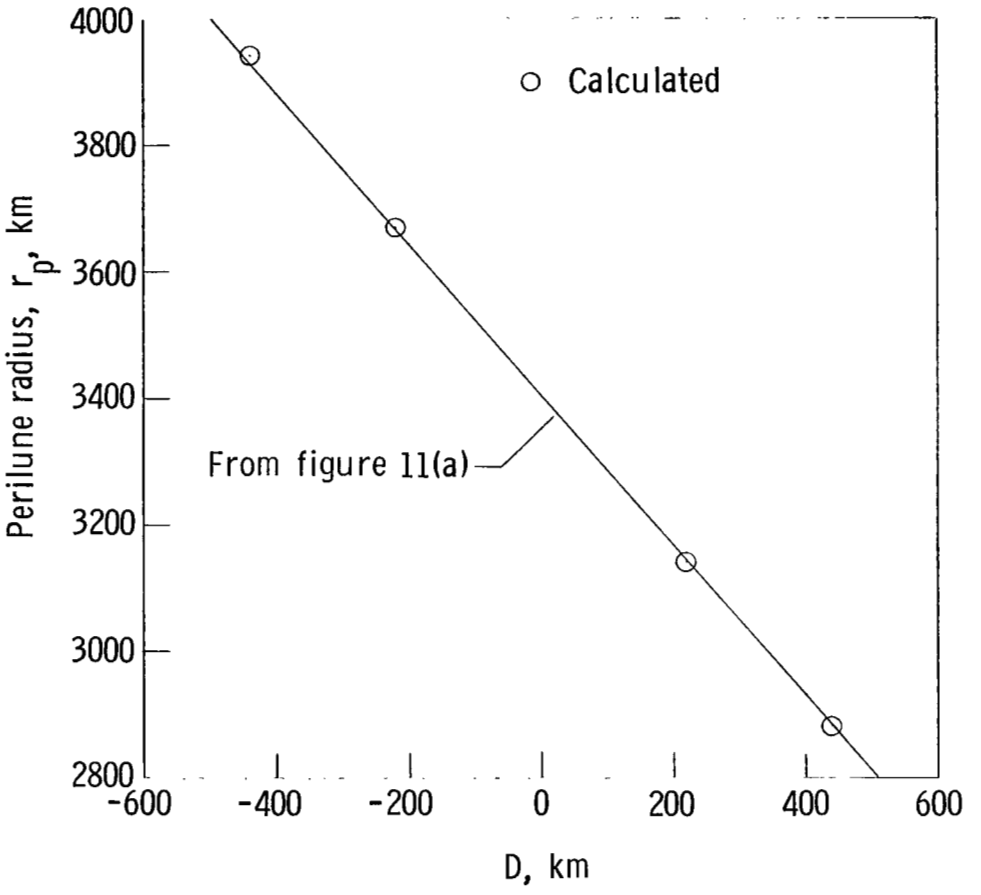

Figure 20.- Comparison of actual variation and calculated variation of r_p with D. T_p = 14.617 hr.

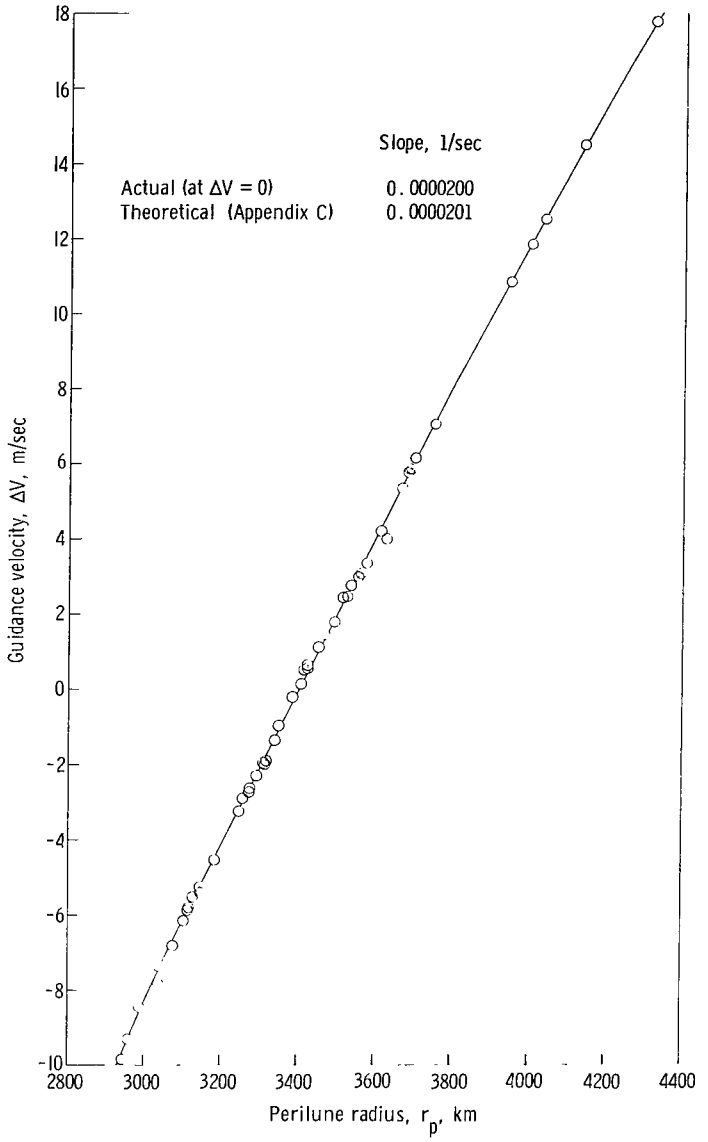

(a) 70-hr translunar trajectory;
$r_{p,n}$ = 3403.6 km; T_p = 14.617 hr.

Figure 21.- Variation of approach-guidance velocity with perilune radius for 50 perturbed trajectories. $\sigma_{r,mc}$ = 22 km.

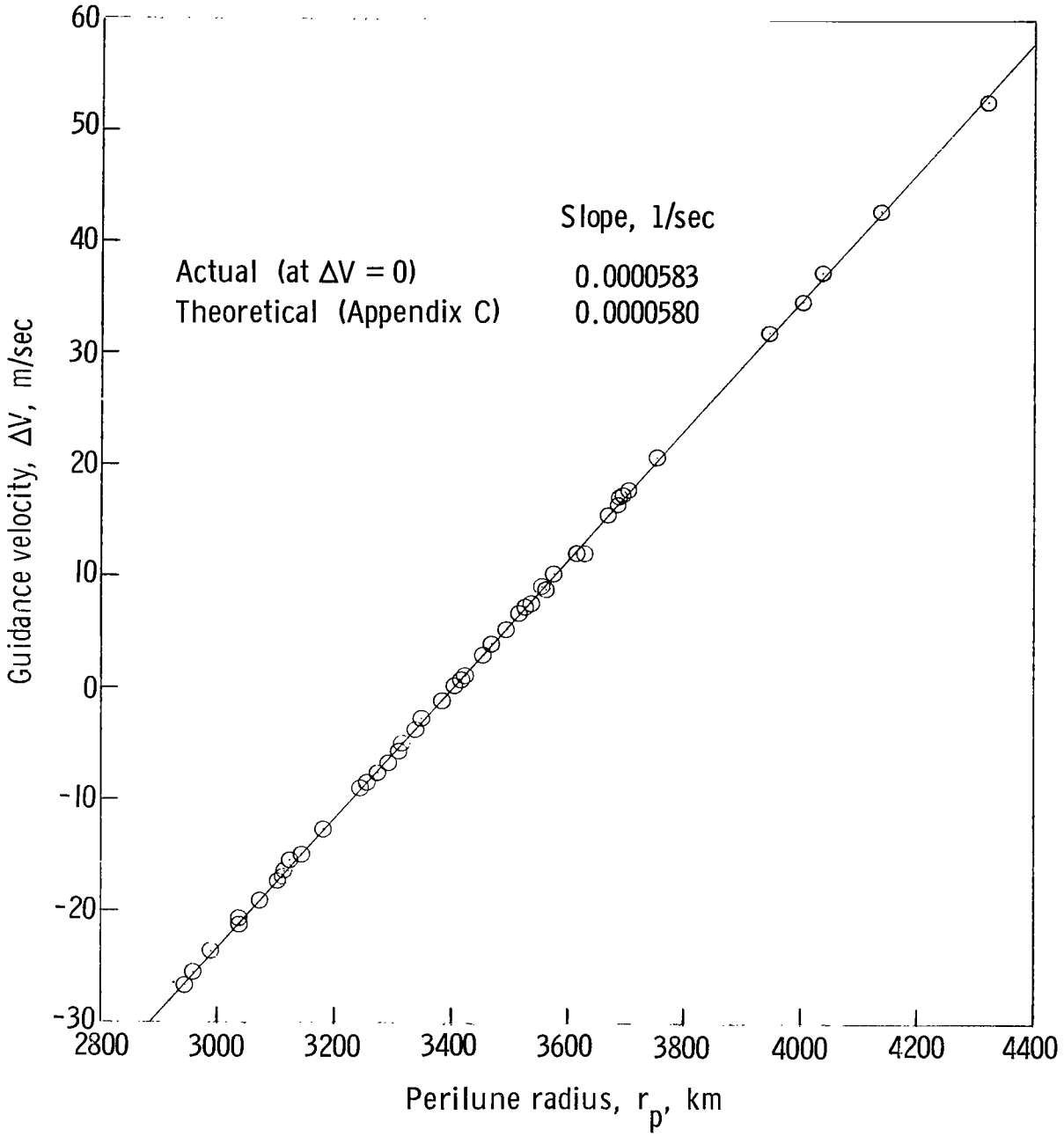

(b) 70-hr translunar trajectory; $r_{p,n}$ = 3403.6 km; T_p = 4.617 hr.

Figure 21.- Continued.

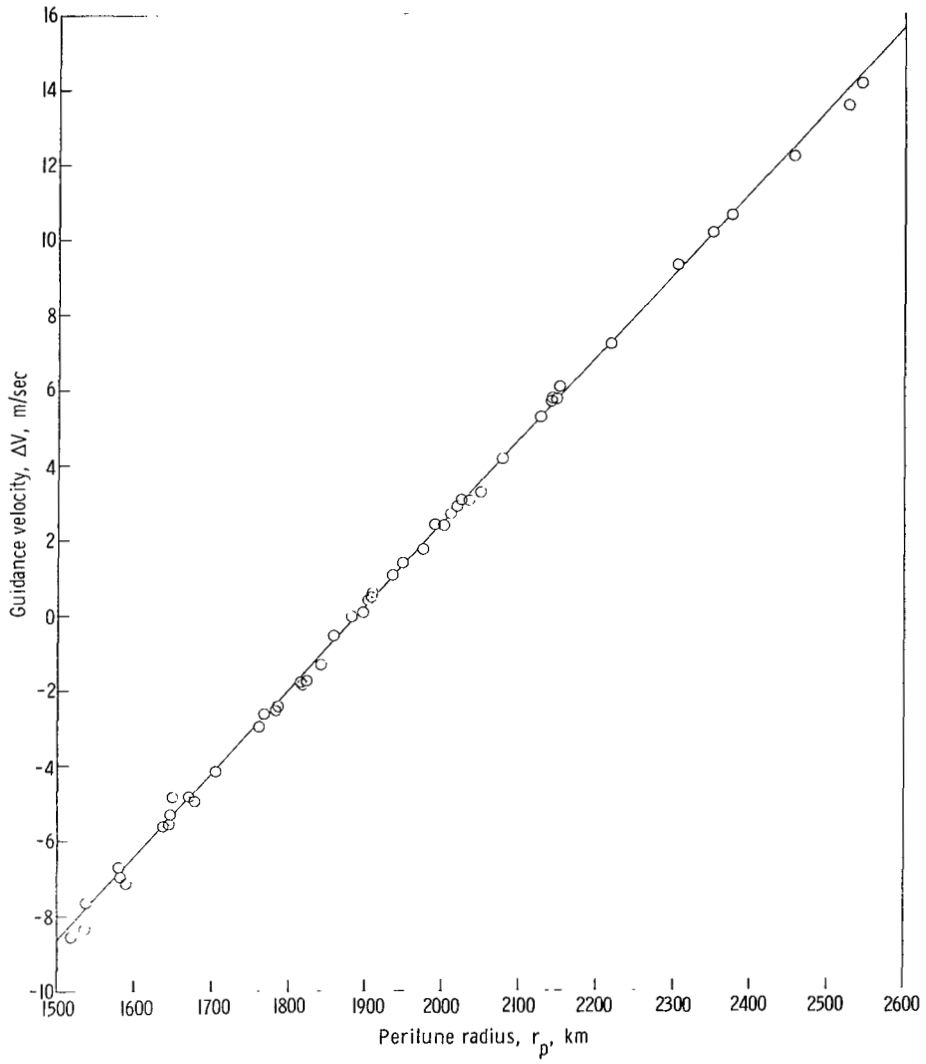

(c) 70-hr translunar trajectory; $r_{p,n}$ = 1892.8 km; T_p = 15.07 hr.

Figure 21.- Continued.

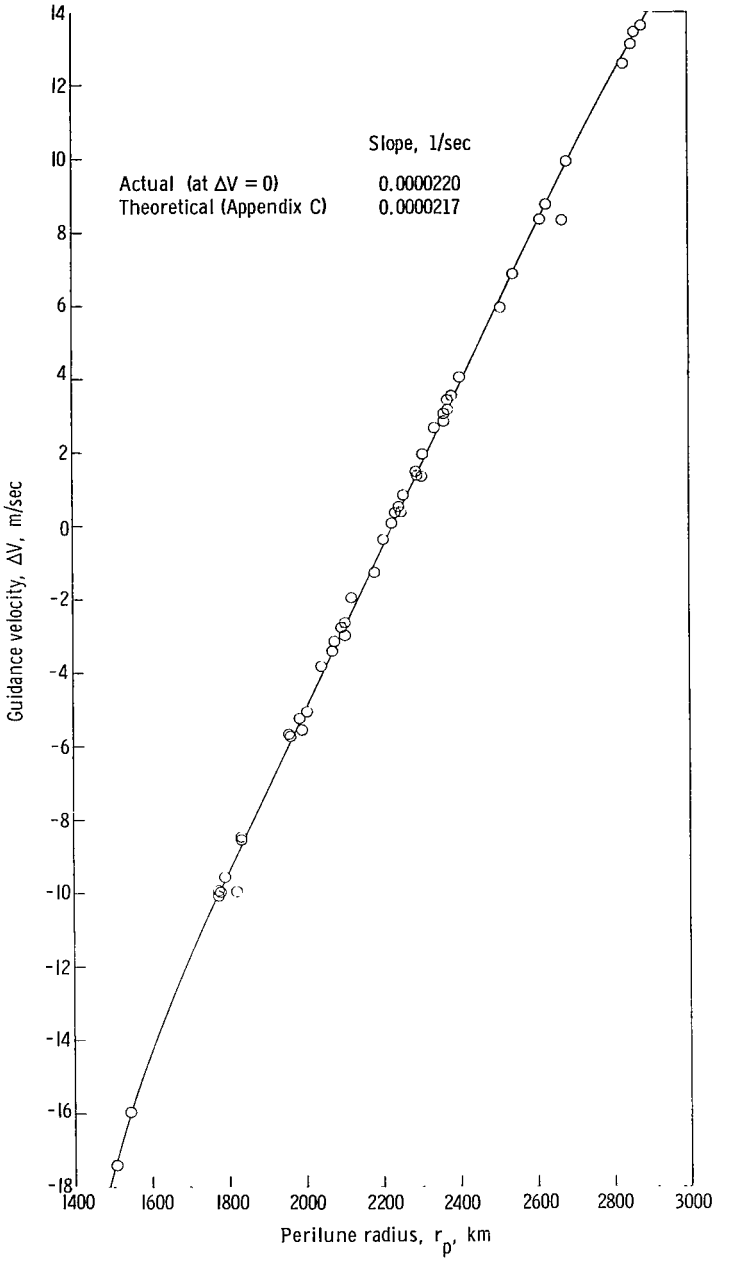

(d) 90-hr translunar trajectory;
$r_{p,n}$ = 2236.6 km; T_p = 15.0 hr.

Figure 21.- Concluded.

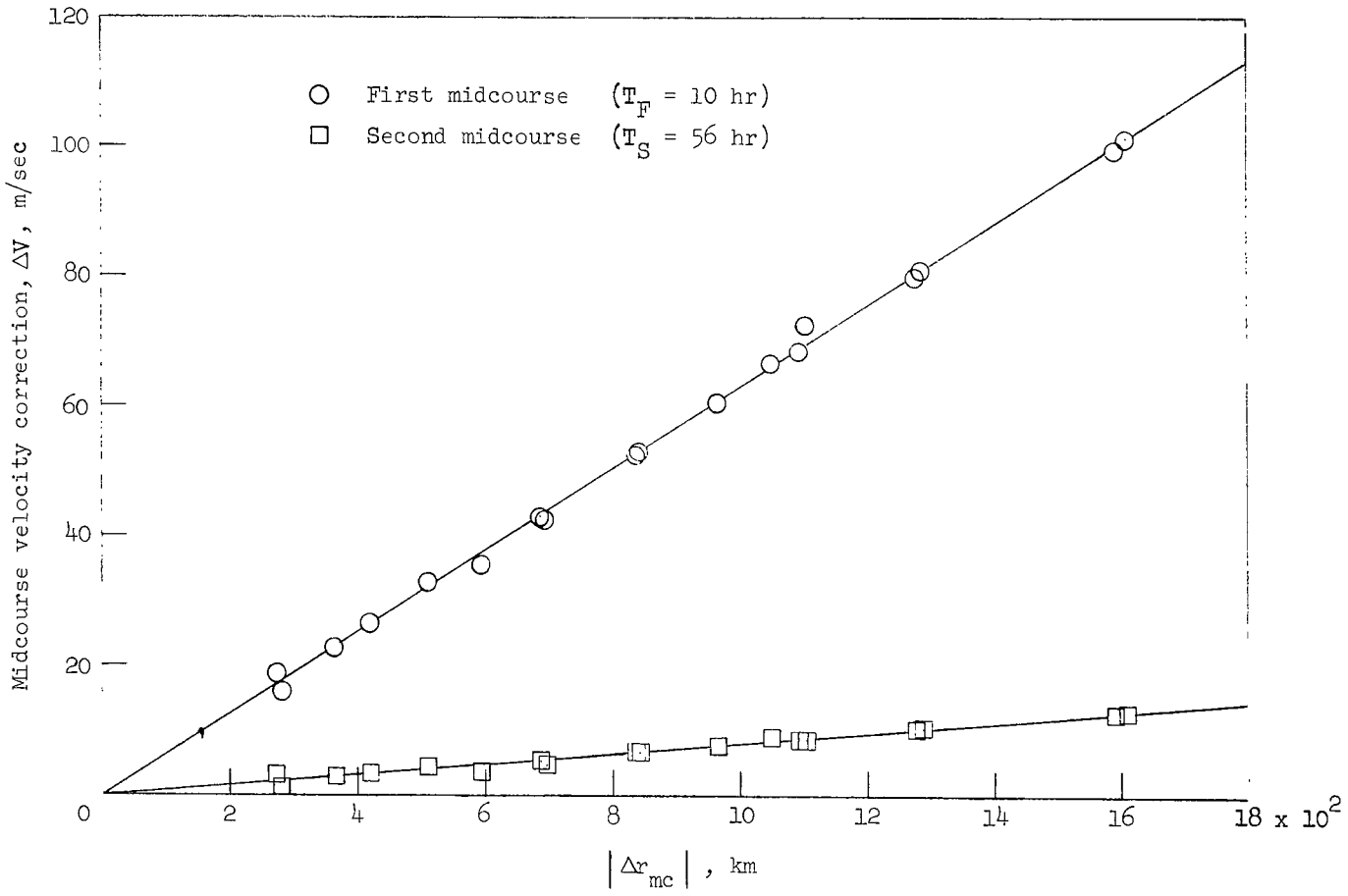

Figure 22.- Midcourse-maneuver velocity requirements. T_{pf} = 9.5 hr.

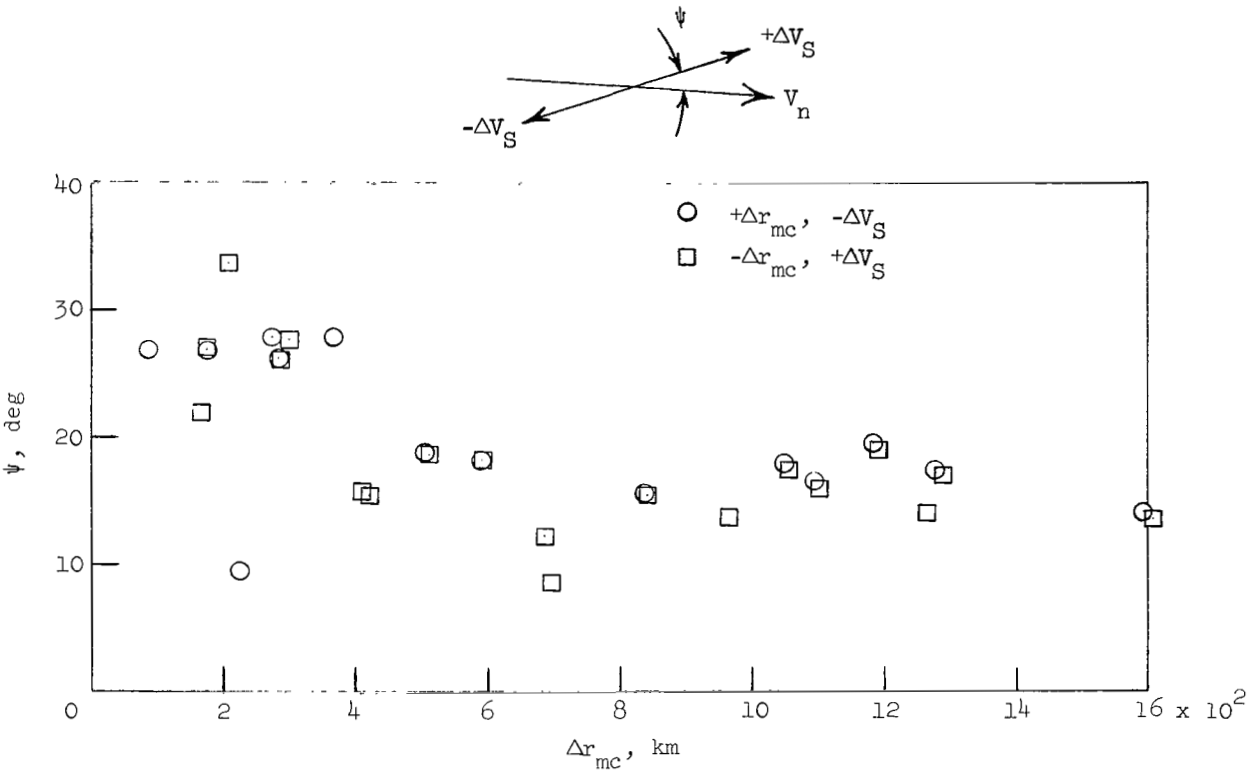

Figure 23.- Variation in direction of second midcourse-velocity vector. T_{pf} = 9.5 hr.

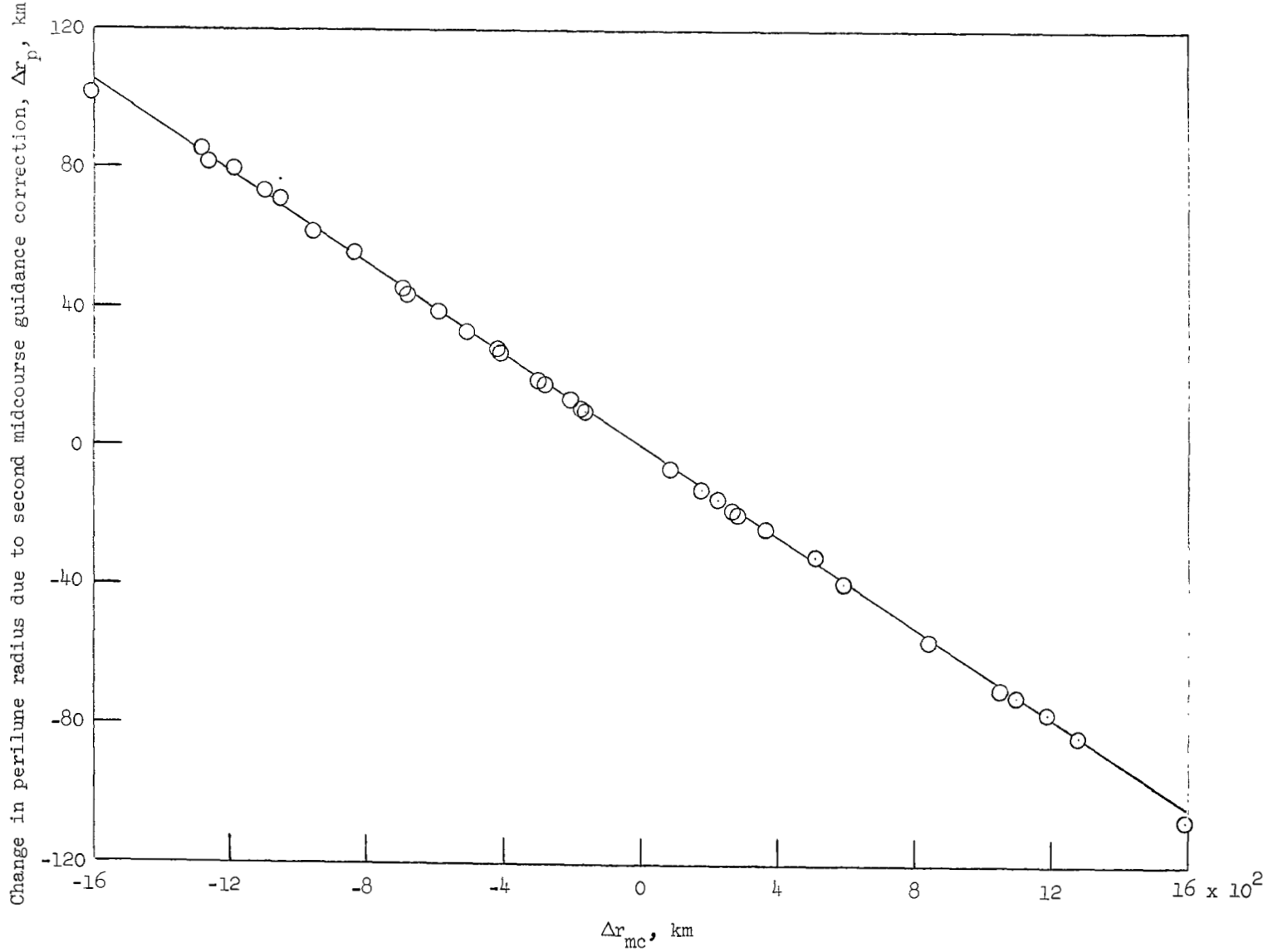

Figure 24.- Effect of second midcourse maneuver on perilune radius. T_{pf} = 9.5 hr.

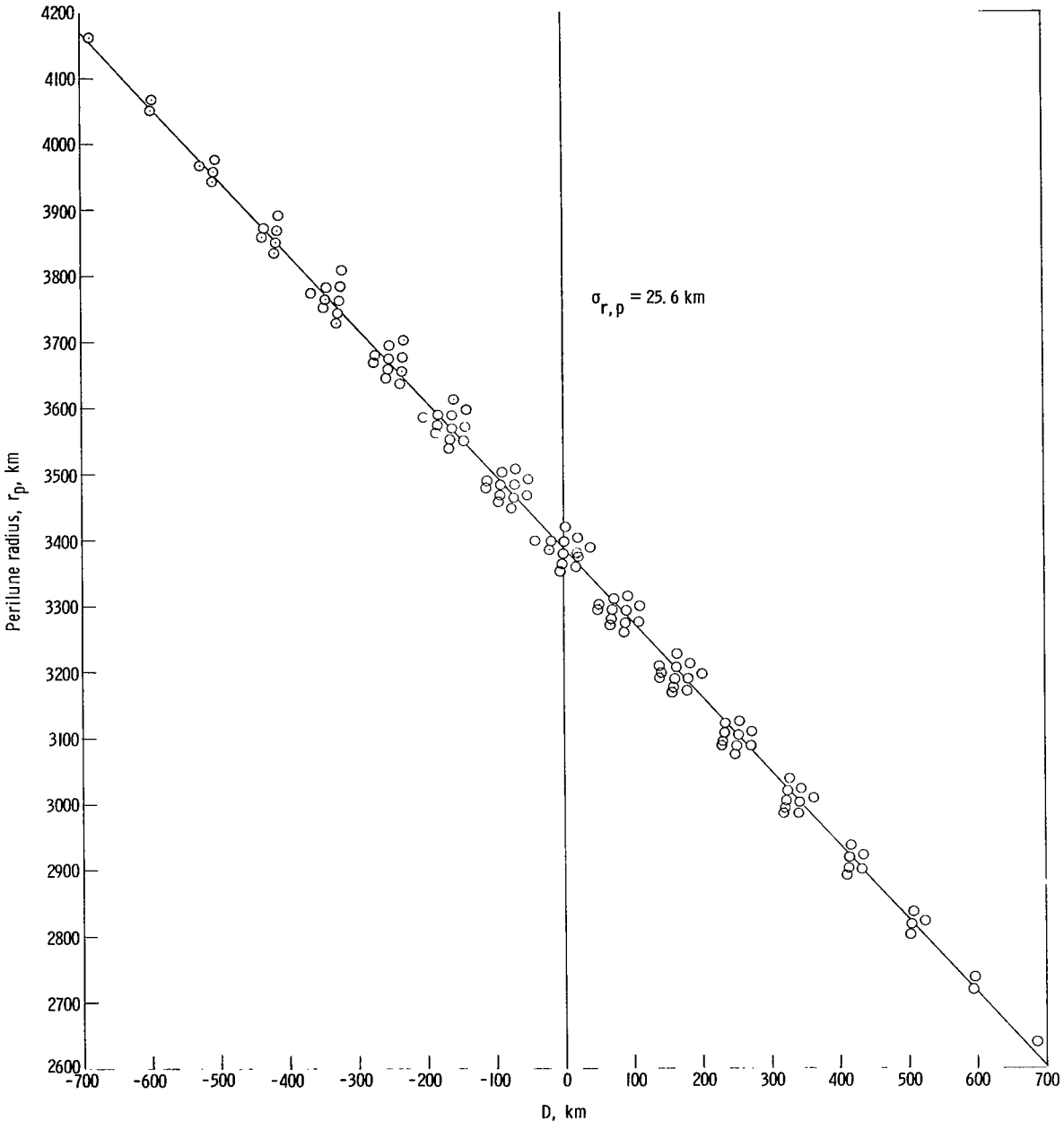

Figure 25.- Prediction of perilune radius resulting from approximately spherical distribution of midcourse-velocity errors. Maximum velocity error, ±2 m/sec in any component; D at T_p = 12.117 hr.

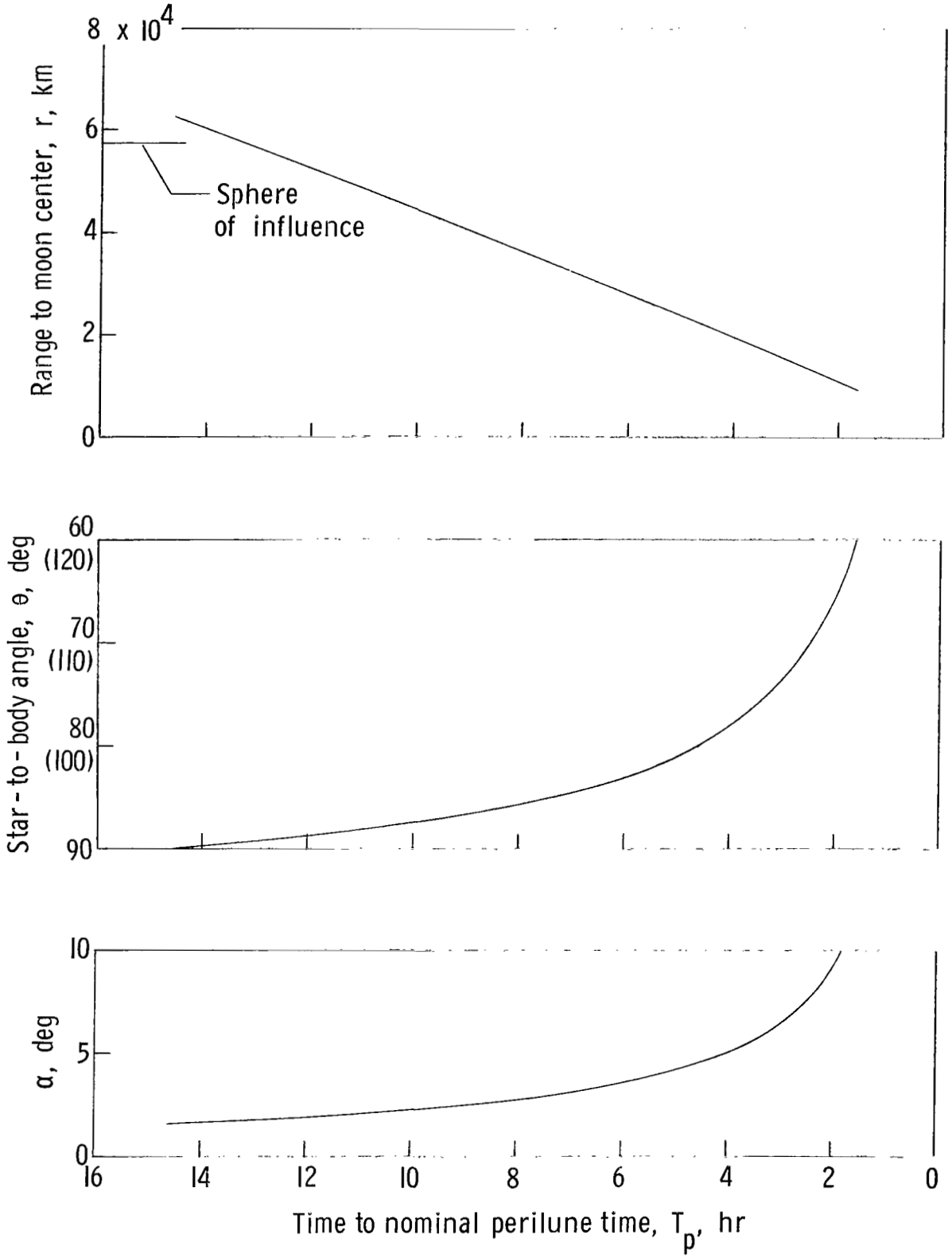

Figure 26.- Characteristics of nominal trajectory. Star is in vehicle orbital plane and in direction perpendicular to range vector at lunar sphere of influence.

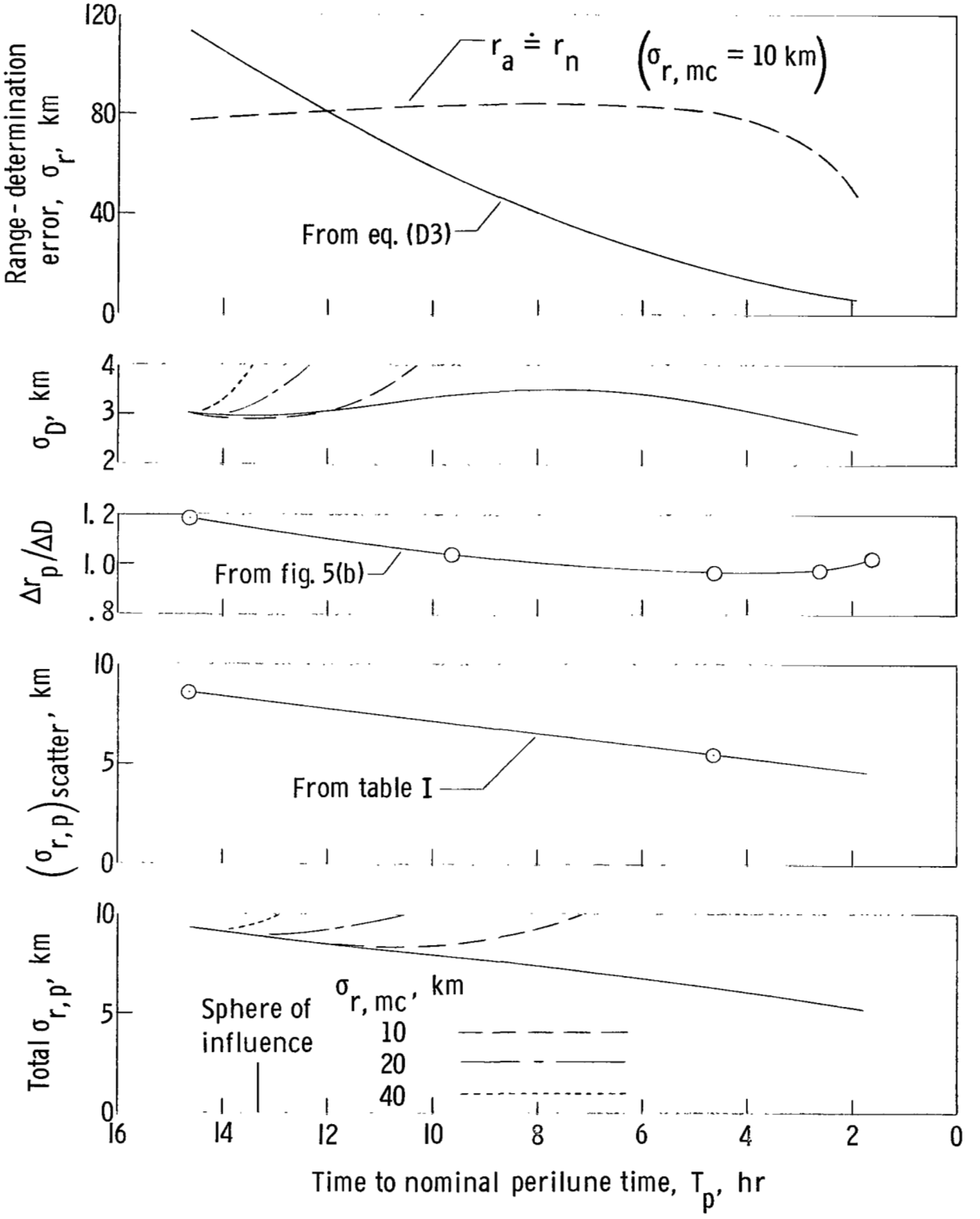

Figure 27.- Approach-guidance-accuracy characteristics due to measurement error and scatter error. Measurement errors σ_α and σ_θ = 10 seconds of arc; moon-radius uncertainty, 0.8 km. Range to moon measurement used for solid lines in upper two plots and lowest plot.

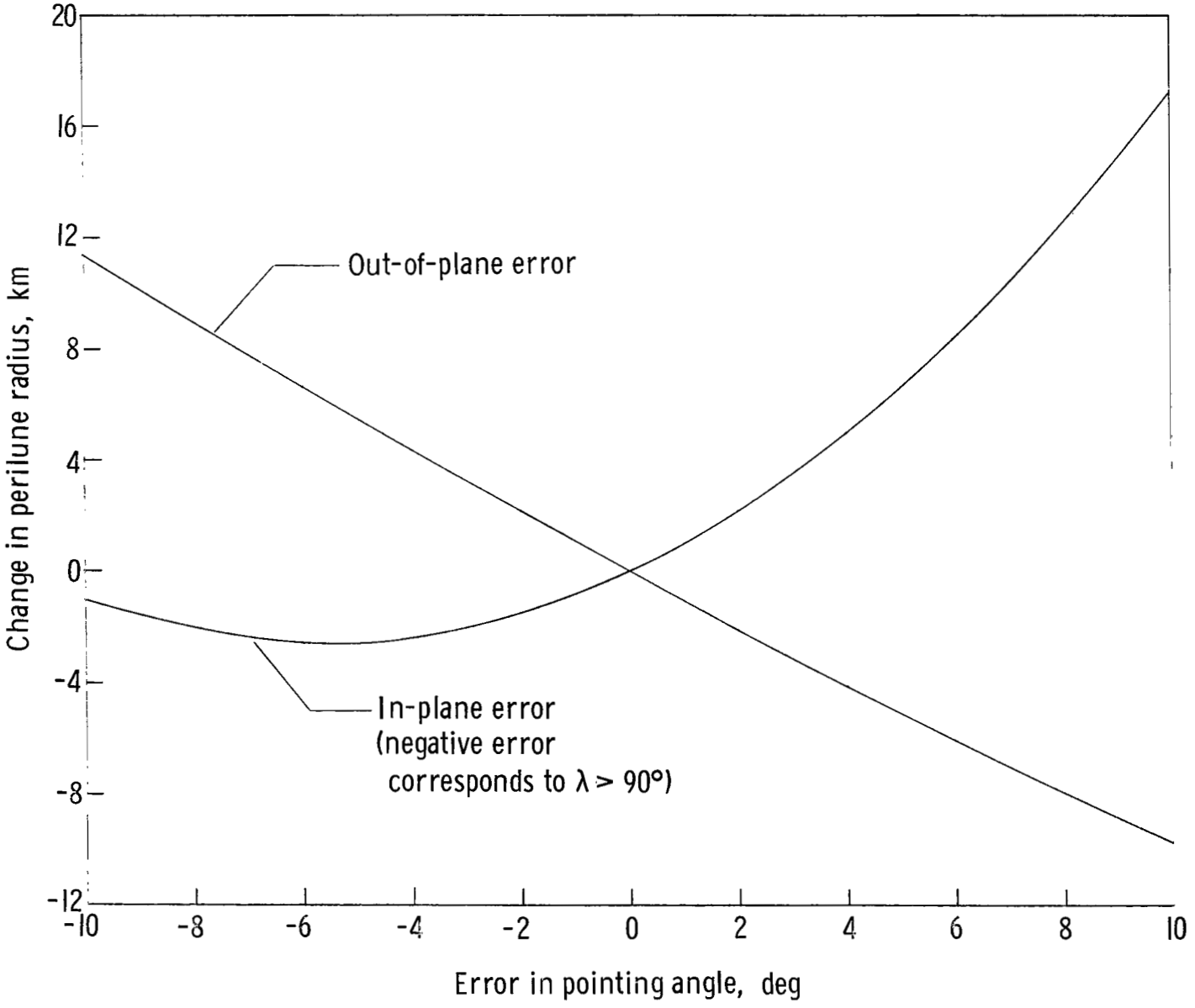

Figure 28.- Effect of error in pointing direction on approach-guidance accuracy. T_p = 14.617 hr; $\lambda_n = 90^\circ$.

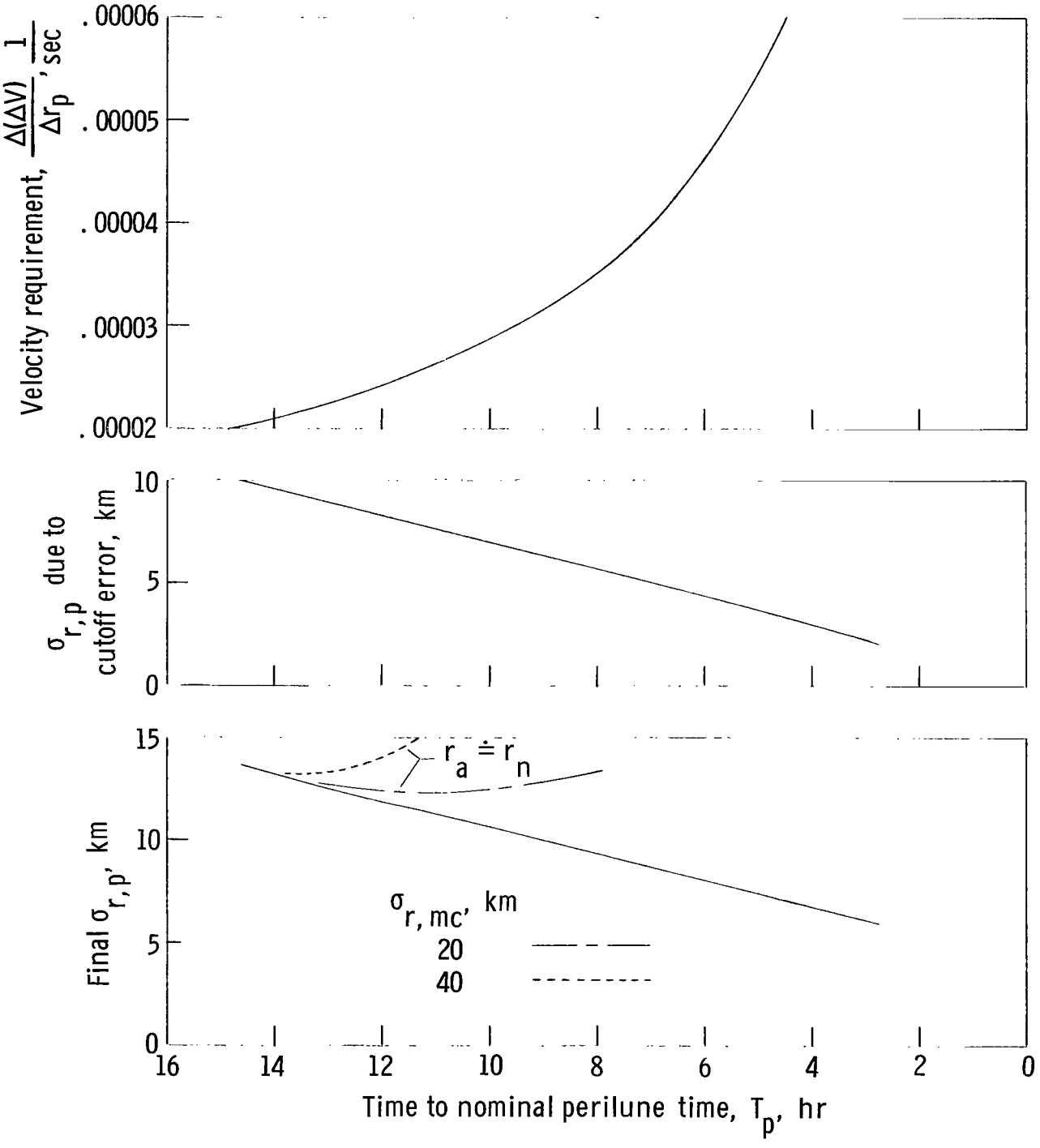

Figure 29.- Approach-guidance error with effect of velocity-cutoff error included. One-sigma value of velocity-cutoff error, 0.2 m/sec. Range to moon measurement used for solid line in bottom plot.

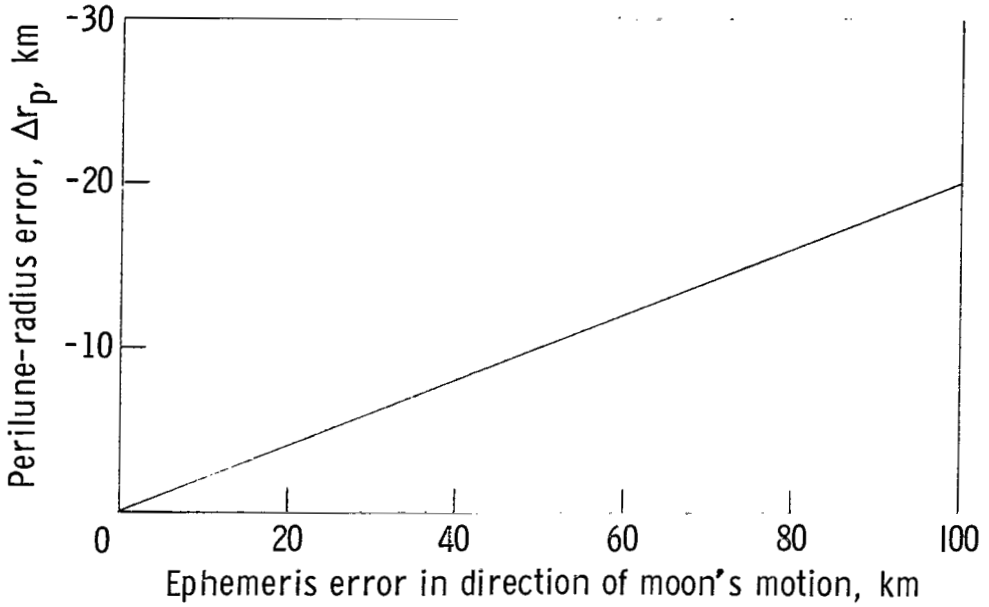

Figure 30.- Effect of lunar ephemeris error on approach-guidance accuracy. T_p = 12.117 hr. (For ephemeris error in direction opposite to moon's motion, direction of Δr_p is away from moon.)

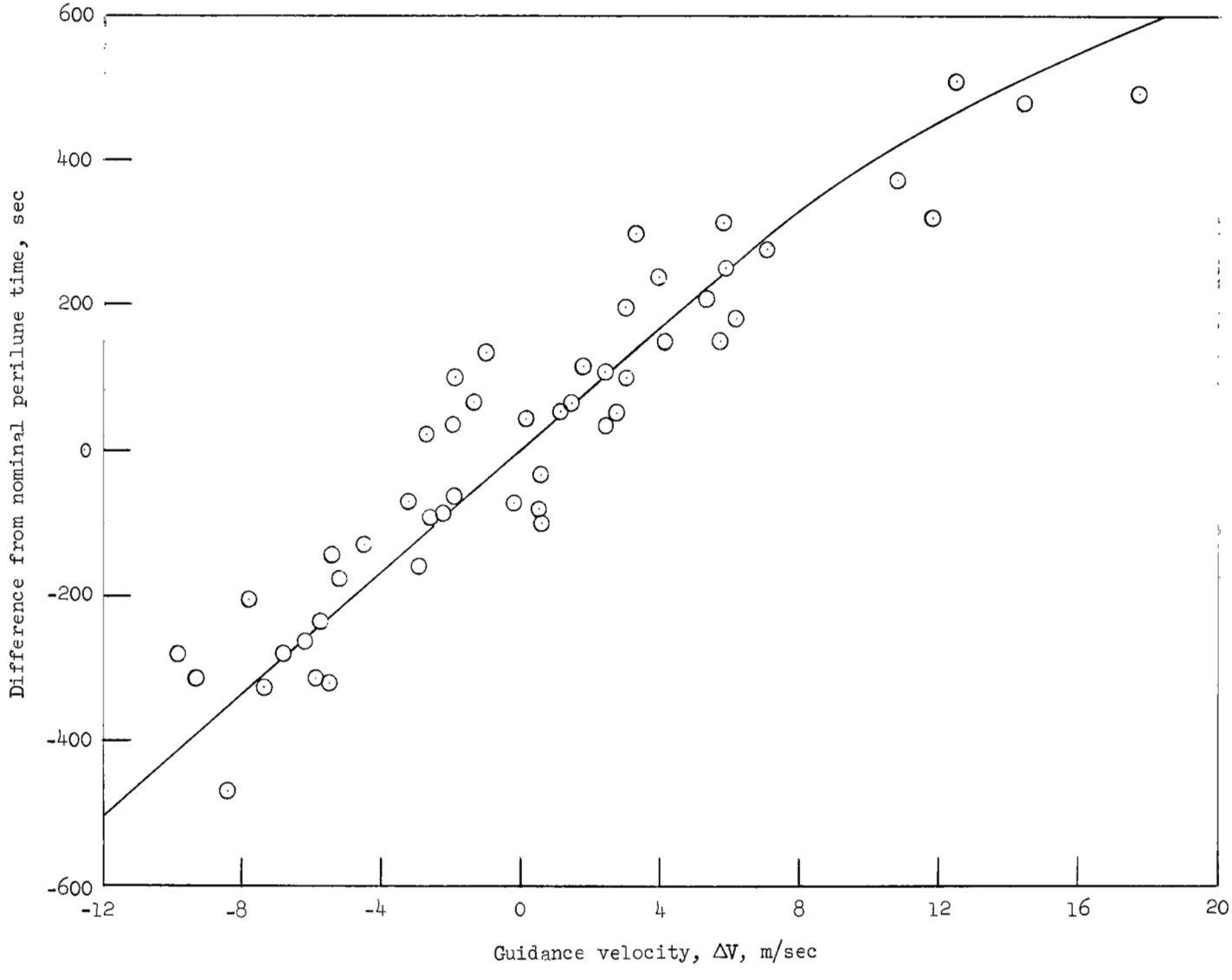

Figure 31.- Prediction capability of perilune time for perturbed trajectories. $\sigma_{r,mc}$ = 22 km.

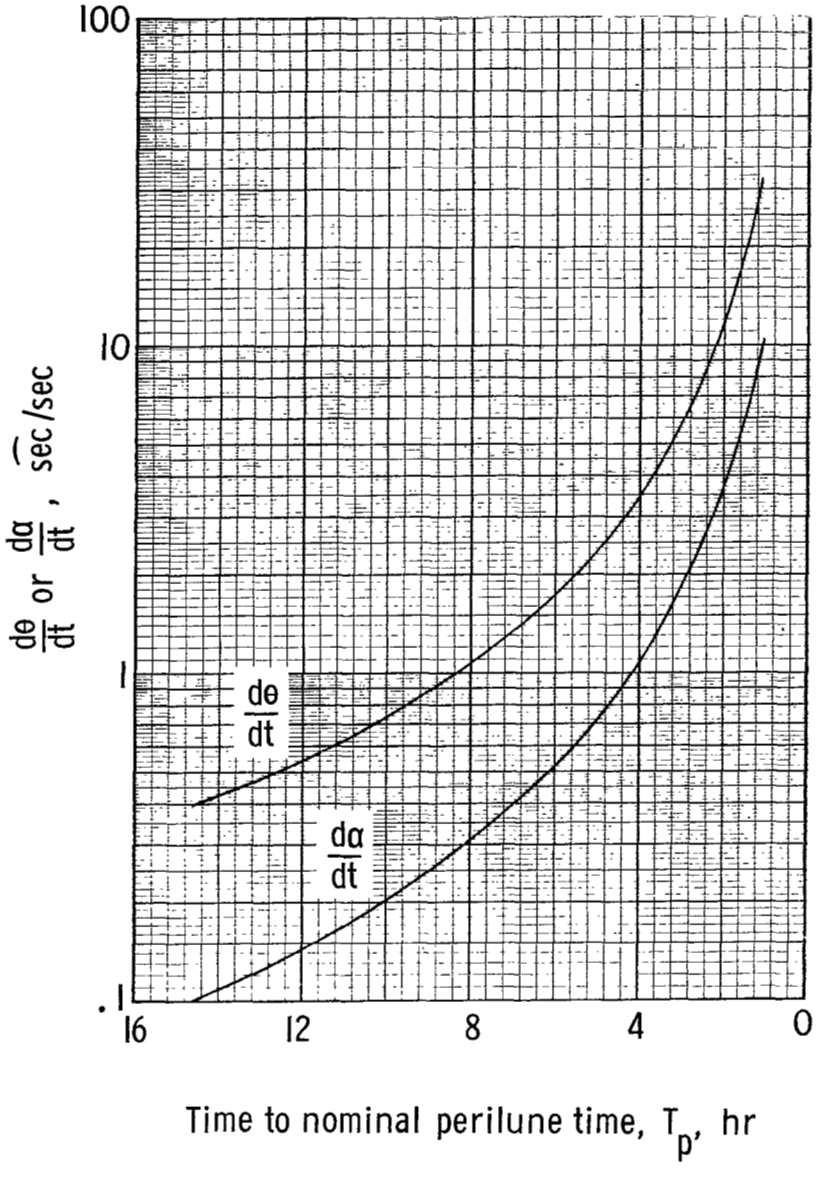

Figure 32.- Rate of change of measurement angles with time along nominal trajectory.

NASA-Langley, 1970 —— 21 L-7053

"The aeronautical and space activities of the United States shall be conducted so as to contribute . . . to the expansion of human knowledge of phenomena in the atmosphere and space. The Administration shall provide for the widest practicable and appropriate dissemination of information concerning its activities and the results thereof."

—NATIONAL AERONAUTICS AND SPACE ACT OF 1958

NASA SCIENTIFIC AND TECHNICAL PUBLICATIONS

TECHNICAL REPORTS: Scientific and technical information considered important, complete, and a lasting contribution to existing knowledge.

TECHNICAL NOTES: Information less broad in scope but nevertheless of importance as a contribution to existing knowledge.

TECHNICAL MEMORANDUMS: Information receiving limited distribution because of preliminary data, security classification, or other reasons.

CONTRACTOR REPORTS: Scientific and technical information generated under a NASA contract or grant and considered an important contribution to existing knowledge.

TECHNICAL TRANSLATIONS: Information published in a foreign language considered to merit NASA distribution in English.

SPECIAL PUBLICATIONS: Information derived from or of value to NASA activities. Publications include conference proceedings, monographs, data compilations, handbooks, sourcebooks, and special bibliographies.

TECHNOLOGY UTILIZATION PUBLICATIONS: Information on technology used by NASA that may be of particular interest in commercial and other non-aerospace applications. Publications include Tech Briefs, Technology Utilization Reports and Notes, and Technology Surveys.

Details on the availability of these publications may be obtained from:

SCIENTIFIC AND TECHNICAL INFORMATION DIVISION

NATIONAL AERONAUTICS AND SPACE ADMINISTRATION

Washington, D.C. 20546